# PART 1

# COAL STRUCTURE AND UPGRADING

## Section 1

# CHEMICAL STRUCTURAL COMPARISON OF LIGNITE, SUBBITUMINOUS, AND BITUMINOUS COALS

K. E. Chung and I. B. Goldberg

Rockwell International Science Center

# ABSTRACT

Chemical structural characteristics of a Texas lignite, a Wyoming subbituminous coal, and an Illinois bituminous coal were compared in terms of the distribution and arrangement of oxygen functional groups, aromatic clusters, linkages between the clusters, and side chains on the clusters. The structural characteristics were used to construct molecular models specific to the coals examined. Also, the structural data were related to their hydroliquefaction yields such as potential product, their distribution and hydrogen consumption.

The arrangements of aromatic clusters and functional groups are similar in the three coals. Two to four aromatic clusters of similar size are linked to each other by alkyl C-C bonds, making a chain of aromatic clusters. Two or more of these chains are connected to each other by ester and ether groups. The size of aromatic clusters ranges from single ring to five-fused ring clusters.

The three coals are different in the distributions of aromatic clusters, oxygen functional groups, and side chains. The lignite and bituminous coal contain fewer large aromatic clusters than the subbituminous coal, although they contain similar amounts of single ring and two-fused ring aromatic clusters. Hydroxyl and ether groups comprise more of the oxygen in lignite than the ester and carbonyl groups. However, the ester and carbonyl groups comprise more of the oxygen than hydroxyl and ether groups in the subbituminous coal. Most oxygen of the bituminous coal was in the form of ether and hydroxyl groups. The lignite and subbituminous coal contain more side chains than the bituminous coal.

The above structural characteristics were determined by controlled solubilization of each coal, followed by solvent fractionation of the product, and detailed analyses of the product fractions. The controlled solubilization was carried out in reactions with NaOH/ethanol/$H_2O$ at temperatures between 215° and 320°C. Elemental balances and other analytical data revealed that the oxygen functional groups of each coal were attacked selectively in the solubilization process, resulting in an orderly, definable degradation of the complex coal structure.

# INTRODUCTION

Since the chemical nature of coal has been understood only in qualitative terms, better understanding of its chemical composition and structural characteristics could result in substantial improvements in coal utilization. Elucidation of the coal structure, however, has been hindered by two major obstacles: the complex composition of coal and its low solubility in known solvents. Recently we have developed an effective methodology to overcome these difficulties, and determined the chemical structural characteristics of specific coals quantitatively in terms of the distribution and arrangement of oxygen functional groups, linkages and aromatic clusters.[1-4] Briefly, our characterization methodology consists of controlled solubilization of each coal, followed by solvent fractionation of the product and detailed analyses of each fraction to obtain molecular structural information.

In this paper, we will compare the structural characteristics of three coals of different ranks, which were determined with our methodology. Our findings reveal substantially different trends in structural characteristics among the different coals from those depicted by previous representative structures.[5] Therefore, the results provide a new insight into the reactivity of coals under, e.g., liquefaction conditions.

# EXPERIMENTAL

Three coal samples were a subbituminous coal from the Rawhide mine in northeastern Wyoming, a lignite from the Big Brown mine in northeastern Texas, and a bituminous coal from Burning Star No. 4 mine in Illinois. Each sample was ground in a ball mill with water. After removing the excess water, the moist coal samples were used in solubilization reactions. The moisture contents of the samples were typically 50%. The Wyoming coal, after drying at 110°C, had the following composition: C, 64.9%; H, 4.2%; N, 0.6%; O and S, 24.8% by difference; and ash, 5.5%. The composition of a dried Texas lignite sample was: C, 59.7%; H, 4.2%; N, 1.2%; O and S, 22.6% by difference; and ash, 12.3%. The composition of a dried Illinois coal sample was: C, 64.1%; H, 4.3%; N, 1.2%; O and S, 14.4% by difference; and ash, 16.0%.

Each coal was solubilized in reactions with NaOH/ethanol/$H_2O$. For the two low-rank coals, three reactions were carried out at 215°, 260° and 300°C, and for the bituminous coal, the reaction temperatures were 260°, 300° and 320°C. Subbituminous coal reactions were denoted by Sub-215, Sub-260 and Sub-300; lignite reactions by Lig-215, Lig-260 and Lig-300; and bituminous coal reactions by Ill-260, Ill-300 and Ill-320. In each reaction, a weighed portion of 50 g of a moist coal sample was mixed with 40 g of ground NaOH, and the mixture was placed in a 1-liter autoclave, followed by the addition of 120 g of ethanol. The reactor was heated to the desired temperature, the reaction was continued for 1 h, and then the reactor was cooled to ambient temperature.

The gaseous product was examined by IR. The condensed product was collected in water and the solution was centrifuged. Figure 2-1 shows the fractionation scheme. The solid material from the centrifugation was called "Basic Solution Insoluble" or BaI. $CO_2$ formed during the reaction appeared as $Na_2CO_3$ in the basic solution and was determined by a forward/backward titration method or absorption of evolved $CO_2$ in a weighed $CO_2$ absorber using an aliquot of the supernatant solution. The rest of the supernatant was acidified to pH 2.7 to obtain a precipitate, which was collected and called "Basic Solution Soluble" or BaS. Acetone extraction was performed only on BaI-HI obtained in the reaction at 300°C. Pyridine extraction was performed at room temperature with the solvent/sample ratio of 10. $H_2O$-soluble material was recovered from the water washes of BaS and BaI by chloroform extraction.

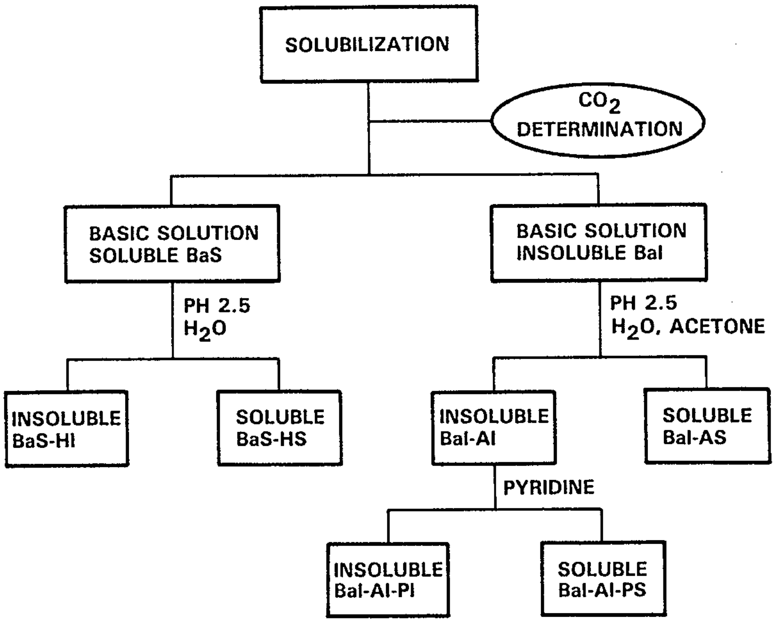

Figure 2-1. Fractionation of Solubilization products.

Most of the condensed-phase product fractions were analyzed for elemental composition, ash content, average molecular weight, hydrogen distribution and functional group contents. Elemental composition was determined with a Perkin-Elmer Model 240B analyzer. The ash content was determined by heating at 750°C in a ventilated furnace. Hydrogen distribution and functional group contents were determined by $H^1$-NMR and IR spectroscopy using a JOEL FX-60-Q NMR spectrometer and a Nicolet MX-1 Fourier transform IR spectrometer. Average molecular weight was determined by vapor phase osmometry using a Corona Model 232A apparatus (Wescan Instruments, Inc.). The experimental procedure and conditions were carefully chosen to ensure the correct determination of molecular weight.[6]

# RESULTS AND DISCUSSION

The progress of the solubilization reaction depends on the reactivity of a feed coal that is governed by functional groups of the coal. Meanwhile, the chemical characteristics of solubilization products depend on the reaction employed as well as on the feed coal. Thus, the correct understanding of the solubilization reaction is necessary to determine the characteristics of the products and, in turn, those of the starting material. We will discuss the solubilization reaction of the Wyoming coal first, and then examine the structural characteristics of the solubilization products, followed by the description of the coal structure and its relationship to liquefaction behavior. The results from the Texas lignite and the Illinois coal will be examined in a similar manner, pointing out major differences from the Wyoming coal.

## CHEMICAL STRUCTURAL CHARACTERISTICS OF WYOMING SUBBITUMINOUS COAL

### Formation of the Solubilization Products

Recently the base/alcohol reaction of coal has been investigated by several groups,[1-3,7-9] but there has been no consistent interpretation of the chemistry involved. During this investigation, we observed the evolution of $CO_2$ on the acidification of the product solutions; this observation has not been reported in the literature. For example, the amount of $CO_2$ evolved was 19.4% in Sub-260. Only a trace of $CO_2$ was detected in the gaseous products by IR. According to a blank test by Makabe et al,[9] NaOH and ethanol produced only a minute amount of $CO_2$, 0.011% based on carbon in ethanol at 300°C. Our observation of $CO_2$ evolution is extremely significant for properly understanding the chemistry of the feed coal.

The product distribution and molecular weights of condensed-phase products from the three reactions of the Wyoming coal are compared in Table 3-1. The yield of $CO_2$ was significant in Sub-215, and it increased by more than a factor of four at 260°C and remained constant at 300°C. Nevertheless, the recovered $H_2O$-soluble and the lost $H_2O$-soluble increased with reaction temperature by a factor of three between 260° and 300°C. The trends of $CO_2$ and the $H_2O$-soluble yields indicate that dissimilar reactions took place at the different temperatures.

Table 3-1

COMPARISON OF YIELDS (wt%) AT DIFFERENT TEMPERATURES

| | | Sub-215 | Sub-260 | Sub-300 |
|---|---|---|---|---|
| BaS-HI | 26.9 | 42.7 (1190)* | | 14.2 (780) |
| BaS-HS | 24.6 | 7.0 (1140) | | 14.9 (770) |
| BaI-AS | - | - | 17.6 (590) | |
| BaI-PS | 14.5 | 25.4 (1400) | | 14.7 (2100) |
| BaI-PI | 28.9 | 6.1 | 4.6 | |
| CO as $CO_2$ | | 3.0 | 12.4 | 12.2 |
| $H_2O$-Soluble | | 0.0 | 1.8 | 5.6 |
| Lost and Error | | 2.1 | 4.6 | 16.2 ($C_1$-$C_2$ Soluble?) |

*Average molecular weight by vapor phase osmometry

The distribution of the condensed-phase products also reflects the different reactions that have taken place. Even at 215°C, 70% of the feed coal was converted to the soluble and gaseous products. Furthermore, 51% was soluble in basic solution. This high solubility indicates a high content of polar functional groups in the products.

At 260°C, the conversion increased to 94%, and the condensed product distribution was altered drastically. The substantially higher yields of BaS-HI and BaI-PS came from BaS-HS and BaI-PI in Sub-215, respectively. Still the yield of BaS-HI and BaS-HS is 50% of the feed, and the high solubility in basic solution indicates a large content of polar functional groups in these fractions as well. Obviously, decarboxylation was responsible for the change as indicated by the large amount of $CO_2$ evolved, but other reactions may have contributed. The yield of the $H_2O$-soluble (recovered and lost) is significant. The average molecular weights of soluble fractions ranged from 1140 to 1400.

At 300°C, the conversion, 95%, remained almost the same as at 260°C, but the product distribution changed from that found at 260°C. Since the $CO_2$ evolution was not altered from that at 260°C, the larger yield of the $H_2O$-soluble material is characteristic to the reaction which occurred at 300°C. The molecular weights of the soluble fractions ranged from 590 to 2100, which were approximately 34% less than those in Sub-260. BaI-AS is a unique fraction which had the lowest molecular weight, but it was mixed with BaI-AI-PS, which had potentially the highest molecular weight among the soluble fractions in Sub-300. The elemental composition revealed that BaI-AS had the lowest oxygen content but the highest H/C ratio: thus, it was not soluble in the basic solution or in $H_2O$. The much larger molecular weight of the BaI-PS fraction in Sub-300 than in Sub-260 reveals that (1) the fraction from Sub-260 consisted of at least two subfractions which differ greatly in molecular weight and functionality, and (2) the BaI-PS fraction obtained from Sub-300 was little changed, even though the reaction temperature was increased by 40°C.

In addition to the product distribution, element balances provide important information. In Sub-215, the total carbon recovery was 97%, as shown in Table 3-2, which indicates that the product collection and its analysis were dependable. However, hydrogen and oxygen recoveries were 110% and 117%, respectively. The high hydrogen recovery and $CO_2$ evolution resulted in significantly higher H/C ratios of the product fractions, BaS-HI, BaS-HS, BaI-HI and BaI-HS, than that of the feed coal.

Similar trends were observed with Sub-260 fractions, as shown in Table 3-3. The total product yield was more than 100%, although the ash recovery was only 31%. The unrecovered ash material was assumed to be lost in the aqueous solution during alkali and acid treatments. As $CO_2$ evolution increased substantially, more

Table 3-2

YIELD AND ELEMENTAL COMPOSITION OF Sub-215 PRODUCTS

| | Yield % | C % | H % | N % | O %* | Ash % | H/C |
|---|---|---|---|---|---|---|---|
| Dry Coal | 100.0 | 64.9 | 4.2 | 0.6 | 24.8 | 5.5 | 0.78 |
| BaS-HI | 26.9 | 67.5 | 4.9 | (0.6)** | 26.1 | 0.9 | 0.86 |
| BaS-HS | 24.6 | 66.7 | 4.9 | (0.6) | 26.8 | 1.0 | 0.89 |
| BaI-HI | 12.8 | 68.4 | 5.6 | (0.6) | 17.3 | 8.1 | 0.98 |
| BaI-HS | 30.6 | 59.4 | 4.5 | (0.6) | 31.6 | 3.9 | 0.91 |
| $CO_2$ | 4.7 | 27.3 | - | - | 72.7 | - | - |
| Total Yield | 99.6 | 62.8 | 4.6 | | 28.9 | 3.6 | 0.88 |
| Total Recovery | | 97% | 110% | | 117% | 66% | 113% |

*By difference
**Assumed value: due to instrument malfunctioning

Table 3-3

YIELD AND ELEMENTAL COMPOSITION OF Sub-260 PRODUCTS

| | Yield % | C % | H % | N % | O %* | Ash % | H/C |
|---|---|---|---|---|---|---|---|
| Dry Coal | 100.0 | 64.9 | 4.2 | 0.6 | 24.8 | 5.5 | 0.78 |
| BaS-HI | 42.7 | 68.8 | 5.5 | 0.7 | 23.1 | 1.9 | 0.96 |
| BaS-HS | 7.0 | 51.6 | 4.0 | 0.5 | 14.8 | 2.1 | 0.93 |
| BaI-PS | 25.4 | 73.6 | 6.9 | (0.6)** | 16.5 | 2.4 | 1.13 |
| BaI-PI | 6.1 | 73.7 | 5.2 | (0.6)** | 18.1 | 2.4 | 0.85 |
| $CO_2$ | 19.4 | 27.3 | - | - | 72.7 | - | - |
| $H_2O$-Soluble | 1.8 | ND | ND | ND | ND | ND | ND |
| Total Yield | 102.4 | 61.5 | 4.7 | | 32.2 | 1.7 | 0.92 |
| Total Recovery | | 95% | 112% | | 130% | 31% | 118% |

*By difference
**Assumed value: due to instrument malfunctioning
ND: Not determined

than four times the amount in Sub-215, the oxygen recovery increased to 130% and the hydrogen recovery increased to 112%. The higher $CO_2$ evolution in this reaction resulted in a greater average H/C ratio of the condensed products than that of Sub-215 products.

The yield and composition of Sub-300 products, Table 3-4, showed variations from the trends observed in Sub-260 and Sub-215. The amount of $CO_2$ evolved remained the same as in Sub-260, while the amount of the $H_2O$-soluble increased by a factor of three. The total product yield, carbon recovery and oxygen recovery decreased substantially, indicating that some product was not recovered. The large amount of the $H_2O$-soluble suggests that the unrecovered material was water soluble species of small molecular size. The average H/O ratio of the condensed product increased beyond that of Sub-260 product. The increased H/C ratio seems to be due to the lost material, which had a high O/C ratio, at least 1.3, based on the carbon and oxygen recoveries.

Results from the three reactions showed that hydrogen incorporation in the products accompanied the oxygen incorporation. Apparently most of the hydrogen and oxygen incorporation took place in Sub-215, and it increased slightly in Sub-260. However, further incorporation in Sub-260 and Sub-300 might not have been detected due to the $H_2O$-soluble lost material.

Table 3-4

YIELD AND ELEMENTAL COMPOSITION OF SUB-300 PRODUCTS

| | Yield % | C % | H % | N% | O %* | Ash % | H/C |
|---|---|---|---|---|---|---|---|
| Dry Coal | 100.0 | 64.9 | 4.2 | 0.6 | 24.8 | 5.5 | 0.78 |
| BaS-HI | 14.2 | 73.7 | 7.0 | (0.6)** | 18.1 | 0.6 | 1.15 |
| BaS-HS | 14.9 | 71.2 | 6.7 | (0.6) | 19.7 | 1.8 | 1.13 |
| BaI-HI | | | | | | | |
| AS | 17.6 | 80.5 | 8.5 | (0.6) | 9.4 | 1.0 | 1.27 |
| AI-PS | 14.7 | 75.5 | 6.6 | (0.6) | 16.3 | 1.0 | 1.04 |
| AI-PI | 3.4 | 80.1 | 5.0 | (0.6) | 13.3 | 1.0 | 0.75 |
| BaI-HS | 1.2 | 73.1 | 6.8 | (0.6) | 18.0 | (1.5)** | 1.12 |
| $CO_2$ | 19.1 | 27.3 | 0 | 0 | 72.7 | 0 | 0 |
| $H_2$-Soluble | 5.6 | 33.2 | 4.1 | - | - | ND | 1.46 |
| Total Yield | 90.7 | 57.0 | 4.7 | | 24.2 | 0.7 | 0.99 |
| Total Recovery | | 88% | 112% | | 97% | 13% | 127% |

*By difference
**Assumed value: due to instrument malfunctioning
ND: Not determined

IR spectra of the feed coal and some product fractions are shown in Figure 3-1. Unlike the coal, two BaS fractions showed a prominent absorption at 1700 $cm^{-1}$ due to the carbonyl group in addition to the strong absorptions at 3600-2500 $cm^{-1}$ due to O-H stretch, 3000-2800 $cm^{-1}$ due to nonaromatic C-H stretch, 1600 $cm^{-1}$ due to aromatic C-C stretch with -O- substituent, and 1500-1000 $cm^{-1}$ due to C-O stretch and nonaromatic C-H bend, which are common to coal-derived liquids or coals. Other fractions, BaI-AS and BaI-PS, had less intense absorptions at 1700 $cm^{-1}$. These carbonyl absorptions are due to carboxylic acids, as evidenced by $CO_2$ evolution and the solubility of the product fractions in basic solutions. Thus the carbonyl groups exist in the feed coal. The origin of the carbonyl groups appears to be mostly esters and some other carbonyl form according to the additions of hydrogen and oxygen to the product, as well as the solution behavior of the product fractions.

The experimental data presented so far indicate that three major reactions have taken place at three different reaction temperatures. The hydrolysis of ester and carbonyl groups was the predominant reaction at 215°C. Decarboxylation was a

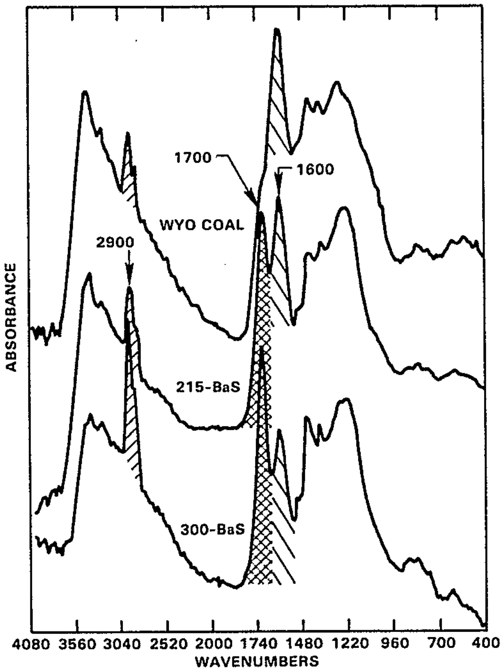

Figure 3-1. IR spectrum of Wyoming coal and products.

major process at 260°C. Another hydrolysis which produced the $H_2O$-soluble material was a major reaction at 300°C. Since no additional $CO_2$ was evolved, it is most likely that ether groups were hydrolyzed at 300°C. This progressive reaction path illustrates the complexity of coal chemistry and the need for carefully controlled liquefaction experiments. The identification of different reactions which took place revealed that different oxygen-functional groups were selectively attacked.

Table 3-5 shows how the composition and yield of the condensed-phase products changed as a result of the oxygen-related reaction steps. The composition and yield were calculated based on 100 carbon atoms of the feed. The differences among the coal and the products at the different reaction temperatures reveal that most hydrogen, 10% of the hydrogen in the feed, was added to the coal at 215°C, while substantial amounts of carbon and oxygen were removed between 260 and 300°C. Consequently, the Sub-300 product had a much higher atomic H/C ratio than the feed, 1.1 vs 0.78, contained 60% less oxygen, and was analyzable in detail. Since the solubilization reaction involves the hydrolysis of different oxygen functional groups, this observation reveals that the Wyoming coal can be

Table 3-5

YIELD AND COMPOSITION OF CONDENSED-PHASE PRODUCT FRACTIONS

| | | Difference | | |
|---|---|---|---|---|
| | | C | H | O |
| Coal | $C_{100}H_{78.0}N_{0.8}O_{28.2}$ | | | |
| | | - 5.3 | + 7.8 | + 0.8 |
| Sub-215 | $C_{94.7}H_{85.8}N_{0.8}O_{29.0}$ | | | |
| | | - 8.1 | + 1.6 | - 8.4 |
| Sub-260 | $C_{86.6}H_{87.4}N_{0.7}O_{20.6}$ | | | |
| | | - 6.8 | - 0 | - 8.9 |
| Sub-300 | $C_{79.8}H_{87.4}N_{0.5}O_{11.7}$ | | | |
| | TOTAL | -20.2 | + 9.4 | -16.5 |

hydrogenated with $H_2O$ instead of $H_2$ or hydrogen-donor solvents as in current liquefaction processes.

The reaction products were further examined by $^1H$-NMR. The spectra of the Sub-300 fractions, Fig. 3-2, show a broad, well-resolved peak with a maximum at 10ppm. The quantitative determination of this acid proton revealed that the ratios of the proton to oxygen atom in the fractions were close to two, as shown in Table 6: almost all oxygen atoms exist in carboxylic groups. The water-soluble fraction, BaS-HS, contains the largest number of carboxylic groups, while the basic-solution insoluble fraction, BaI-AS, contains the smallest number of carboxylic groups.

The spectroscopic data and the elemental balances examined indicate that the oxygen functional groups in the feed coal underwent a drastic change during the NaOH/ethanol/$H_2O$ reaction. The result is a reduction of molecular weight and a large increase in the H/C ratio of the products. The determination of the carboxyl group contents in the Sub-300 fractions revealed that most of the oxygen linkages were cleaved, while nonoxygen structural features of the feed coal remained intact during the solubilization reaction. A similar conclusion, i.e., the conservation of aromatic clusters, has been drawn in the same reaction with a Utah bituminous coal.[1,2] The following structural analysis of the experimental data is intended to provide more information on the stable structures of the coal as well as on the products themselves.

## Structural Parameters of Sub-300 Product Fractions

Although the solubilization product fractions are complex mixtures of numerous components, they can be characterized in terms of average molecular structural parameters to describe their chemical nature and the related chemistry on a

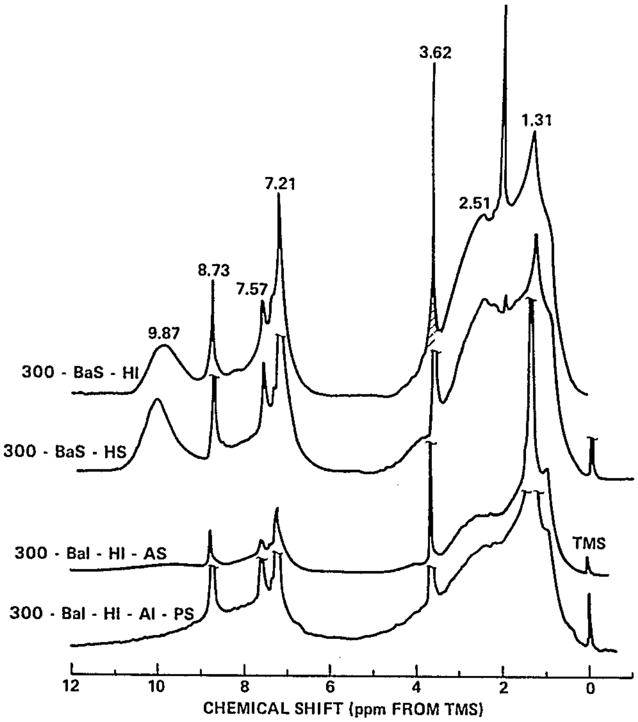

Figure 3-2. Acid protons in Sub-300 fractions.

Table 3-6

OXYGEN AND CARBOXYL GROUP CONTENTS IN SUB-300 FRACTIONS

| Empirical Formula | | M.W. | Number of Carboxyl Groups* | Number Other Oxygens |
|---|---|---|---|---|
| BaS-HI | $C_{48}H_{55}O_{8.6}N_{0.3}$ | 780 | 3.5 | 1.6 |
| BaS-HS | $C_{45.6}H_{51.4}O_{9.9}N_{0.3}$ | 770 | 5.0 | 0.0 |
| BaI-HI-AS | $C_{39.6}H_{50.1}O_{3.7}N_{0.3}$ | 590 | 1.7 | 0.3 |

*From acid protons determined by NMR

molecular level. The usefulness of the average structural parameters depends upon how well the product fractions were separated, and the preparation of the product fractions including their fractionation is a critical step in obtaining the desired information.

To derive molecular information, each solubilized coal product fraction was represented by an average molecule. The characteristics of the average molecule were quantified from various analytical data in terms of structural parameters. The commonly used formulae to calculate structural parameters[1,10] were modified to account for the carbonyl groups observed in the products as listed in Table 3-7. C and H are the numbers of carbon and hydrogen atoms in the empirical formula of an average molecule. $C_c$ represents the number of carbon atoms in carbonyl groups in an average molecule. Hydrogen (H) was divided into five types based on $^1$H-NMR spectra: $H_A$, 5-9 ppm; $H_{2\alpha}$, 2.2-5 ppm; $H_{3\alpha}$, 2.0-2.2 ppm; $H_\beta$, 1.1-2.0 ppm; and $H_\gamma$, 0.0-1.1 ppm. In most cases $H_{3\alpha}$ was included in $H_{2\alpha}$, since the NMR spectra did not show a well-defined separation between these two proton groups.

In the product fractions, the aromaticity and the total number of rings can be calculated by adding a term, $C_c$, to the formulae. However, the positions of the carbonyl groups must be known to calculate the other parameters. For example, whether or not a carboxylic group is attached directly to an aromatic ring makes a large difference in the calculated number for aromatic clusters and aromatic rings in an average molecule. The significance of the structural parameters are illustrated in Figure 3-3.

The structural parameters of the Sub-300 fractions are listed in Table 3-8. The aromaticities of the four fractions were low, ranging from 0.43 to 0.58. This result indicates that the aromaticity of the feed coal should be lower than 0.4, taking into account the carbonyl carbon (nonaromatic) which was removed as $CO_2$. There are several aromatic and hydroaromatic rings in average molecules of these fractions. Nevertheless, these rings are separated by nonaromatic bonds, forming individual aromatic clusters as indicated by the number of aromatic clusters, $N_{cl}$.

The cluster parameters show large differences among the three Sub-300 fractions. BaS-HS was made of single-aromatic-ring clusters, BaI-AS consisted of two-fused-ring clusters and BaS-HI was a mixture of single-ring clusters and two-fused ring clusters, as indicated by cluster size, CS. For example, CS of benzene, naphthalene and anthracene or phenanthrene are 1.0, 2.0 and 3.0, respectively. BaI-PS consisted of four- or more-fused aromatic-ring clusters. There was little evidence of three-fused ring clusters in these fractions. The cluster weights of these fractions increase as CS increases.

Three important observations may be made from the large differences in the cluster parameters among the fractions. First, the separation method to obtain these

## Table 3-7

## FORMULAE FOR STRUCTURAL PARAMETERS WITH SAMPLES CONTAINING C = O GROUPS

Number of Aromatic Carbon Atoms:

$$C_A = C - \frac{1}{2}(H_{2\alpha} + H_{2\beta}) - \frac{1}{3}(H_{3\alpha} + H_{\gamma}) - C_c \tag{1}$$

Fraction of Carbon Atoms which are Aromatic (= Aromaticity):

$$f_A = \frac{C_A}{C} \tag{2}$$

Total Number of Rings:

$$R_T = \frac{2C - H + 2}{2} - \frac{1}{2} C_A - C_c \tag{3}$$

Number of Aromatic Clusters:

$$Ncl = \frac{1}{3}(C_{AP} - \frac{1}{2} C_A) \tag{4}$$

$$C_{AP} = H_A + \frac{1}{2} H_{2\alpha} + \frac{1}{3} H_{3\alpha} + C_c(?) \tag{5}$$

Number of Aromatic Rings:

$$R_A = \frac{C_A - 2Ncl}{4} \tag{6}$$

Number of Naphthenic Rings:

$$R_N = R_T - R_A \tag{7}$$

Cluster Size:

$$CS = R_A/Ncl \tag{8}$$

Cluster Weight:

$$CW = M.W./Ncl \tag{9}$$

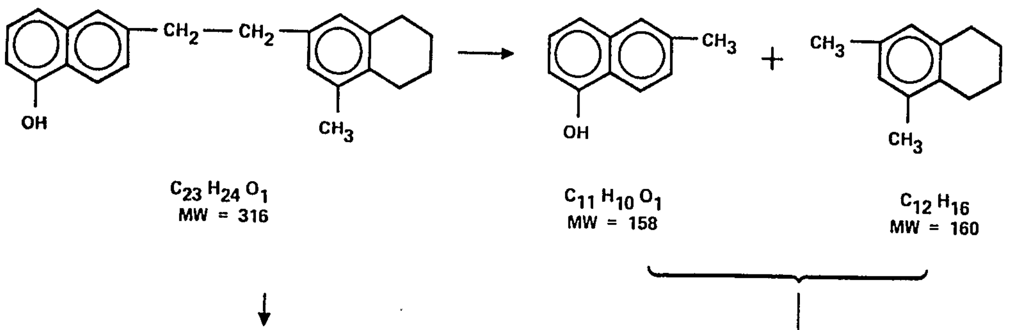

| | | Parameter | |
|---|---|---|---|
| | 0.7 | $f_A$ = CARBON AROMATICITY | 0.7 |
| AVG. MOLECULE | 3 | $R_A$ = NUMBER OF AROMATIC RINGS | 1.5 |
| | 1 | $R_N$ = NUMBER OF NAPHTHENIC RINGS | 0.5 |
| | 4 | $R_T$ = TOTAL NUMBER OF RINGS | 2 |
| | 2 | $N_{Cl}$ = NUMBER OF AROMATIC CLUSTERS | 1 |
| AVG. CLUSTER | 1.5 | CS = CLUSTER SIZE = $R_A/N_{Cl}$ | 1.5 |
| | 158 | CW = CLUSTER WEIGHT = $MW/N_{Cl}$ | 160 |

Figure 3-3. Illustration for structural parameters.

Table 3-8

STRUCTURAL PARAMETERS OF SUB-300 FRACTIONS

| | Yield, Wt% | M.W. | $f_A$ | $R_T$ | $N_{cl}$ | CS | CW |
|---|---|---|---|---|---|---|---|
| BaS-HI | 14.2 | 780 | 0.46 | 7.1 | 2.8 | 1.5 | 280 |
| BaS-HS | 14.9 | 770 | 0.47 | 5.3 | 3.6 | 1.0 | 210 |
| BaI-AS | 17.6 | 590 | 0.43 | 5.3 | 1.8 | 2.0 | 340 |
| BaI-PS | 14.7 | 2100 | 0.58 | 26.1 | 3.7 | 4.8 | 580 |

fractions was effective in apportioning the condensed product according to aromatic cluster size. Second, since it is unlikely that those clusters were altered during their preparation process, the feed coal itself must have consisted of the different aromatic clusters characterized by the cluster parameters. Furthermore, these aromatic clusters seemed to be linked to one another in an orderly manner. For example, single-aromatic-ring clusters in BaS-HS were connected to, on the average, 3.6 other similar clusters as revealed by CS and $N_{Cl}$. In BaI-AS, two-fused-aromatic-ring clusters were connected to, on the average, 1.8 other similar clusters. These structural characteristics of the Sub-300 fractions can be related to the original structures of the feed coal as well as to the potential product distribution resulting from complete liquefaction of the coal.

## Chemical Structure of the Wyoming Coal and Its Liquefaction Potential

Since the Sub-300 product fractions were obtained by selective cleavage of oxygen functional groups as discussed in the first section, the stable structures such as the aromatic clusters and aliphatic linkages remaining in these fractions must be the same as those in the feed coal. Thus the characteristics of the stable structures of Sub-300 fractions are equivalent to those of the coal, and provide information on two important aspects of coal composition, polymeric nature and heterogeneity. The molecules of the coal consist of repeating structural units (such as aromatic clusters) of similar size, although the actual structures of each unit may vary. The coal, however, is a mixture of different polymeric constituents, e.g., the BaS-HS fraction of the coal consisted of small clusters, while the other fractions consisted of larger clusters.

In addition, much information on weak functional groups or linkages of the Wyoming coal is available. The involvement of oxygen functional groups in Sub-215, Sub-260 and Sub-300 reveals that the stable structures like those found in Sub-300 product fractions are held together by oxygen functional groups in the feed coal. Three major functional groups connect the aromatic clusters: ester and carbonyl, ether, and alkyl. Ester linkages have not been considered a major functional group in bituminous or subbituminous coals.[11,12] Our observation of $CO_2$ evolution at 260°C and the addition of hydrogen and oxygen showed that as much as 58% of the oxygen in the coal is in ester and carbonyl groups. The production of more $H_2O$-soluble material at 300°C than at 260°C without $CO_2$ evolution reveals the presence of a substantial amount of ether groups. The remaining linkages in Sub-300 fractions must be alkyl groups, since almost all oxygen atoms in the fractions are in carboxylic groups.

The information on the oxygen functional group distribution was combined with that on the stable structures of the coal to give an overall chemical structural picture of the coal as shown in Fig. 3-4. All these structural features are important for understanding and controlling the liquefaction and upgrading chemistry. In the following discussion, the findings on the chemical structure and reactivity of the Wyoming coal will be used to obtain a potential product distribution upon complete liquefaction of the coal.

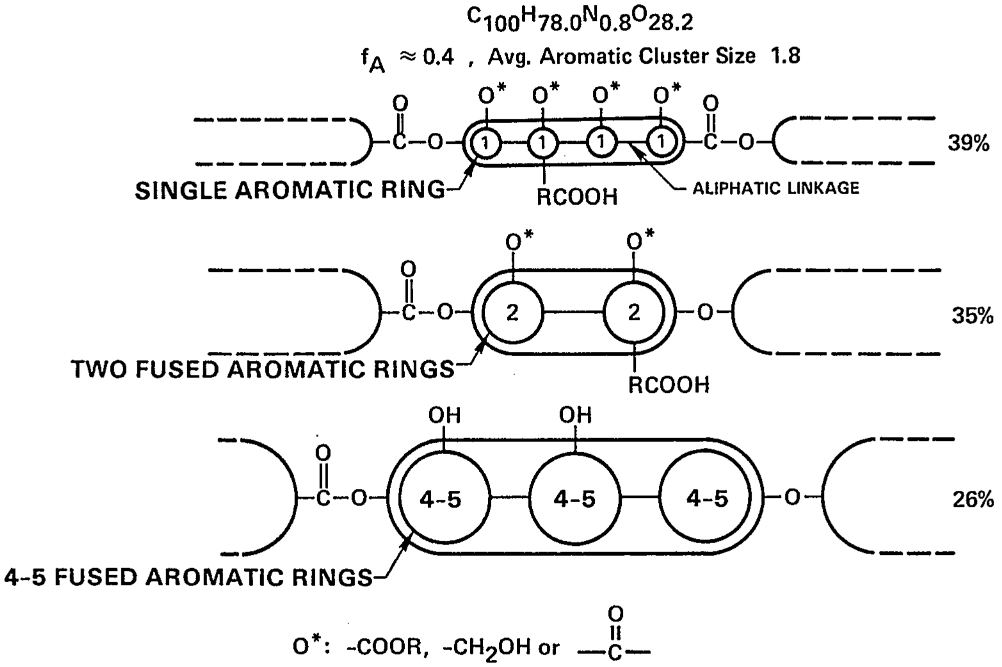

Figure 3-4. Chemical structure of Wyoming No. 1 coal.

Since Sub-300 product fractions retain the stable structures of the coal, structural characteristics of these fractions provide valuable information on potential condensed products which will be formed upon liquefaction of the coal. As shown in Table 3-8, the average molecules of the three Sub-300 fractions, BAS-HI, BaS-HS and BaI-AS, were made of aromatic clusters and nonaromatic linkages. Although the linkages were not cleaved in the NaOH/ ethanol/$H_2O$ reaction at 300°C, they are expected to be cleaved under hydroliquefaction conditions, e.g., at 400° to 450°C. Thus, upon further liquefaction, the average molecule of BaS-HI, which had 2.8 aromatic clusters, will become 2.8 smaller molecules, each having only one aromatic cluster with the average molecular weight, 280.

Similarly, BaS-HS and BaI-AS will become products having average molecular weights of 210 and 340, respectively. Assuming that the carboxyl groups in these fractions will be removed or reduced during liquefaction, all of the new products should be distillable under vacuum, according to our previous observations on the Utah coal.[1,2] In the previous work, a coal-derived product fraction with an average molecular weight larger than 390 was not distillable. In a liquefaction process with a hydrogen-donor solvent, the yield of distillable product from the

Wyoming coal should be at least 52% of the feed according to the yields of BaS-HI, BaS-HS, BaI-AS and $H_2O$-soluble. The yield could be even larger if part of the BaI-PS is included in the product and some carbonyl groups are reduced to methylene groups, $-CH_2-$. The material that was lost in the wash water in the NaOH/ethanol/$H_2O$ reaction will become a gaseous product, e.g., $CH_4$ and $C_2H_6$, under hydrogenation conditions. It was found earlier that 8.2% of the carbon in the coal evolved as $CO_2$ (Table 3-4).

This product distribution is compared to that of a separate liquefaction experiment on the same coal at 450°C with a hydrogenated coal-derived solvent[12] in Table 3-9. The predicted yields of distillate product and $C_1$-$C_3$ gas are very close to those obtained in the hydroliquefaction experiment. The yields of $CO_2$ and CO, however, show a large difference, 8.2% C vs 3.4% C. This difference is due to the dissimilar nature of the NaOH/ethanol/$H_2O$ reaction and the hydrogenative liquefaction, but it does not significantly affect the overall excellent agreement.

Table 3-9

COMPARISON OF THE PRODUCT DISTRIBUTION FROM NaOH-ETHANOL REACTION AND "WYO" LIQUEFACTION

| | NaOH/EtOH Reaction | U. of Wyoming* |
|---|---|---|
| Distillable Product | 52% Wt | 55% Wt |
| $C_1$-$C_3$ Gas | 12% C | 13.1% C |
| $CO_2$ and CO | 8.2% C | 3.4% C |

*Ref. 13

The agreement in the $C_1$-$C_3$ gas yield shows that the gaseous products primarily arise from cleaving the side chains containing oxygen functional groups in the original structure of the coal. This observation indicates that some side chains may be retained in liquid products by not cleaving off as gaseous product: e.g., hydrogenation of $\phi\text{-}\overset{O}{C}\text{-}CH_2CH_3$ to $\phi\text{-}CH_2\text{-}CH_2CH_3$. Recent results from the two-stage catalytic liquefaction of Illinois No. 6 coal revealed such a possibility.[14]

In addition, the structural parameters of Sub-300 product fractions can be used to estimate the number of strong linkages (i.e., nonoxygen or aliphatic linkages) to be cleaved and the amount of hydrogen required to obtain the predicted product distribution. The number of strong linkages in the average molecule of a product fraction is equal to $N_{cl}$-1, where $N_{cl}$ is the number of aromatic clusters in Table 3-8. These linkages are aliphatic, and the clevage and quenching of each linkage under hydroliquefaction conditions require two hydrogen atoms to result in two smaller molecular species: the hydrogen consumption is directly related to the number of aliphatic linkages. Based on this relationship, the amount of hydrogen required in cleaving strong linkages in order to obtain the product distribution in Table 3-8 is 0.3% of the coal. This number compares to 61% in the "Wyo" liquefaction. The difference, 5.7%, represents the amount of hydrogen consumed to cleave or remove oxygen functional groups of the coal in the "Wyo" liquefaction.

## CHEMICAL STRUCTURAL CHARACTERISTICS OF TEXAS LIGNITE

### Formation of the Solubilization Products

The product yields shown in Table 10 reveal that the lignite behaved similarly to the Wyoming subbituminous coal in the solubilization reaction with NaOH/ethanol/$H_2O$. However, the distribution of the products was different. The formation of BaS from the lignite was completed at 215°C, while that from the subbituminous coal continued even beyond 260°C (See Table 3-1). The $CO_2$ evaluation was approximately 50% of that from the subbituminous coal. The amounts of $H_2O$-soluble and lost material increased apparently in a similar manner, but a detailed analysis showed a different trend with the lignite.

Table 3-10

SUCCESSION OF PRODUCT FORMATION (WT% YIELD)

| | Lig-215 | Lig-260 | Lig-300 |
|---|---|---|---|
| BaS-HS | 55.3 | 22.6 | 23.1 |
| BaS-HI | 20.1 | 38.9 | 4.4 |
| BaI-AS | -- | -- | 19.7 |
| BaI-AI-PS | 21.1 | 11.1 | 15.4 |
| BaI-AI-PI | | 11.5 | 8.6 |
| CO as $CO_2$ | 3.5 | 6.6 | 6.9 |
| $H_2O$-Sol | 0 | 0.1 | 4.0 |
| Lost and Error | 0.1 | 9.2 | 17.9 |

Elemental balances indicated that substantial amounts of hydrogen and oxygen were added to the feed, while substantial amounts of carbon and oxygen were removed as $CO_2$ and $H_2O$-soluble material. These changes resulted in different yield and composition of the condensed-phase products at the three reaction temperatures, as shown in Table 3-11. The difference between the lignite and the Lig-215 product shows that 8 hydrogen atoms were added to the feed base on 100 carbon atoms of the feed, while six carbon atoms and one oxygen atom were removed. Between Lig-215 and Lig-260 products, eight carbon atoms and six oxygen atoms were removed from Lig-215 product without any change in the hydrogen content. Between Lig-260 and Lig-300 products, eight hydrogen atoms were added, while ten oxygen atoms were removed with no change in the carbon content. This large amount of removed oxygen accounts for the difference between "lost and error" in Lig-300 and that in Lig-260 in Table 3-10.

Table 3-11
YIELD AND COMPOSITION OF CONDENSED-PHASE PRODUCTS

| | | Difference | | |
|---|---|---|---|---|
| | | C | H | O |
| Lignite | $C_{100}H_{84.6}O_{28.4}$ | | | |
| | | - 5.9 | + 8 | - 1.1 |
| Lig-215 | $C_{94.1}H_{92.6}O_{27.3}$ | | | |
| | | - 8.3 | 0 | - 6.0 |
| Lig-260 | $C_{85.8}H_{92.6}O_{21.3}$ | | | |
| | | 0 | + 8.3 | -10.1 |
| Lig-300 | $C_{85.9}H_{101}O_{11.2}$ | | | |
| | TOTAL | -14.2 | +16.3 | -17.2 |

Taking into account the $CO_2$ evolution and the $H_2O$-soluble formation in Table 3-10, the above differences in yield and composition reveal that hydrolysis and decarboxylation were the main reactions taking place at 215°C. In Lig-260, decarboxylation and $H_2O$-soluble formations were major processes. In Lig-300, the substantial amount of deoxygenation without additional $CO_2$ evolution indicates that dehydration took place. However, the substantial amount of hydrogen addition suggests that reduction of carbonyl or carboxyl groups might have taken place.

In comparison with the Wyoming coal, the hydrolysis accompanying hydrogen and oxygen addition and decarboxylation took place at the same temperatures, 215 and 260°C, respectively. However, the formation of $H_2O$-soluble material took place at the lower temperature, 260°C, with the lignite than at 300°C with the Wyoming subbituminous coal. Another major difference concerns the large amounts of hydrogen addition and oxygen removal without any change in carbon recovery with the lignite; this was not observed with the Wyoming coal. These differences in the reactivity indicate that oxygen functional groups of the lignite are dissimilar to those of the Wyoming coal in their distribution and even in their identities.

Supporting data for the dissimilar distribution of oxygen functional groups are shown in Table 3-12. The hydroxyl and carboxyl group contents in Lig-300 fractions were determined from $^1$H-NMR spectra, elemental composition and molecular weight. Two fractions, BaS-HS and BaS-HI, contained carboxyl groups and hydroxyl groups.

Table 3-12

HYDROXYL AND CARBOXYL GROUPS IN LIG-300 FRACTIONS*

| | Empirical Formula | M.W. | Number of Carboxyl Groups | Number of Hydroxyl Groups |
|---|---|---|---|---|
| BaS-HS | $C_{48.6}H_{55.3}O_{8.2}$ | 770 | 1.4** | 5.5** |
| BaS-HI | $C_{48.9}H_{54.2}O_{9.3}$ | 790 | 2.5** | 4.2** |
| BaI-AS | $C_{37.1}H_{48.0}O_{2.9}$ | 540 | 0 | 2.9 |
| BaI-AI-PS | $C_{126}H_{144}O_{18}$ | 1940 | 0 | 15.7 |

* Based on $^1$H-NMR data.

** All oxygen atoms were assumed to be in carboxyl and hydroxyl groups.

However, the other two fractions did not contain carboxyl groups but rather hydroxyl groups. In contrast, most oxygen of similar product fractions from the Wyoming coal was in carboxyl groups, as listed in Table 3-6. The larger number of hydroxyl groups in these fractions from the lignite supports the possible substantial deoxygenation due to dehydration.

Further structural characteristics of Lig-300 fractions are described in terms of average molecular structural parameters, as shown in Table 3-13. Fractions BaS-HS and BaS-HI are almost the same. An average molecule of each fraction consists of 3.7 aromatic clusters. The cluster size, 1.3, revealed that each fraction is a 70:30 mixture of single- and two-fused ring clusters. The average molecule of BaI-AS consisted of 1.7 aromatic clusters, and the average cluster was a two-fused ring cluster, as indicated by the cluster size, CS. The average molecule of BaI-AI-PS had 4.9 aromatic clusters, and the average cluster was a three-fused ring cluster. The average cluster weight in each of the four fractions ranges

Table 3-13

STRUCTURAL PARAMETERS OF LIG-300 FRACTIONS

| | Yield, % | M.W. | $f_A$ | $R_T$ | Ncl | CS | CW |
|---|---|---|---|---|---|---|---|
| BaS-HS | 23.1 | 770 | 0.55 | 6.7 | 3.7 | 1.3 | 210 |
| BaS-HI | 4.4 | 790 | 0.54 | 6.5 | 3.7 | 1.3 | 210 |
| BaI-AS | 19.7 | 540 | 0.46 | 5.0 | 1.7 | 2.0 | 320 |
| BaI-AI-PS | 15.4 | 1940 | 0.55 | 20.7 | 4.9 | 3.0 | 390 |

from 210 to 390. These structural parameters of Lig-300 fractions can be combined with the information on the oxygen functional groups to construct a chemical structural model of the Texas lignite as we did with the Wyoming subbituminous coal.

## Chemical Structure of the Texas Lignite and Its Liquefaction Potential

Extensive chemical information was derived from the formation of the solubilization products and from the structural characteristics of the product fractions in the previous section. This can be used to determine detailed chemical characteristics of the Texas lignite. The structural parameters of Lig-300 fractions showed the distribution and arrangement of stable structures, i.e., aromatic clusters and aliphatic linkages, of the lignite. Combining the data on the stable structures with those on oxygen functional groups, we constructed an overall chemical structural picture of the lignite as shown in Fig. 3-5. The general arrangement of aromatic clusters, aliphatic linkages and oxygen functional groups is similar to that of the Wyoming coal in Fig. 3-4. Aromatic clusters of a similar size are joined by aliphatic linkages to form a group of aromatic clusters. The aromatic cluster groups are linked to each other by oxygen functional groups. However, major differences from the Wyoming coal pertain to the distributions of the aromatic clusters and oxygen functional groups.

The difference in the distribution of aromatic clusters between the subbituminous coal and the lignite is shown in Fig. 3-6. The two coals contained a similar amount of single- and two-fused ring clusters, 50 wt% of each coal. However, the amount of three-fused aromatic ring clusters was 15% in the lignite, while there were few such clusters in the subbituminous coal. The amount of four- or more-fused-aromatic-ring clusters was 9% in the lignite, while it was 19% in the subbituminous coal.

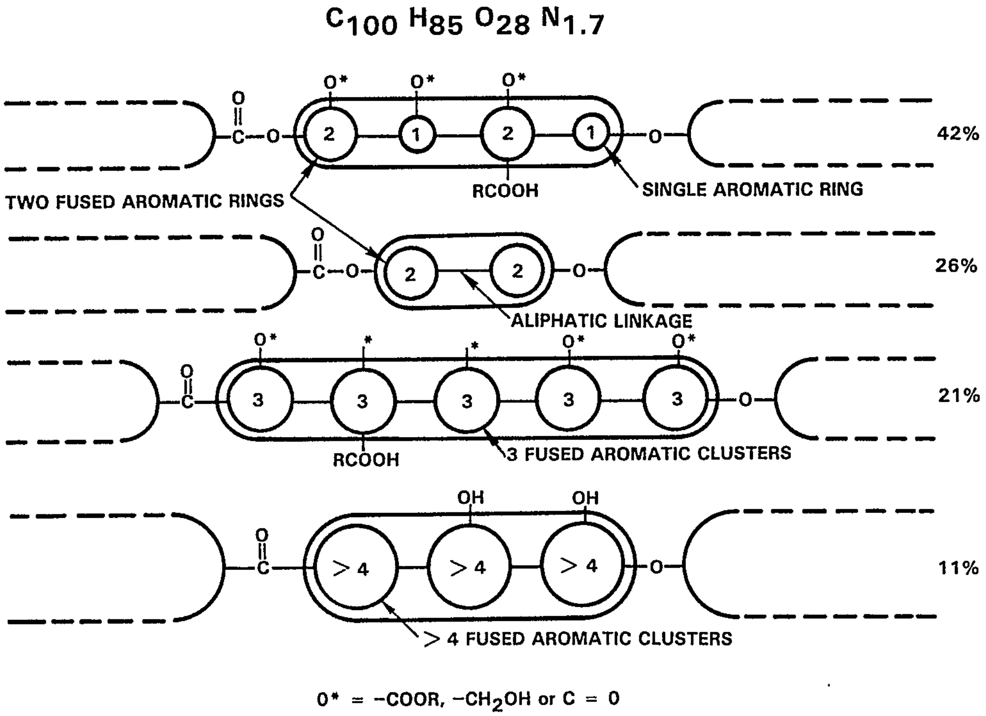

Figure 3-5. Chemical Structure of a Texas Lignite

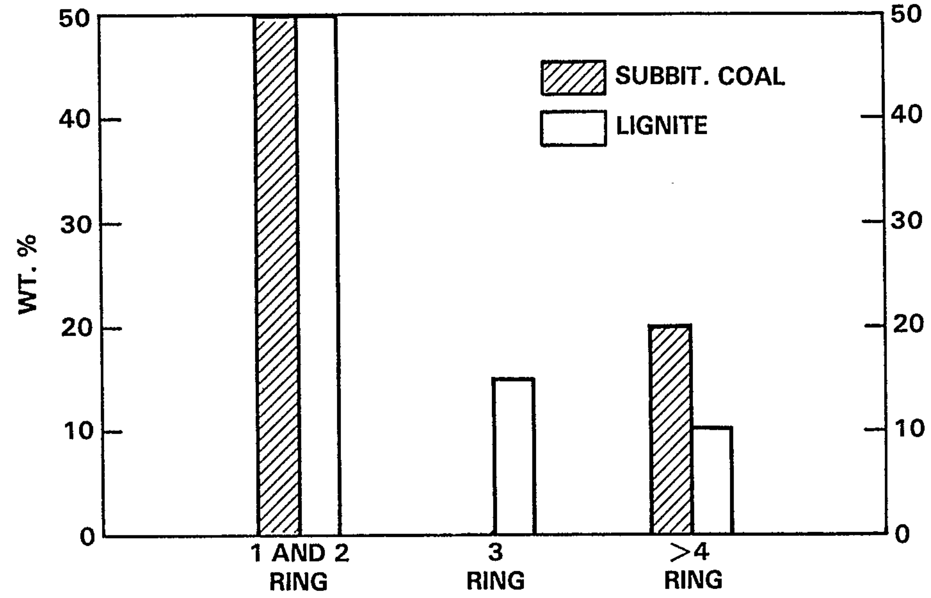

Figure 3-6. Comparison of the Two Coals (Aromatic Ring Composition)

Another major difference between the lignite and the subbituminous coal was the distribution of oxygen functional groups, as shown in Fig. 3-7. The distribution was estimated from the amount of $CO_2$ evolved, the yields of $H_2O$-soluble products, elemental balances, and the molecular weight of the soluble product fractions. Approximately 75% of the oxygen in the lignite was in hydroxyl and ether groups, while the rest of the oxygen was in ester and carbonyl groups. Most of the ester and carbonyl groups seemed to be linkages between aromatic clusters, while most of the ether and hydroxyl groups seemed to be on side chains. In the Wyoming subbituminous coal, approximately 60% of the oxygen was in ester and carbonyl groups. More than half of these functional groups appeared to be linkages between aromatic clusters. The rest of the oxygen was in ether and hydroxyl groups, and most of them were on side chains.

The product distribution in Table 3-10 and structural parameters in Table 3-13 were used to predict the product distribution from the hydroliquefaction of the lignite. The distribution in Table 3-14 was calculated in the same manner as that for the Wyoming coal. The potential yield of distillable product is 60% of the feed. This yield was larger by 15% than that in the subbituminous coal due to the larger amount of three-fused ring clusters in the lignite. Approximately one-half of the amount of three-fused ring clusters was estimated to be distillable because of the large cluster weight.

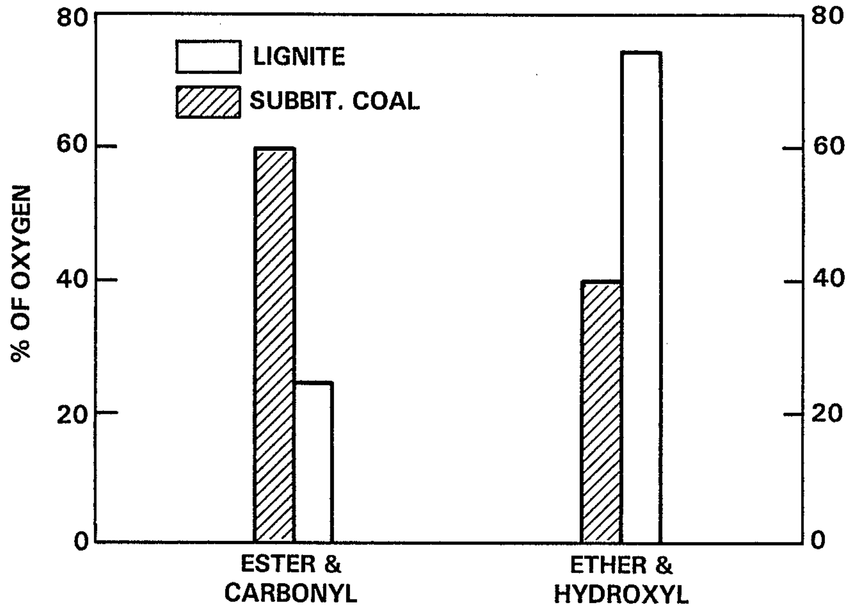

Figure 3-7. Comparison of the Two Coals (Oxygen Function Group Distribution)

Table 3-14

POTENTIAL PRODUCT DISTRIBUTION IN THE LIQUEFACTION OF THE LIGNITE

| | |
|---|---|
| Distillable Product | 60% wt |
| $C_1$-$C_2$ Gas | 10% C |
| $CO_2$ and CO | 4% C |
| Residue | 9% wt |
| $H_2$ consumption | (0.3% wt)* |

* Amount to be required in cleaving alkyl linkages.

The estimated hydrogen consumption required in cleaving alkyl linkages was 0.3 wt% of the feed. This amount was much less than 5% hydrogen consumption in current hydroliquefaction processes, and indicates that substantial improvements in the liquefaction technology is possible.

## CHEMICAL STRUCTURAL CHARACTERISTICS OF ILLINOIS BITUMINOUS COAL

### Formation of the Solubilization Products

Product distributions from the three solubilization reactions are listed in Table 3-15. The conversion based on the pyridine solubility was 88% in Ill-260, 92% in Ill-300 and 94% in Ill-320. As the reaction temperature increased, BAI-AI-PS yield decreased, while that of BAI-AS increased. The $CO_2$ yield was minute at 260°C,

Table 3-15
PRODUCT DISTRIBUTION FROM THE SOLUBILIZATION REACTIONS

| | ILL-260 | ILL-300 | ILL-320 |
|---|---|---|---|
| BaS-HS | 7.2 | 5.1 | 4.2 |
| BaS-HI | 10.4 | 11.9 | |
| BaI-AS | 13.5 | 31.5 | 42.1 |
| BaI-AI-PS | 54.7 | 31.2 | 27.2 |
| BaL-AI-PI | 11.1 | 8.0 | 6.3 |
| CO AS $CO_2$ | 1.0 | 3.0 | 10.1 |
| $H_2O$-SOL | 0.0 | 0.5 | 1.0 |
| LOST & ERROR | 2.1 | 8.8 | 9.1 |

but it increased by three times at 300°C, and another three times at 320°C. The yield of $H_2O$-Sol was minute but increased with the temperature. The lost material including experimental error was 2.1% in Ill-260, increased to 8.8% in Ill-300, and remained at a similar level, 9.1%, in Ill-320. These data on $H_2O$-Sol and the lost material indicate that the large increase in the lost material in Ill-300 is due to $H_2O$-soluble species of small molecular weight that escaped the chloroform extraction. The variation in the lost material between Ill-300 and Ill-320 reveals that insignificant amounts of $H_2O$-soluble small species were produced in Ill-320.

These product distributions are significantly different from those obtained from the low-rank coals. Although the conversions were similarly high at 260° and 300°C, the Wyoming subbituminous coal converted substantially more to base-soluble fractions, $CO_2$, $H_2O$-Soluble, and the lost material. These differences must be due to dissimilar chemical characteristics of the two coals.

Elemental composition of the production fractions from Ill-260 is shown in Table 3-16. The carbon recovery is 97.3% indicating that the product collection and analysis were dependable. Hydrogen and oxygen recoveries were 108% and 123%, respectively. The oxygen recovery is based on an assumption that all pyrite sulfur was removed. This assumption is supported by 5.9% recovery of the ash and a strong odor of $H_2S$ during acidification of the product fractions. The incorporated atomic H/C ratio is close to 2, which reveals that hydrolysis of oxygen functional groups took place during the solubilization. The incorporated hydrogen increased the H/C ratio of the condensed-phase product to 0.89, compared with 0.80 of the feed coal.

Element recoveries and $CO_2$ yield from the three reactions are compared with those from similar reactions of the Wyoming subbituminous coal in Fig. 3-8. With the Wyoming coal, hydrogen and oxygen incorporations were substantial at 215°C as indicated by 110% and 117% recoveries. At 260°C, the oxygen recovery increased further to 130%, while the hydrogen recovery increased slightly to 112%. At 300°C, the oxygen recovery decreased drastically to 97%, while the hydrogen recovery remained the same. The recoveries of hydrogen and oxygen from the Illinois coal reaction at 260°C are similar to those from the Wyoming coal reactions at 215 and 260°C. At 300°C, C, H and O recoveries show similar trends with both the coals. However, there are two major differences in $CO_2$ evolution. The $CO_2$ yields from the Wyoming coal were 12 and 4 times higher at 260 and 300°C respectively than those from the Illinois coal. The $CO_2$ evolution from the

## Table 3-16

## YIELD AND ELEMENTAL COMPOSITION OF ILL-260 PRODUCTS (wt%,daf)

| | Yield | C | H | N | O + S | ASH*1 | H/C |
|---|---|---|---|---|---|---|---|
| Coal | 100 | 76.3 | 5.1 | 1.4 | 17.2*2 | 16.0 | 0.80 |
| BaS-HS | 7.2 | 74.7 | 5.7 | 1.3 | 18.3 | 1.5 | 0.92 |
| BaS-HI | 10.4 | 74.9 | 6.1 | 1.2 | 17.8 | 1.5 | 0.98 |
| BaI-PS | 68.2 | 76.1 | 5.7 | 1.5 | 16.7 | 0.6 | 0.90 |
| BaI-PI | 11.1 | 78.8 | 5.3 | 1.2 | 14.7 | 3.6 | 0.81 |
| $CO_2$ | 1.6 | 27.3 | - | - | 72.7 | - | - |
| Total Yield | 98.5 | 74.3 | 5.5 | 1.4 | 17.3 | 0.9 | 0.89 |
| Recovery | 98.5 | 97.3 | 108 | 100 | 123*3 | 5.9 | 112 |

*1 On Dry Basis
*2 Sulfur Content: Organic 1.9% and Inorganic 3.2%.
*3 Assumption: all pyrite sulfur was removed.

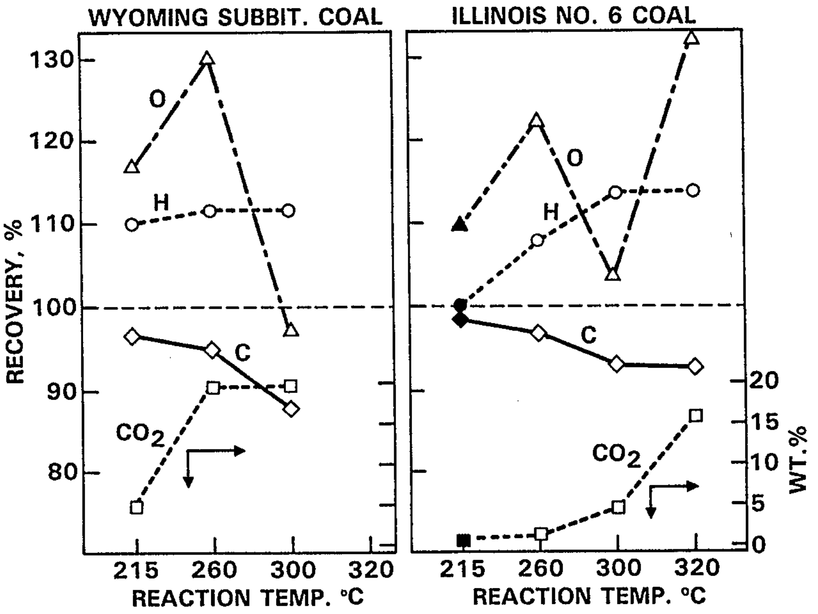

Figure 3-8. Elemental Recoveries and $CO_2$ Yield in the Solubilizaiton Reactions

Wyoming coal was completed at 260°C and remained the same at 300°C, while from the Illinois coal it increased by 3 times at 300°C and another 3 times at 320°C. The similarities in hydrogen and oxygen incorporation indicate that hydrolysis took place in the solubilization reactions of both the coals; differences in $CO_2$ evolution reveal that dissimilar oxygen functional groups in the two coals were hydrolyzed.

Figures 3-9 and 3-10 show IR and $^1$H-NMR spectra of Ill-300 product fractions. The IR spectra show a sharp absorption at 1700 $cm^{-1}$ due to the carbonyl group, in addition to broad strong absorptions at 3600-2500 $cm^{-1}$ due to O-H stretch, and at 1500-1000 $cm^{-1}$ due to C-O stretch. However, the carbonyl absorptions in BaS-HS and BaS-HI are substantially weaker than those in the similar fractions from the Wyoming coal. The carbonyl absorptions in BaI-AS and BaI-AI-PS spectra are much weaker than those in the former two fractions. Also in the $^1$H-NMR spectra of BaS-HS and BaS-HI, there are little absorptions at 10 ppm, compared with well-

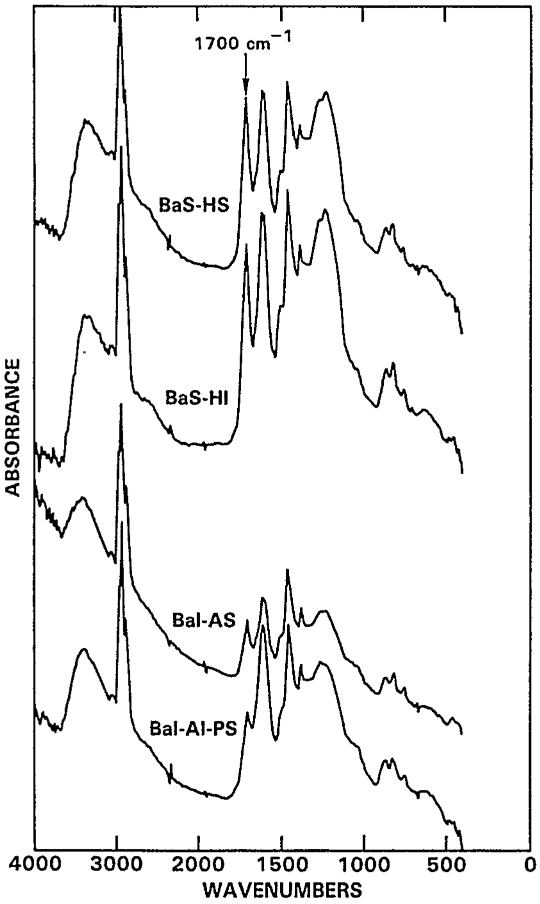

Figure 3-9. IR spectra of Ill-300 fractions.

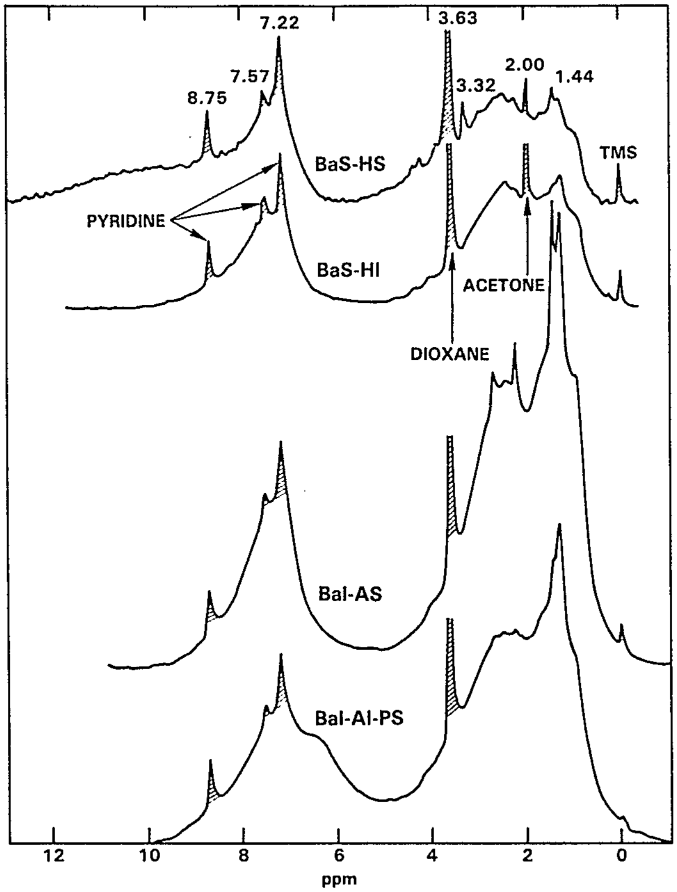

Figure 3-10. $^1$H-NMR spectra of Ill-300 fractions.

resolved strong absorptions in the spectra of similar fractions from the Wyoming coal. The spectra of BaI-AS and BaI-AI-PS show little absorption at 10 ppm. These NMR spectra reveal that almost no acid protons, COOH, exist in the product fractions, and that strong IR absorptions are due to -OH and C-O. These spectroscopic data on the product fractions support the observation from element recoveries and $CO_2$ yield that the oxygen functional groups of the Illinois coal differ from those of the Wyoming coal.

Based on the experimental data presented so far, major possible reactions are listed in Fig. 3-11. Hydrolysis of ester and carbonyl groups takes place around 215°C, followed by a substantial decarboxylation at 260°C. These reactions are minor as indicated by the small amounts of $CO_2$ evolved in Ill-260 and Ill-300, and by weak absorptions due to carbonyl groups in the IR spectra and acid protons in the $^1$H-NMR spectra. Thus, the hydrolysis of ether groups was the major reaction in the solubilization of the Illinois coal at temperatures between 260° and 300°C.

$$\mathrm{RCOOR'} + \mathrm{H_2O} \xrightarrow[\mathrm{EtOH}]{\mathrm{NaOH}} \mathrm{R'OH} + \mathrm{RCOONa} \qquad \leq 215°\mathrm{C}$$

$$\mathrm{RCOR} + \mathrm{H_2O} \xrightarrow[\mathrm{EtOH}]{\mathrm{NaOH}} \mathrm{RCOOH} + \mathrm{RH} \qquad \leq 215°\mathrm{C}$$

$$\mathrm{RCOOH} \xrightarrow[\mathrm{EtOH}]{\mathrm{NaOH}} \mathrm{RH} + \mathrm{CO_2} \qquad 215°\mathrm{C} - 260°\mathrm{C}$$

$$\mathrm{R\text{-}O\text{-}R} + \mathrm{H_2O} \xrightarrow[\mathrm{EtOH}]{\mathrm{NaOH}} \mathrm{ROH} + \mathrm{ROH} \qquad 260°\mathrm{C} - 300°\mathrm{C}$$

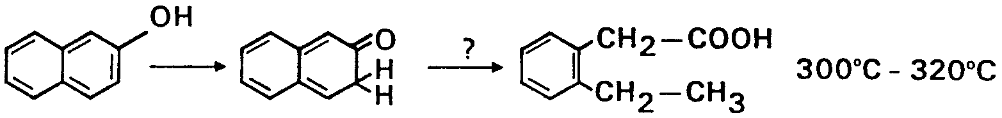

Figure 3-11. Important reactions in coal solubilization.

The large increase in decarboxylation at temperatures between 260 and 320° is unique to the bituminous coal. Since the Ill-300 product contained no significant amount of carboxylic groups according to IR and NMR analysis, the large amount of $CO_2$ in Ill-320 was derived most likely from phenols that can ketonize readily under basic conditions.[15]

These major reactions during the solubilization indicate that oxygen functional groups are attacked selectively: thus, aliphatic and aromatic structures remained intact. In other words, aliphatic linkages and aromatic clusters in the solubilization product should be the same as those of the feed coal. We will examine these stable structures in the next section.

Specific reactions involving oxygen functional groups formed the condensed-phase products. In Fig. 3-12, the yields and compositions of the products from the three reactions are compared based on the stoichiometry of 100 carbon atoms of the feed. The differences between the coal and Ill-260 product show that 2.7 carbon atoms were removed from the coal, while 6.4 hydrogen atoms and 2.1 oxygen atoms were added.

The differences between Ill-260 and Ill-300 products reveal that additional 5.9 carbon and 4.0 oxygen atoms were removed from the Ill-260 product, while additional 4.7 hydrogen atoms were added. Comparison of Ill-300 and Ill-320 products indicates that additional 4.6 carbon and 4.2 oxygen atoms were removed from the Ill-300 product while only 0.7 hydrogen atoms were removed. In total, 13.2 carbon and 6.1 oxygen atoms were removed from the coal, while 10.4 hydrogen atoms

| YIELD AND COMPOSITION BASED ON 100 C-ATOMS | | | | DIFFERENCE | | |
|---|---|---|---|---|---|---|
| | | | | C | H | O |
| COAL | $C_{100}$ | $H_{80.2}$ | $O_{13.8}$ | | | |
| | | | | -2.7 | +6.4 | +2.1 |
| ILL-260 | $C_{97.3}$ | $H_{86.6}$ | $O_{15.9}$ | | | |
| | | | | -4.3 | +4.7 | -4.0 |
| ILL-300 | $C_{93.0}$ | $H_{91.3}$ | $O_{10.9}$ | | | |
| | | | | -6.2 | -0.7 | -4.2 |
| ILL-320 | $C_{86.8}$ | $H_{90.6}$ | $O_{6.7}$ | | | |
| | | | TOTAL | -13.2 | +10.4 | -6.1 |
| | | | NET REACTION | $+5.2\ H_2O - 12\ CO$ | | |

Figure 3-12. Condensed-phase product composition.

were added to form the Ill-320 product. Since the hydrogen was supplied by the hydrolysis, the total change is equivalent to the addition of 5.2 $H_2O$ molecules and the removal of 12 carbon and oxygen atoms. The hydrogen from $H_2O$ was retained in the product, while oxygen in the coal was removed as $CO_2$. This observation shows that the Illinois bituminous coal can be hydrogenated with $H_2O$ instead of $H_2$ or hydrogen-donor solvents as used in current liquefaction processes.

## Chemical Strucural Characteristics of Ill-300 Product Fractions

To derive molecular structural information, each soluble fraction from Ill-300 was represented by an average molecule. The characteristics of the average molecule were quantified in terms of structural parameters as we did with Sub-300 in Section 3. The structural parameters of Ill-300 fraction are listed in Table 3-17. Molecular weight and the total number of rings, $R_T$, of the first three fractions are similar, but those of the last fraction are much larger. Carbon aromaticity of these fractions ranges from 0.6 to 0.7. The last three parameters provide very useful information on the molecular structure of these fractions. $N_{cl}$ dislcoses that the average molecules of the fractions are made of 2.3 to 6.9 aromatic clusters. These aromatic clusters are connected to each other by aliphatic linkages, since most oxygen linkages were cleaved during the solubilization as discussed in the previous section.

Table 3-17

STRUCTURAL PARAMETERS OF Ill-300 FRACTIONS

| | Yield,% | M.W. | $f_A$ | $R_T$ | $N_{c1}$ | CS | CW |
|---|---|---|---|---|---|---|---|
| BaS-HS | 5.1 | 740 | 0.70 | 7.5 | 4.1 | 1.5 | 180 |
| BaS-HI | 11.9 | 770 | 0.65 | 8.8 | 3.3 | 2.0 | 240 |
| BaI-AS | 31.5 | 620 | 0.59 | 7.7 | 2.3 | 2.2 | 270 |
| BaI-AI-PS | 31.2 | 2350 | 0.68 | 29.8 | 6.9 | 3.3 | 340 |

The cluster parameters, CS and CW, reveal large differences among the four fractions. The cluster size, CS, shows that BaS-HS is composed of a mixture of single-ring and two-fused-ring aromatic clusters, BaS-HI and BaI-AS consist of mostly two-fused-ring aromatic clusters, and BaI-AI-PS consists of mostly three-fused-ring aromatic clusters. The cluster weights, CW, of these fractions increase as the cluster size increases.

These structural characteristics of the Ill-300 fractions can be related to the original structures of the feed coal, as well as to the potential product distribution in a complete liquefaction of the coal, which will be discussed in the next section.

## Chemical Structural Model of the Illinois Coal and Its Liquefaction Behavior

A molecular structural model, Fig. 3-13, of the Illinois coal was constructed using the data on the stable structures and oxygen functional groups. One- and two-fused aromatic clusters are joined by aliphatic linkages to make a group of small aromatic clusters. Three-fused aromatic clusters make a group of medium aromatic clusters: on the average, seven clusters are connected to each other by aliphatic linkages. Four- or more-fused aromatic clusters are joined to themselves by aliphatic linkages to make a group of large aromatic clusters. The small, medium, and large clusters constitute 56%, 36%, and 8%, respectively, of the coal. Each group of aromatic clusters, small, medium, and large, is connected to others by oxygen functional groups, i.e., mostly ether linkages.

The arrangement of aromatic clusters and aliphatic linkages is similar to those of the low-rank coals. The Illinois coal, however, contains a large amount of three-fused aromatic clusters, compared with a negligible amount in a Wyoming

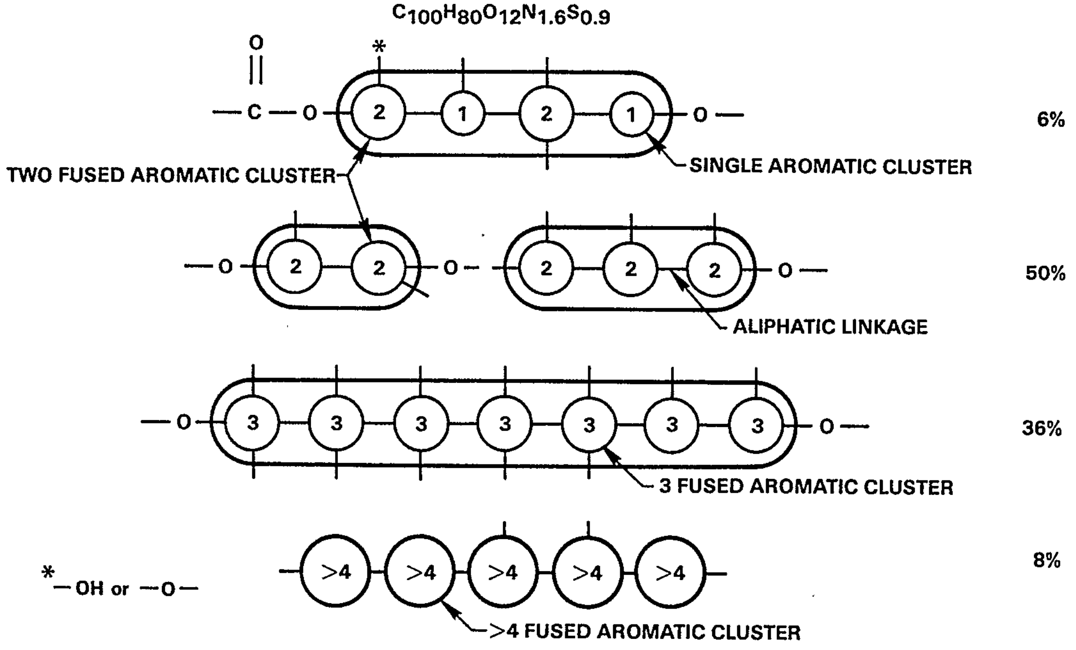

Figure 3-13. Chemical structure of an Illinois coal.

subbituminous coal as shown in Fig. 3-14. Also, the distribution of oxygen functional groups, Fig. 3-15, is substantially different between the two coals due to higher oxygen and ester group contents in the Wyoming coal.

The structural data on the condensed-phase product and the information on oxygen functional groups were used to predict the product distribution and hydrogen consumption in the hydroliquefaction of the coal. Table 3-18 shows the predicted values together with recent liquefaction data from the Advanced Coal Liquefaction R&D Facility at Wilsonville, Alabama.

Although an identical sample of the Illinois coal used at Wilsonville was not examined in this study, the overall agreement between the predicted values and the liquefaction data is reasonable. The predicted distribution reveals that the distillable product yield at the Wilsonville plant was significantly lower than the potential yield by 20% in 1985 and 10% in 1986, taking into account the hydrogen added to the total product. Accordingly, the residue yields were higher than the predicted value.

The predicted $C_1$-$C_3$ gas yield is close to the Wilsonville yield, since the value based on the carbon is similar to that based on the weight in this case. The predicted yield of $CO_2$ and CO will become 4 to 6% on weight basis, which agrees

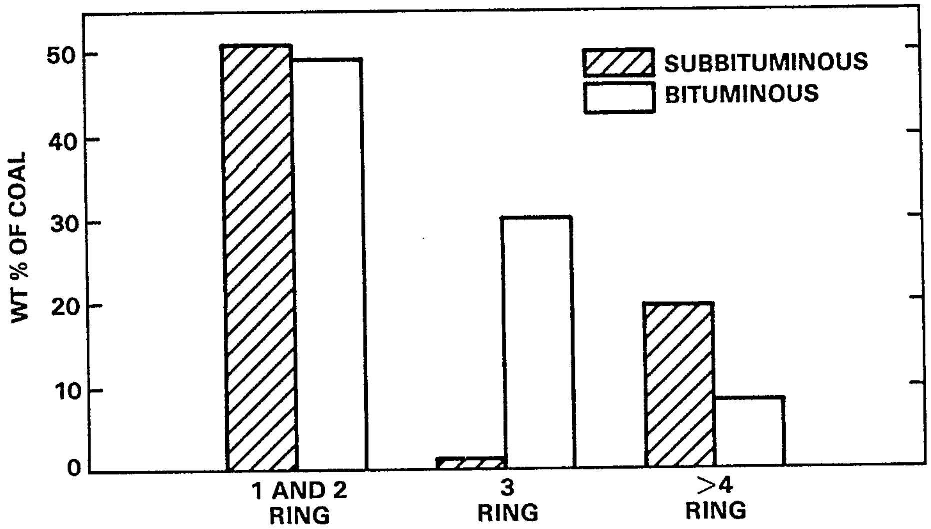

Figure 3-14. Aromatic cluster composition of the two coals.

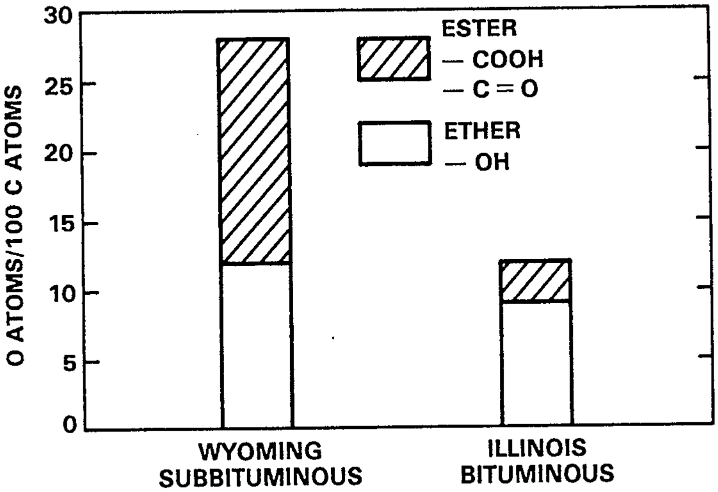

Figure 3-15. Oxygen Functional Group Distribution in the Two Coals

well with the Wilsonville yield. This agreement in gaseous product yields indicates that the gaseous products were derived from ester and carbonyl groups and side chains containing oxygen functional groups as the characterization data of the coal revealed. On the other hand, the agreement indicates that the processing conditions at the Wilsonville plant were mild, and little $C_1$-$C_3$ gas was produced from aliphatic side chains containing no oxygen functional groups.

The estimated hydrogen consumption required in cleaving aliphatic linkages is 0.4%wt of the feed coal. This amount is much less than 6.8% hydrogen consumption in the current hydroliquefaction process, and indicates that substantial improvements in the liquefaction technology is possible by reducing the hydrogen consumption.

Table 3-18

PREDICTED YIELDS VS LIQUEFACTION DATA:
ILLINOIS NO. 6 BITUMINOUS COAL (BURNING STAR)

| | NaOH/EtOH | Wilsonville* | |
|---|---|---|---|
| | Reaction | 1985 | 1986 |
| Distillable Product | 70%wt | 62%wt | 70%wt |
| $C_1$-$C_3$ Gas | 7%C | 6%wt | |
| $CO_2$ and CO | 2%C | 6%wt(?) | |
| Residue | 8%wt | 25%wt** | 15%wt |
| H2 Consumption | (0.4%wt)*** | 6.1%wt | 6.8%wt |

*Lamb, et al, EPRI Contractor's Conf. on Clean Liquid and Solid Fuels, 1985, and Hollenack, Illinois Coal Development Board Technical Meeting, 1986.
**Includes coal product rejected to ash concentrate.
***Amount to be required in cleaving alkyl linkages.

# CONCLUSION

An Illinois bituminous coal, a Wyoming subbituminous coal and a Texas lignite were characterized and compared in terms of the distribution and arrangement of aromatic clusters, linkages, and oxygen functional groups. The characterization consisted of solubilization of each coal by reactions with NaOH/ethanol/ $H_2O$, solvent fractionation of the product, and detailed analyses of the product fractions to obtain average molecular structural parameters.

The three coals behaved similarly in the solubilization reactions, but each coal showed its peculiar reactivity. Elemental balances and other analytical data revealed that the oxygen functional groups of each coal were attacked selectively and the complex coal structure underwent an orderly, definable diminution. The solubilization reaction proceeded in a well-defined manner: hydrolysis of ester and carbonyl groups at 215°C, decarboxylation at 260°C, and another hydrolysis or dehydration/hydrogenation at 300°C. Thus, the reaction resulted in the addition of hydrogen from $H_2O$ to the soluble product and the removal of oxygen as $CO_2$. The solubilization reaction takes place at a higher temperature as the rank of a coal increases. $CO_2$ production was the highest from the subbituminous coal at temperatures between 215° and 300°C, while it was the lowest from the bituminous coal. Nevertheless, $CO_2$ production from the bituminous coal increased substantially with the reaction temperature between 260° and 320°c; the two low-rank coals did not show this trend.

The arrangement of aromatic clusters and oxygen functional groups were similar in the three coals. Two to four aromatic clusters of a similar size were linked to each other by alkyl C-C bonds, making a chain of aromatic clusters. Two or more of these chains were connected to each other by ester and ether groups. The size of aromatic clusters ranged from single ring to five-fused ring clusters.

Major differences between the three coals were in the distributions of aromatic clusters, aliphatic side chains, and oxygen functional groups. The lignite and bituminous coals contained fewer large aromatic clusters than the subbituminous coal, although the three coals contained similar amounts of single- and two-fused ring aromatic clusters. The amount of aliphatic chains containing an oxygen functional group ranged from 7% to 12% of carbon in the coals. More than 70% of the oxygen in the lignite was in hydroxyl and ether groups, while the rest of the oxygen was in ester and carbonyl groups. In the subbituminous coal, 60% of the oxygen was in ester and carbonyl groups, and the rest was in ether and hydroxyl groups. Most of the oxygen functional groups were on side chains. Most of the oxygen in the bituminous coal was in the form of ether and hydroxyl groups.

These structural data were related to the liquefaction behavior of each coal. The predicted distribution of liquefaction products from the subbituminous coal agreed closely with experimental values in an independent liquefaction study. According to the predicted distribution, the lignite has 15% more potential yield of distillable product than the subbituminous coal. The predicted product distribution from the Illinois bituminous coal revealed that the distillate yield at the Wilsonville plant was lower by 10% than the potential yield.

For the three coals, the amount of hydrogen required to cleave aliphatic linkages should be 0.3% of feed, compared to the 5 to 7% used in current hydroliquefaction processes. This indicates that more than 90% of the hydrogen consumption is due to deoxygenation and the production of gaseous species. Our observation of the reactions between $H_2O$ and oxygen functional groups indicated that a major fraction of oxygen in these coals can be removed without consuming molecular hydrogen. Thus, the chemistry of oxygen functional groups can play a major role in substantial improvements of the liquefaction technology.

# REFERENCES

1. Chung, K.E., Ph.D. Thesis, University of Utah (1980).
2. Anderson, L.L., Chung, K.E., Pugmire, R.J. and Shabtai, J. in New Approaches in Coal Chemistry, Blaustein, B.D., Bockrath, B.C. and Friedman, S., Eds., ACS Symp. Series 169, 223 (1981).
3. Chung, K.E., Anderson, L.L. and Wiser, W.H., preprints, Div. of Fuel Chem., ACS 24(3), 243 (1979).
4. Chung, K.E., Goldberg, I.B. and Ratto, J.J., "Chemical Structure and Liquefaction Reactivity of Coal," EPRI AP-4995, Final Report, Vol. 1, Jan. 1987.
5. Wender, I., Catal. Rev.-Sci. Eng. 14 (1), 97 (1976).
6. Chung, K.E., Anderson, L.L. and Wiser, H.H., Fuel 58, 849 (1979).
7. Ross, D.S. and Blessing, J.E., Fuel 58, 433, 438 (1979).
8. Winans, R.E., Hayatsu, R., McBeth, R.L., Scott, R.G., Moore, L.P. and Studier, M.H., Prepr. Div. Fuel Chem., ACS 24 (2), 196 (1979).
9. Makabe, M., Hirano, Y. and Ouchi, K., Fuel 57, 289 (1978).
10. Chapter XXII in Reference (10); Clutter, D.R., Petrakis, L., Stenger, R.L. Jr. and Jensen, R.K., Anal. Chem. 44 (8), 1395 (1972); Kanda, N., Itoh, H., Yokoyama, S. and Ouchi, K., Fuel 57, 677 (1978).
11. Van Krevelan, D.W., Coal, Elsevier Publishing, NY (1961).
12. Ruberto, R.G. and Croanuer, D.C., Chapter 3 in Organic Chemistry of Coal, Larsen J.W., Eds., ACS Sym. Series 71 (1978).
13. Silver, H.F., Corry, R.G. and Miller, R.L. Coal Liquefaction Studies, EPRI, AP:-2779, Final Report (December 1982).
14. MacArthur, J.B., Comolli, A.G. and McClean, J.B., "HRI's Two-Stage Catalytic Coal Liquefaction Program," 9th Annual EPRI Contractors' Conference on Coal Liquefaction, May 1984.
15. Forsen, S. and Nilsson, M., Chapter 3 in The Chemistry of the Carbonyl Groups, J. Zabicky, ed., Interscience Pub., 1970.

## Section 2

# STRUCTURAL STUDIES ON A WYODAK SUBBITUMINOUS COAL
# THE POTASSIUM - CROWN ETHER REACTION

R. Narayan and S. L. Huang

Purdue University

# ABSTRACT

Detailed K-CE reaction studies as a continuation of our efforts on the gentle dismantling of the coal to produce soluble coal oligomers amenable to chemical and spectroscopic analysis, is presented. A modified work-up procedure for the K-CE reaction, incorporating a THF extraction step for the alkali solubles, gave total THF soubles of 31%. Further corroborating evidence for polymethylene groups as pendant side chains and linkages joining coal clusters in the coal macromolecule is documented. A possible biogenesis scheme for the formation of polymethylenes is offered. Detailed NMR studies identified carboxyl groups(~COOH) as a major oxygen functionality along with dioxy aromatic structures. Molecular weight studies of the soluble fractions depicts a coal macromolecule as comprised of coal clusters of polymethylene compounds with molecular weight Mn = 400-600 and Mw = 1400-1980 , dioxy-carboxy coal oligomers of molecular weight_Mn = 500-1000 & Mw = 1450-3350, and a polar hydrocarbon fraction with Mn = 900-1300 and Mw = 4000 linked by K-CE cleavable linkages.

## INTRODUCTION

In this paper we report on the continuation of our studies on the structure of a wyodak subbituminious coal. The approach involves using a site specific reagent namely potassium - crown ether (K-CE) to gently dismantle the coal macromolecular structure at room temperature and atmospheric pressure. This resulted in the formation of soluble chunks of coal oligomer fragments which are now amenable to detailed chemical and structural analysis.In previous work, we have shown that the K-CE reagent dismantles the coal macromolecule to produce soluble coal oligomers. Fifty percent of the wyodak coal is soluble in THF and alkali-fractions, with the alkali soluble fraction accounting for 90% of the total solubles.A total solubility of 70% is obtained after successive K-CE reactions. The formation of large amounts of alkali soluble material indicates that the K-CE reagent has cleaved linkages in coal resulting in the formation of phenolic and carboxylic coal fragments. Based on IR, NMR, Field Ionization Mass Spectral (FIMS) analysis and Tandem Mass Spectrometry (MS/MS) analysis of the alkali soluble fraction, one, two and three rings dihydroxy aromatics / dihydroxy aromatic precursors (precursors like hydroxyethers or diether aromatics) and their alkyl analogs i.e C-1, C-2, C-3, ... C-5, C-7 alkyl hydroxy aromatics have been identified as major structural units comprising the coal macromolecule. Using a Periodate - Borohydride reaction sequence , we corroborated the presence of dioxy aromatics and identified quinonoidal groups in the coal.(See Figure 1.).

These findings indicating the presence of dihydroxy aromatics / dihydroxy aromatic precursors as major oxygen functional units in the coal is significant because dihydroxy aromatics are not substantial constituents of coal liquefaction products or pyrolysis products. Therefore dihydroxy aromatics were never seriously considered as major structural units of the coal macromolecule. These dihydroxy aromatics and their alkyl analogs do not evolve until a temperature of 300°C is reached during the mass spectroscopy analysis. Thus, suggesting that thermal rupture of the large molecular weight coal oligomers of the alkali soluble fraction was responsible for the production of these alkyl substituted dihydroxy aromatics detected in the FIMS and MS/MS. Analysis of the THF-1 fraction by IR, proton and carbon NMR showed the presence of polymethylene groups i.e. $\sim(CH_2)_n\sim$ which are present as pendant chains on aromatic rings and/or linkages joining coal cluster units.

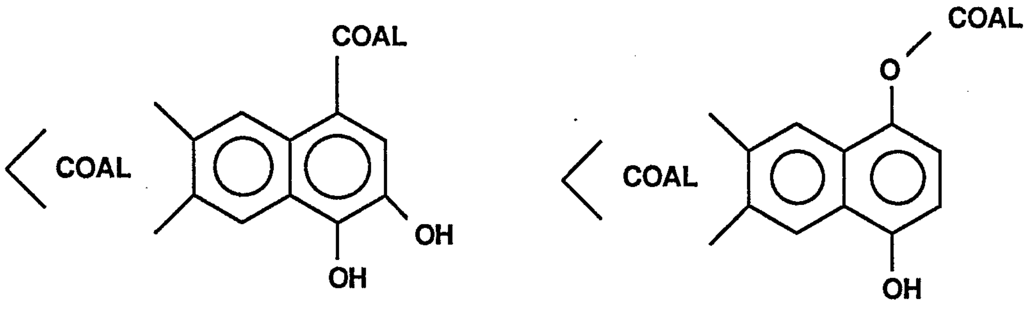

**Dihydroxy aromatics** **Dihydroxy aromatic precursor**

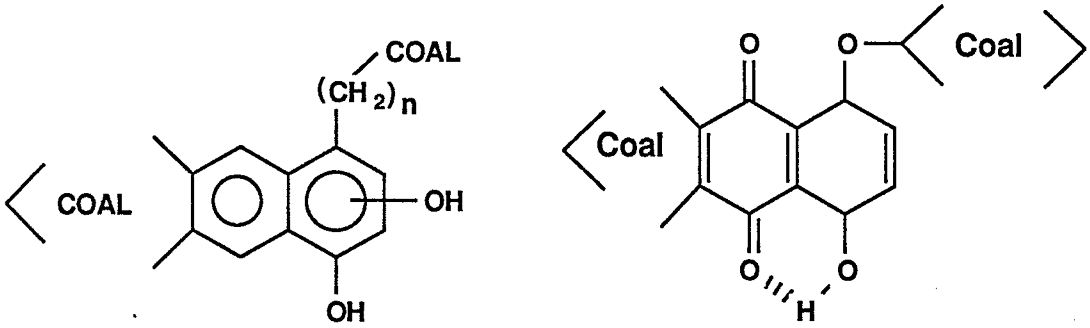

**Alkyl dihydroxy aromatics** **Hydrogen Bonded Quinonoid Structure**

Figure 1. Basic Structural Units

In this paper we report on more detailed K-CE reaction studies including a modified work-up procedure for the reaction, and the extension of the K-CE reaction to a wyodak coal from the Argonne Premium Coal Sample Bank.

## PRESENT RESULTS AND DISCUSSION

### SOLUBILITY STUDIES - POLYMETHYLENE LINKAGES IN COAL.

A modified work-up procedure for the reaction mixture, incorporating a THF extraction of the alkali soluble coal oligomers was adopted as shown in Figure 2.

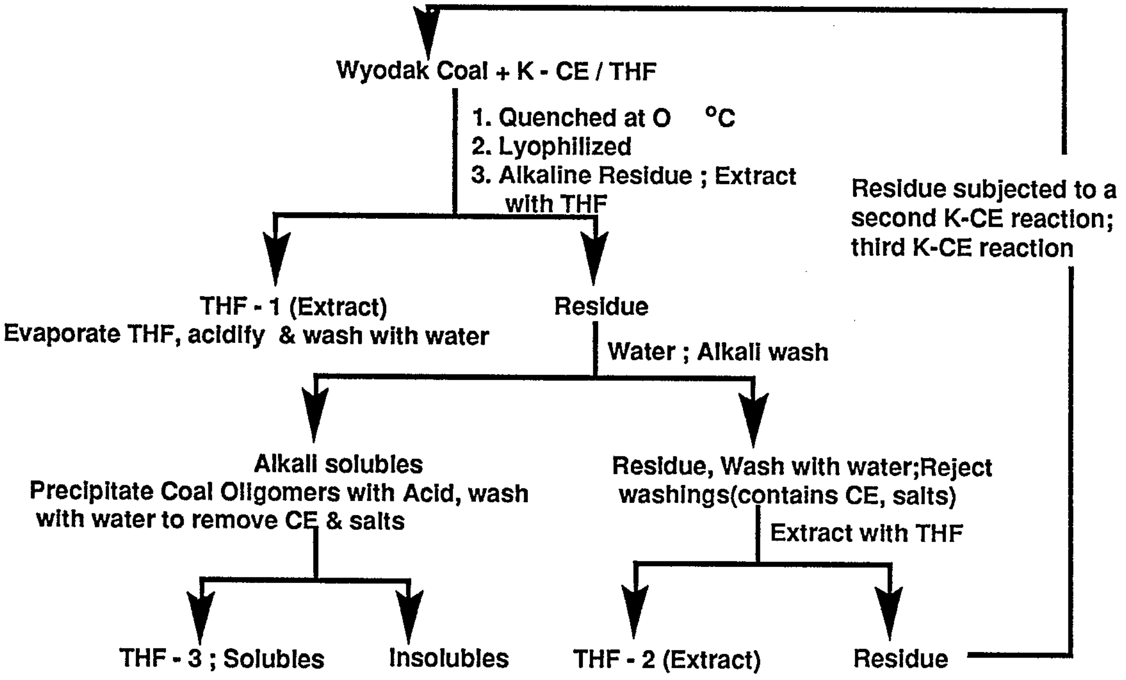

Figure 2. Work-up Procedure for the Coal-K-CE Reaction

The precipitated coal oligomers from the alkali soluble fraction were subjected to a THF extraction and more than 50% of the material were THF extractable. Table 1 gives the solubility data of two independent runs confirming the reproducibility of our results. Table 2 shows the THF extractability of the precipitated alkali soluble coal oligomers after first and second K-CE reaction. It was interesting to note that the THF extractability of the alkali soluble coal oligomers from the second K-CE reaction was higher than the first K-CE reaction.During the second K-CE reaction, a higher percentage reduction of the polar groups of the coal structure , such as aromatic hydroxyl to a less polar dihydro-ketone group accounts for the higher THF solubility.

Table 1

SOLUBILITY OF K-CE TREATED COAL

| REACTION | THF-1 | ALKALI SOLUBLE | THF-2 | TOTAL SOLUBLES |
|---|---|---|---|---|
| H4-22 | 2.8% | 44.8% | 3.0% | 50.6% |
| H4-37 | 0.4% | 47.9% | 3.8% | 52.1% |

Table 2

THF EXTRACTABILITY OF ALKALI SOLUBLE COAL OLIGOMERS

| REACTION | THF SOLUBLE | THF-INSOLUBLE |
|---|---|---|
| H4-22<br>(1st. K-CE Rxn) | 58.3% | 56.7% |
| H4-33<br>(2nd.K-CE Rxn) | 70.7% | 25.4% |

Increasing the concentration of solvated electrons in the reaction by using more crown ether increased the amount of THF-1 fraction 3- to 6-fold as shown in Table 3.

Table 3

EFFECT OF SOLVATED ELECTRON CONCENTRATION ON SOLUBILITY

| K:CE mole Ratio | Reaction time | THF-1 (%) | Alkali soluble (%) | THF-2 (%) |
|---|---|---|---|---|
| 5:1 | 4 days | 2 | 59 | 5 |
| 3:1 | 20 hrs | 6 | 40 | 3 |
| 2:1 | 20 hrs | 12 | 35 | 4 |

* The percent solubility is sum total of two K:CE reactions. The ratio of K:Coal was 3:1 for all the reactions.

The proton and carbon NMR spectrum of these fractions are identical to the earlier reported spectra for the THF-1 fraction , which would mean that the major component is the polymethylene compounds i.e ~ $(CH_2)_n$ ~. The enhanced THF solubility is at the expense of alkali solubility which decreases. This means that the increased electron concentration has promoted more cleavage reactions and polymethylene groups that are attached to coal clusters in alkali soluble fractions or in the residue are being cleaved and are now extractable in the THF-1 fraction. (Figure 3).

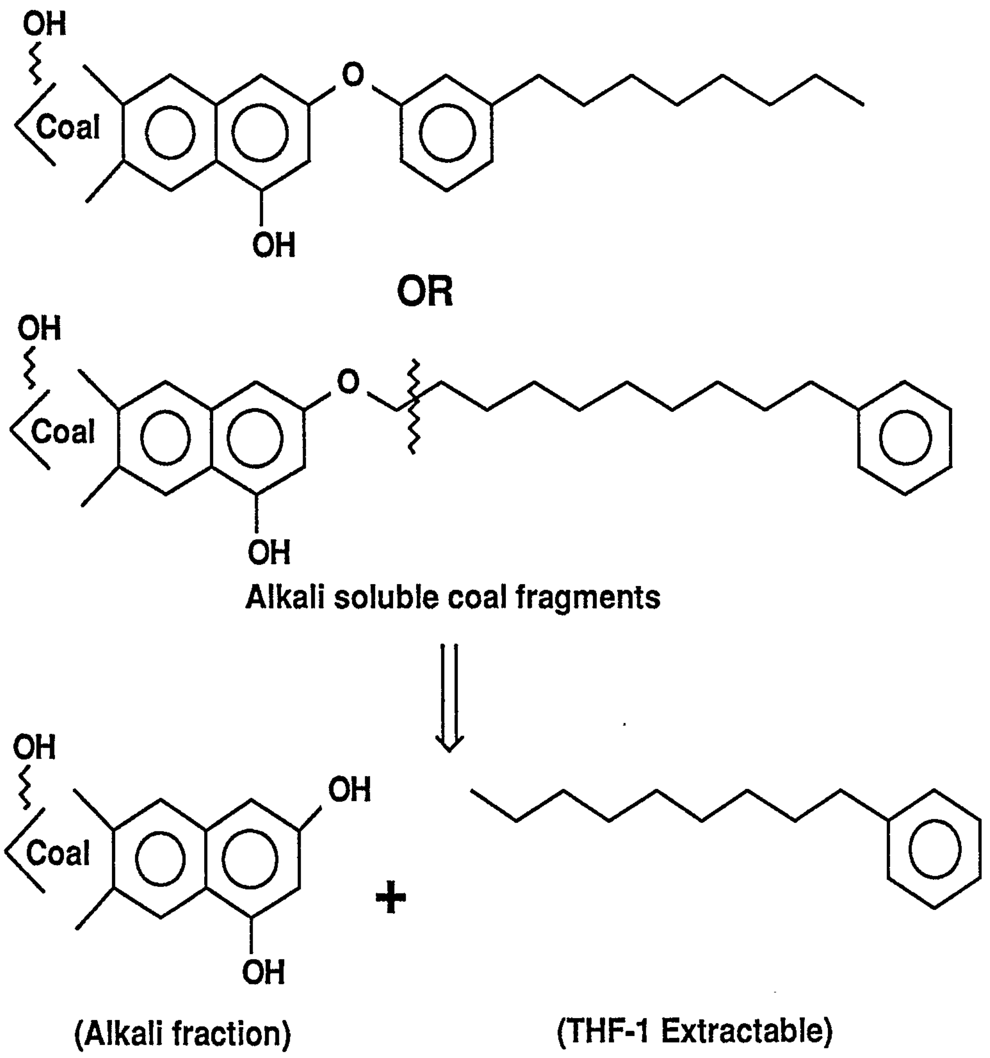

Figure 3. Mechanism for Enhanced THF-1 Extract Yields Using Concentrated Solution of Electrons

Thus, polymethylene groups are present as pendant sidechains and as linkages joining coal clusters in the coal macromolecule. They are definitely not present merely as trapped molecules as is generally perceived. These results nicely corroborates the FIMS and MS/MS analysis of the alkali soluble fraction, wherein C-1, C-2, C-3, ...C-5, C-7 alkyl dihydroxy aromatics were identified.

## Biogenesis of Polymethtylene Linkages in Coal

Carotenoids could be the possible biological precursor for these polymethylene compounds in the coal. Thus, gamma carotene during early diagenesis through microbial intervention, in a manner similar to that described on the biodegradation of acrylic isoprenoids by *pseudomonas* species first undergoes clipping of the methyl groups attached to the carbon chain. During continued maturation in a reducing environment, the alkene chains are hydrogenated and catagenic aromatization of the cyclic ring takes place to give a $C_{33}H_{52}$ polymethylene chain crosslinked aromatic. (Figure 4) This would have a molecular weight of 448 and H/C ratio of 1.5, which is identical to that obtained for the THF-1 extract.

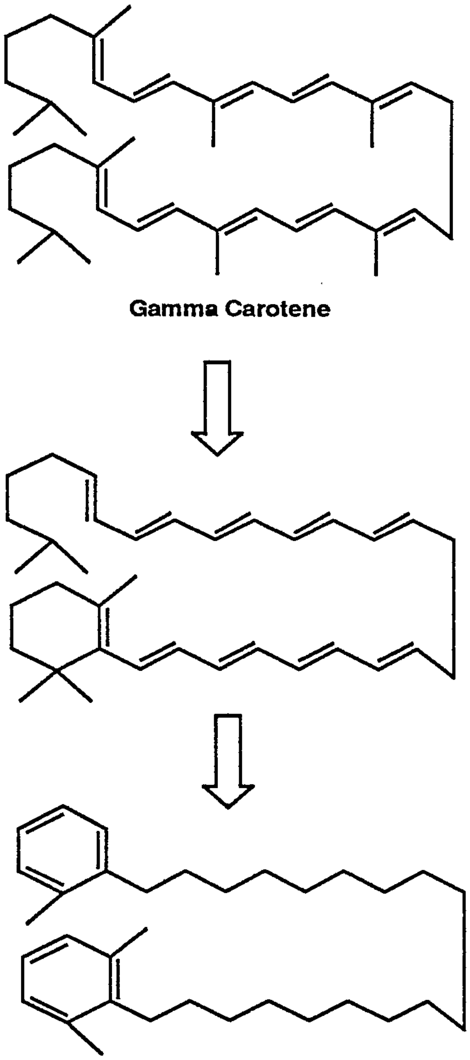

Figure 4. Biogenesis of Polymethylene Crosslinks in Coal

## K-CE REACTION WITH A PRISTINE WYODAK COAL(ARGONNE PREMIUM COAL SAMPLE.

In order to ensure that our results with the EPRI supplied Wyodak coal was representative of that coal, the K-CE reaction was performed on a **pristine** wyodak coal sample from the Argonne Premium Coal Sample Bank. Table 1 lists the percent solubility obtained after K-CE reaction. A smaller coal particle size (-20 mesh to -100 mesh) increased the amount of alkali solubles obtained by two fold, although the amount of THF-1 and THF-2 fractions did not change significantly. Table 2 gives the amount of THF extractable obtained from the precipitated alkali soluble coal.

Table 4

PERCENT SOLUBILITY OF COAL AFTER K-CE REACTION

| Reaction | THF-1 | Alkali soluble | THF-2 | Total |
|---|---|---|---|---|
| One K-CE (-20 mesh) | 7 | 25 | 2 | 34 |
| Total of two K-CE(-20 mesh) | 9 | 29 | 6 | 44 |
| One K-CE (-100 mesh) | 4 | 47 | 2 | 53 |

Table 5

THF SOLUBILITY OF ALKALI SOLUBLES AND TOTAL THF SOLUBILITY OF COAL

| Reaction | % THF Solubility of Alkali Soluble | Total % THF solubility Includes THF-1 & THF-2 |
|---|---|---|
| Unreacted Coal | – | 1.5 - 5 |
| First K-CE(-20 mesh) | 55 | 24 |
| Second K-CE(-20 mesh) | 72 | 15 |
| First K-CE(_100 mesh) | 53 | 31 |

IR's, NMR spectra of the various fractions are identical to that obtained from the EPRI coal. The solubility data are also similar and therefore data analysis from either coal are representative of the wyodak subbituminous coal. An important point to be noted from Table 2 is that a total THF solubility of 31% by weight of the original coal is obtained after one K-CE reaction, as compared to a THF extract yield of only 1.5-5% from the untreated coal.

## NMR STUDIES

The proton NMR spectrum (Figure 5a) of the alkali-soluble fraction showed signals due to the phenolic protons (5-7 ppm or 8.5-11 ppm) and carboxylic protons (8.5-11 ppm). Classical methylation of the alkali soluble coal with Dimethyl Sulfate gave a methylated coal which precipitated from the alkaline solution.

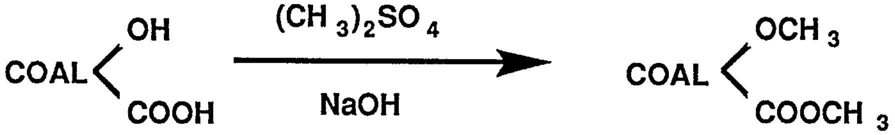

The $^1$H NMR spectrum (Figure 5b) of the methylated coal sample showed the disappearance of the phenolic and carboxylic proton signals and the appearance of a broad signal at 3.8 - 4.2 ppm due to the ~OCH$_3$ protons. This is readily observed on seeing the difference spectrum (Figure 5c) which shows only the broad hump due to the ~OCH$_3$ protons. $^{13}$C NMR spectrum of the methylated coal (figure 6) showed distinct signals at 55 and 52 ppm which can be readily attributed to the carbon resonances of ~OCH$_3$ and COOCH$_3$ respectively.Figure 7 shows the carbon spectrum of the methylated coal after the second K-CE reaction. Again one can readily see the 55 & 52 ppm resonances of ~OCH$_3$ ~COOCH$_3$. Both spectra are very similar except for one striking difference. The 100-120 olefinic carbon resonance band is much more stronger in the spectra of the second K-CE reaction product than the first. This implies that during the second K-CE reaction of the coal more aromatic rings are being reduced to dihydro

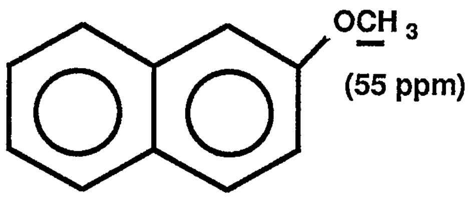

2-methoxynapthalene

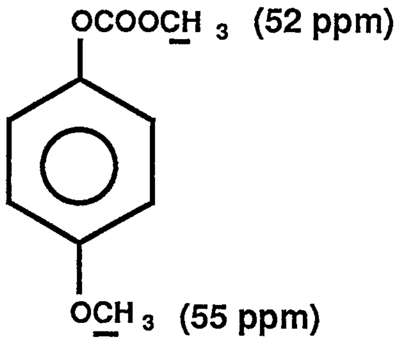

methyl-4-methoxybenzoate

a) Wyodak Coal - Alkali Soluble

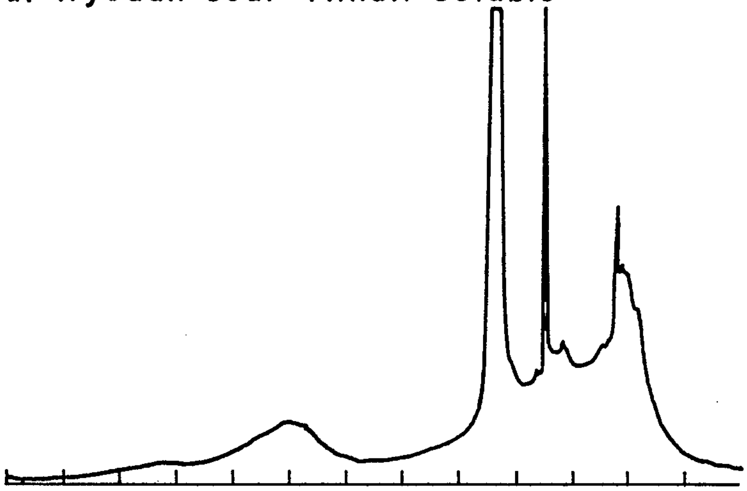

b) Wyodak Coal-Methylated Alkali Soluble

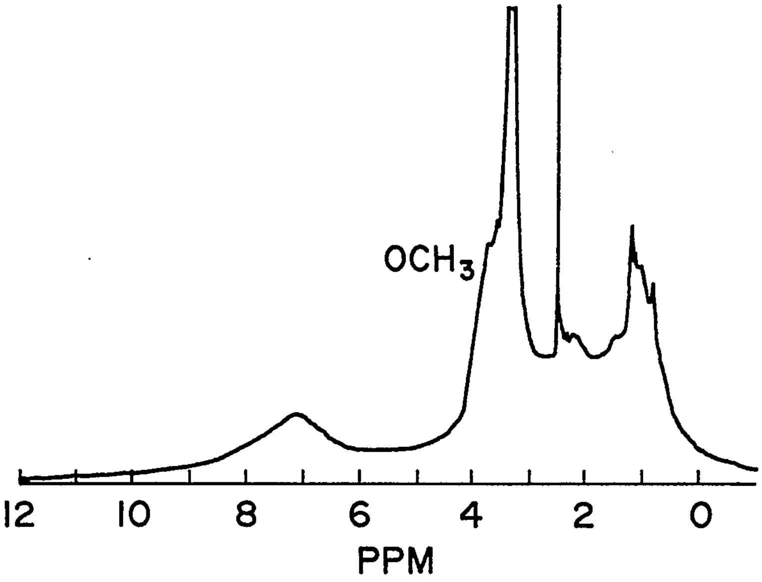

c) Spectrum B Minus Spectrum A

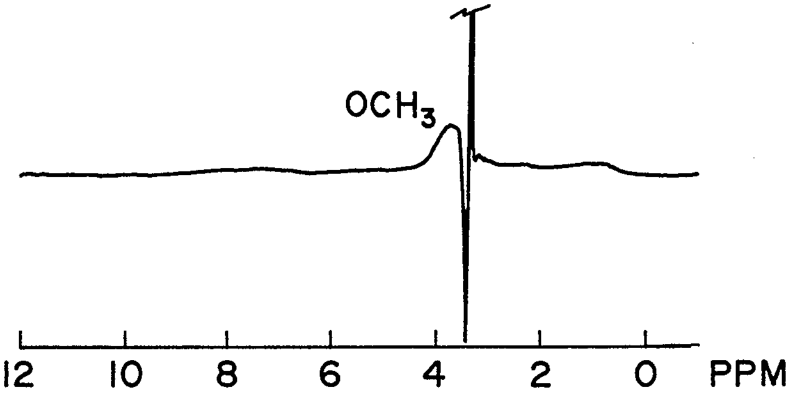

Figure 5. 470 MHz $^1$ NMR Spectra of Alkali Soluble Coal Oligomers

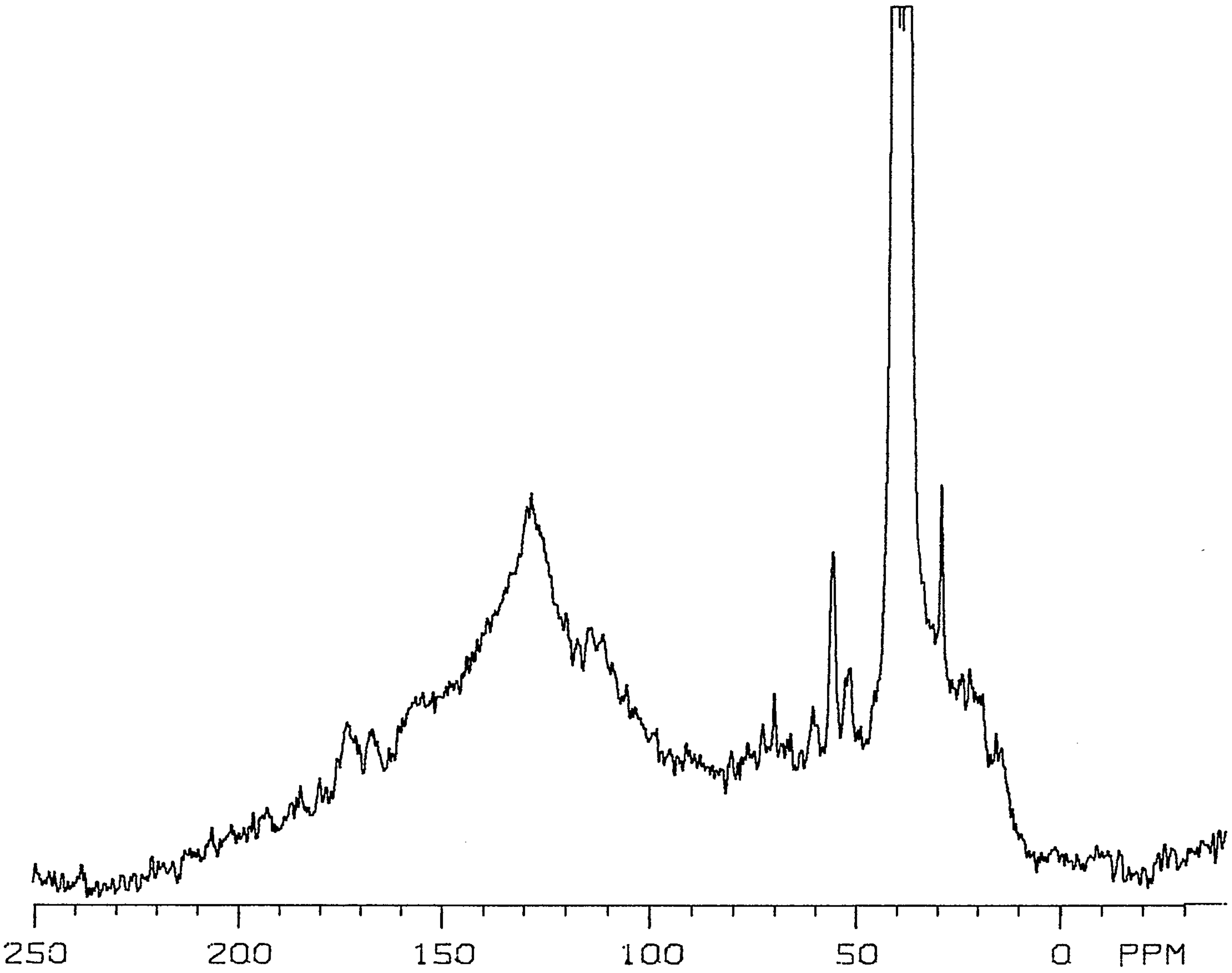

Figure 6. 200 MHz $^{13}$C NMR Spectrum of Alkali Soluble - Methylated Coal, First K-CE Reaction

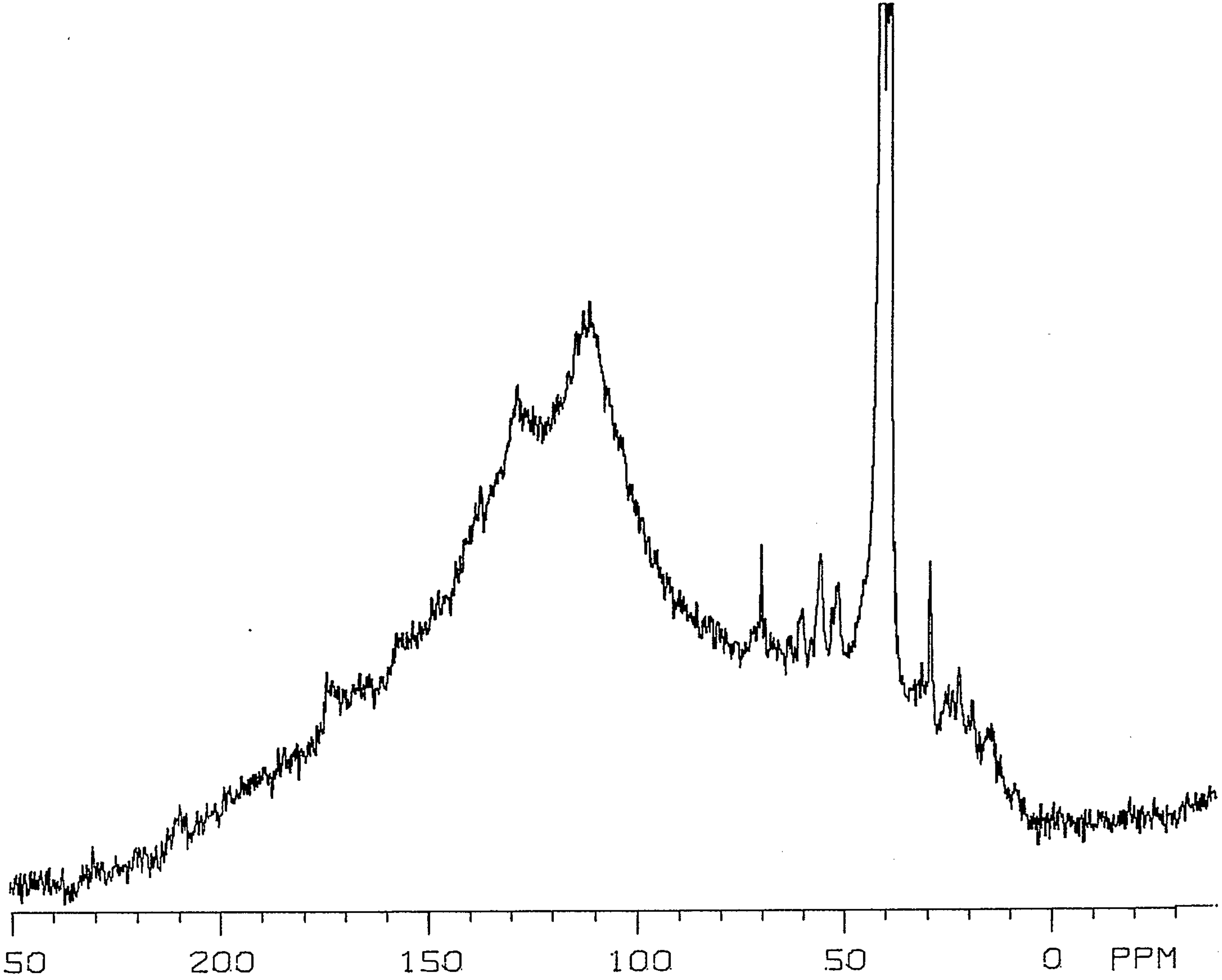

Figure 7. 200 MHz $^{13}$C NMR Spectrum of Alkali Soluble - Methylated Coal, Second K-CE Reaction

and tetrahydro ring systems. $^{13}C$ NMR spectra of model compounds 2-methoxynaphthalene and methyl-4-methylbenzoate established that the 55 ppm signal is due to the $OCH_3$ carbon resonance and the 52 ppm signal is due to the $COOCH_3$ carbon resonance, i.e $^{13}C$ NMR of the methylated coal was obtained using gated decoupling without NOE and adding chromium acetyl acetonate as a relaxing reagent, to quantitate the peak intensities at 55 ppm and 52 ppm. (Figure 8). The ratio of the 55 ppm peak to the 52 ppm peal was 3:2, that is for every 3 phenolic groups in the alkali soluble coal fraction, there was 2 carboxyl groups. Extrapolating to the starting coal macromolecule, these results suggest that for every three phenolic / ether groups (ether cleavage by the K-CE reagent would contribute to the phenolic groups in the alkali soluble coal fraction) there are two carboxyl group. Thus, along with ethers/phenolics (present as dioxy aromatics) carboxyl groups (**~COOH**) are a major oxygen functionality in the wyodak coal.

Figure 9 shows the $^{13}C$ NMR spectra of the alkali soluble fraction in NaOD/$D_2O$ after successive K-CE reactions. A distinctive broad signal at 170-180 ppm is seen in all the spectra corroborating the presence of **~COOH** groups. Broad signals appeared at 0-50 ppm and 100-160 ppm due to the aliphatic and aromatic carbons respectively. The spectra are similar suggesting that the same type of oligomer fragments are being released during successive K-CE reactions.

## MOLECULAR WEIGHT STUDIES

The molecular weights/molecular weight distribution of the various coal oligomer fractions obtained from the coal-K-CE reaction is an important parameter because it allows to piece together the composition of the macromolecular structure of the coal. Thus, molecular weights of the coal oligomer fragments would establish the size of the aromatic clusters being held together by K-CE cleavable linkages. Table 6 lists the molecular weights obtained for the various fractions by Size Exclusion Chromatography using polystyrene standards.

Thus, the coal macromolecule may be envisioned as comprised of coal clusters of molecular weight Mn = 400-600 and Mw = 1400-1980 polymethylene compounds, dioxy-carboxy coal oilgomers of molecular weight Mn = 500-1000 & Mw = 1450-3350, and a second hydrocarbon fraction containing few

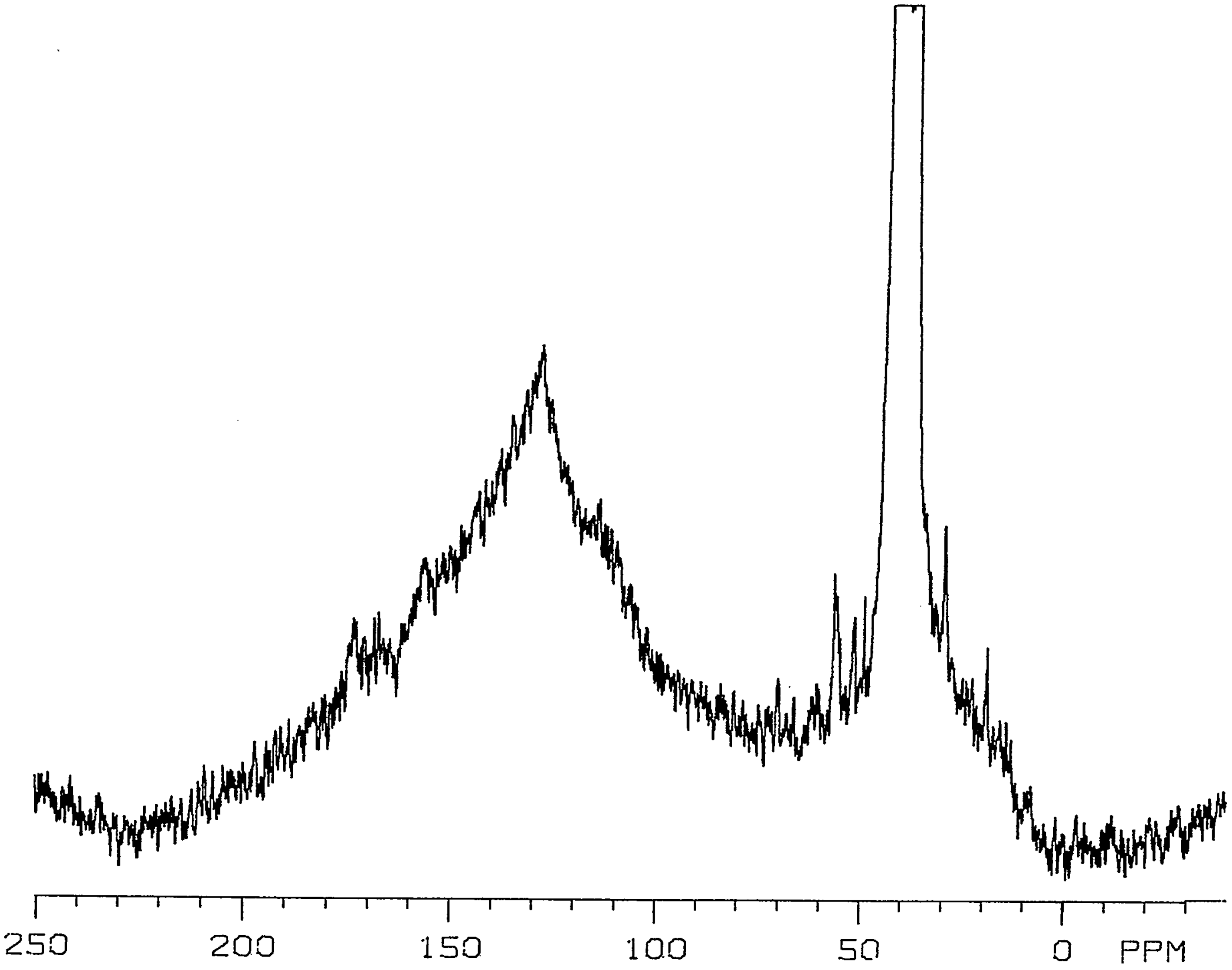

Figure 8. 200 MHz $^{13}C$ NMR Spectrum of Alkali Soluble - Methylated Coal, With Gated Decoupling and No NOE

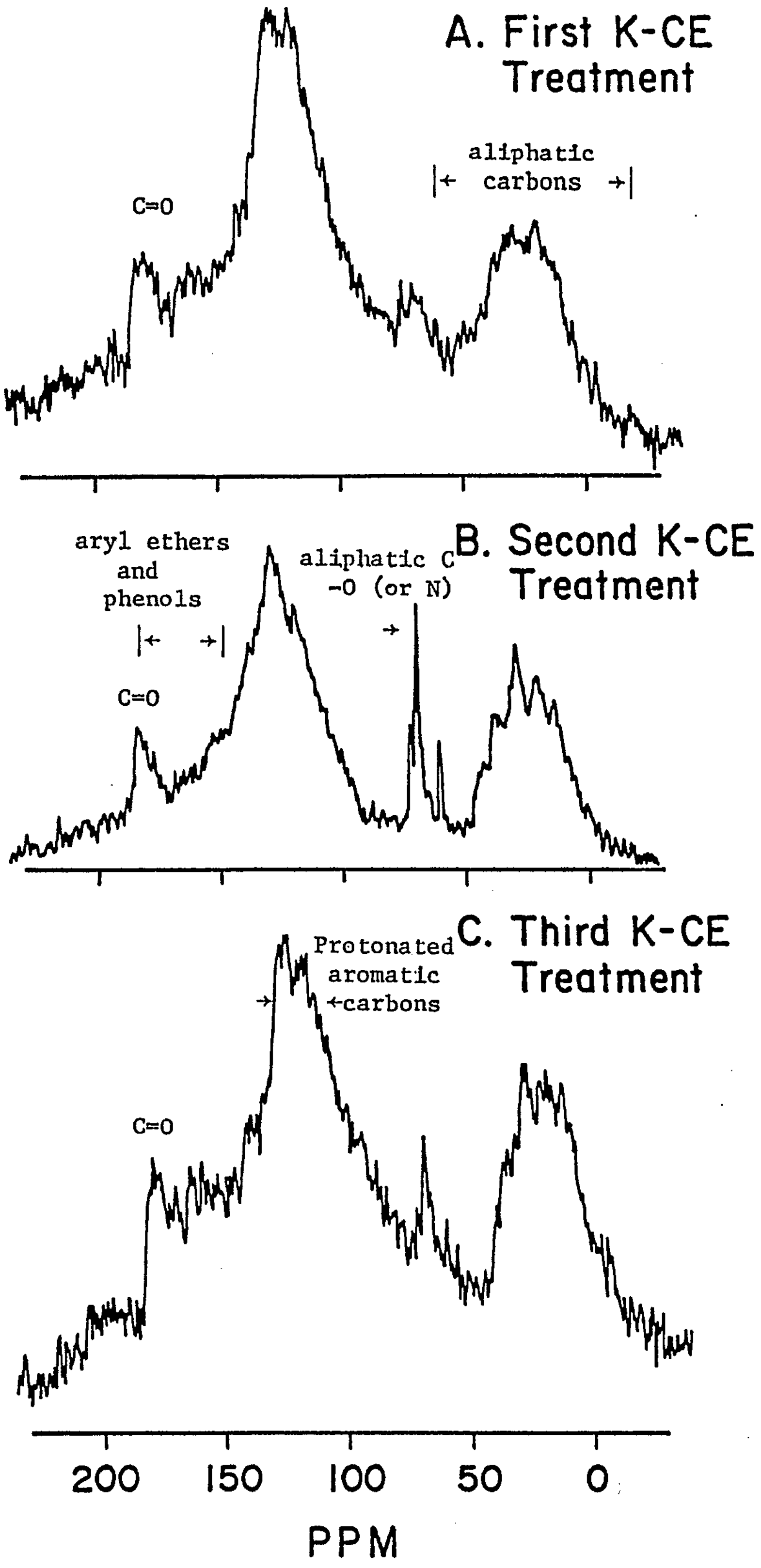

Figure 9. Proton Decoupled $^{13}$NMR Spectra of Alkali Solubles in NAOD/$D_2O$ After Successive K-CE Reactions

linked by K-CE clevable linkages (ether, diaryl alkane, hydrogen bonds). The alkali-THF fraction shows a bimodal molecular weight distribution, with a minor high molecular weight component (Mn=20,000-32,000 & Mw=27,100-35,000), in

Table 6

MOLECULAR WEIGHTS OF THE VARIOUS FRACTIONS

| Coal Oligomer | Molecular Weights | | |
|---|---|---|---|
| Fractions | Number Average $M_n$ | Weight Average $M_w$ | Peak Mol. Wt |
| First K-CE Rxn[a] | | | |
| THF-1 fraction | 414 | 1441 | 1117 |
| THF-2 fraction | 986 | 4029 | 2244 |
| Alkali-THF | 532 (Major) | 1457 | 930 |
| | 23990 (Minor) | 27170 | 33880 |
| Second K-CE Rxn[a] | | | |
| THF-1 | 641 | 1981 | 906 |
| THF-2 | 1079 | 4059 | 1319 |
| Alkali-THF | 863 (Major) | 3355 | 1114 |
| | 32345 (Minor | 35030 | 42204 |
| One K-CE Rxn[b] | | | |
| THF-1 | 522 | 1606 | 956 |
| THF-2 | 1310 | 4070 | 1784 |
| Alkali-THF | 1062 (Major) | 2553 | 1395 |
| | 20080 (Minor) | 24860 | 35714 |
| Wyodak coal - Untreated | | | |
| THF extract | 1712 | 5520 | 594 |
| Wyodak coal+aqueous KOH Precipitate. | | | |
| THF extract | 597 | 1068 | 597 |

a. The coal particle size was -20 mesh.

b. The coal particle size was -100 mesh.

addition to the major low molecular weight component described earlier. This may be construed as another type of coal cluster comprising the coal macromolecule — a condensed ring large molecular weight component. However, it seems more likely that because of diffusion and mass transfer limitations the K-CE reagent has not been able to cleave all the K-CE cleavable linkages, resulting in this larger molecular weight component. The alkali-THF fraction is being subjected to a K-CE reaction to verify this. It was also gratifying to note that our SEC molecular weight results for the alkali-THF fraction are very similar to that obtained by SEC using a continuous viscosity detector combined with a refractive index detector done by a commercial vendor and reported by us at the last EPRI meeting.

# Section 3

# PROGRESS IN BIOLOGICAL CONVERSION OF LOW RANK COALS

B. W. Wilson, J. W. Pyne, R. M. Bean, D. L. Stewart,
R. B. Lucke, B. L. Thomas, M. T. Thomas and J. A. Campbell

Battelle Pacific Northwest Laboratories

and

M. S. Cohen

University of Hartford

# ABSTRACT

Substantial progress has been made during the last year in understanding the phenomenon of coal solubilization by fungi and bacteria. Screening of additional organisms for biosolubilization capability, and screening of coals for amenability to biosolubilization continues. Chemical characterization of the initially obtained biosolubilized product has been completed, and reported in a paper to Energy and Fuels.

Work by the BNW/Hartford group over the last several months has focused primarily on the development and use of cell-free enzyme extracts to solubilize lignite coals. Enzymes from *Polyporous versicolor*, responsible for solubilization of lignite, have been isolated and characterized. Model compounds have been used to study the catalytic capabilities of these enzymes. Results from these studies were compared to those using intact *P. versicolor* and *Phanetochaete chrysosporium*. Additional bioreactor studies have been done, and a conversion metric has been developed to compare conversions obtained from different organisms on various coals.

## INTRODUCTION

Biosolubilization of coals is being investigated as a possible low cost alternative for recovery and utilization of low rank or marginal coals, and as a possible first step in a microbial desulfurization process. In the last year, substantial progress has been made in understanding the biochemical reactions associated with microbial attack on the coal structure and in decreasing the reaction times required to effect solubilization. Chemical characterization of the biosolubilized product from P. versicolor on leonardite was completed during the last year, and the results published in the open literature (1).

Work during the last 3 quarters has been aimed primarily at developing and improving cell-free systems for solubilization. This paper will report progress in this and related areas, including continued organism and substrate screening studies, model compound studies, and the use of various pretreatments to facilitate solubilization. Planned work on the project including evaluation of the biosolubilized material as a feedstock for methane production, and encapsulation and recovery of enzymes from the enzyme/coal reaction mixture, as well as proposed surface analyses to compare coals amenable and non-amenable to biosolubilization will also be discussed.

## ORGANISM AND SUBSTRATE SCREENING

Screening of new organisms for coal solubilization activity and testing of various coals for amenability to solubilization have been ongoing components of the project since its inception. In conjunction with the screening tests, we have evaluated the effects of heating as a pretreatment to facilitate the solubilization of coal. Table 2-1 lists the major results from these studies. Note that there are definite differences in the amenability to solubilization among the coals tested. These differences were seen among coals of the same rank as well as between ranks.

Nitric acid treatment has been used by a number of laboratories to help effect solubilization. Although we consider nitric acid as a severe and impractical

Table 2-1

SUMMARY OF MICROBIAL SOLUBILIZATION OF COALS[a]

| Microorganisms | Type of Coals | | | |
|---|---|---|---|---|
| | Texas Lignite | Beulah Std. #3 | Beulah Zap II | Illinois #6 |
| *P. versicolor* | Trace[b] | --[c] | Trace[b] | -- |
| *P. chrysosporium* | -- | -- | -- | Trace[b] |
| *Candida* sp. | -- | -- | -- | |
| *Penicillium* sp. | -- | -- | -- | Profuse |
| *Cunninghamella* sp. | Profuse | Moderate | Moderate | Trace |
| *P. versicolor var. vulpinus* ATCC 22318 | Moderate[d] | Moderate[d] | N.T.[e] | Trace[d] |
| *Poria placenta* ATCC 32568 | Trace[d] | N.T. | N.T. | -- |
| *Poria placenta* ATCC 11538 | -- | -- | N.T. | -- |
| *Percniporia subacida* ATCC 14710 | -- | -- | N.T. | -- |
| *Heterobasidion annosum* ATCC 9852 | Profuse[d] | Moderate[d] | N.T. | -- |
| *Streptomyces viridosporus* ATCC 39115 | Moderate[d] | N.T. | N.T. | Trace[d] |
| *Streptomyces badius* ATCC 39117 | Moderate[d] | -- | N.T. | Moderate[d] |
| *Streptomyces setonii* ATCC 39116 | Moderate[d] | -- | N.T. | Trace[d] |

---

[a] All coals except leonardite pretreated with heat at 150°C for 7 days

[b] Conversion measured as straw color droplet formation

[c] -- = No Conversion

[d] Required nitric acid treatment (8M) for conversion (i.e., liquid production formation)

[e] N.T. = Not Tested

Table 2-1 (contd)

SUMMARY OF MICROBIAL SOLUBILIZATION OF COALS[a]

| | Type of Coals | | |
|---|---|---|---|
| | | Pennsylvania | |
| Microorganisms | Pittsburgh #8 | Upper Freeport | Leonardite |
| *P. versicolor* | --[c] | -- | Moderate |
| *P. chrysosporium* | -- | -- | Profuse |
| *Candida* sp. | -- | -- | Moderate |
| *Penicillium* sp. | Moderate | Moderate | Moderate |
| *Cunninghamella* sp. | Profuse | -- | Profuse |
| *P. versicolor* var. *vulpinus* ATCC 22318 | N.T.[e] | N.T. | Profuse |
| *Poria placenta* ATCC 32568 | N.T. | N.T. | Trace |
| *Poria placenta* ATCC 11538 | N.T. | N.T. | Profuse[f] |
| *Percniporia subacida* ATCC 14110 | N.T. | N.T. | -- |
| *Heterobasidion annosum* ATCC 9852 | N.T. | N.T. | Trace |
| *Streptomyces viridosporus* ATCC 39115 | N.T. | N.T. | N.T. |
| *Streptomyces badus* ATCC 39117 | N.T. | N.T. | Moderate[b,d] |
| *Streptomyces setonii* ATCC 39116 | N.T. | N.T. | Moderate[b,d] |

---

[a] All coals except leonardite pretreated with heat at 150°C for 7 days

[b] Conversion measured as straw color droplet formation

[c] -- = No Conversion

[d] Required nitric acid treatment (8M) for conversion (i.e., liquid product formation)

[e] N.T. = Not Tested

[f] Conversion measured by complete darkening of media with trace droplet formation

treatment on any larger scale, we have carried out some tests using this treatment in order to compare our progress with that of other laboratories. Use of nitric acid as a pretreatment should be considered carefully when evaluating data on biosolubilization. Note that we have obtained reasonable conversions on coals of several ranks without the use of nitric acid.

Figures 2-1 through 2-3 are photographs of agar cultures as they are used in screening studies. Figure 2-1 shows the comparative conversion of leonardite by Candida, Penicillium and Cunninghamella. Figure 2-2 shows an increase in solubilization after pretreating with heat only. In Figure 2-3 Illinois #6 bituminous coal is shown to be solubilized by a Penicillium strain.

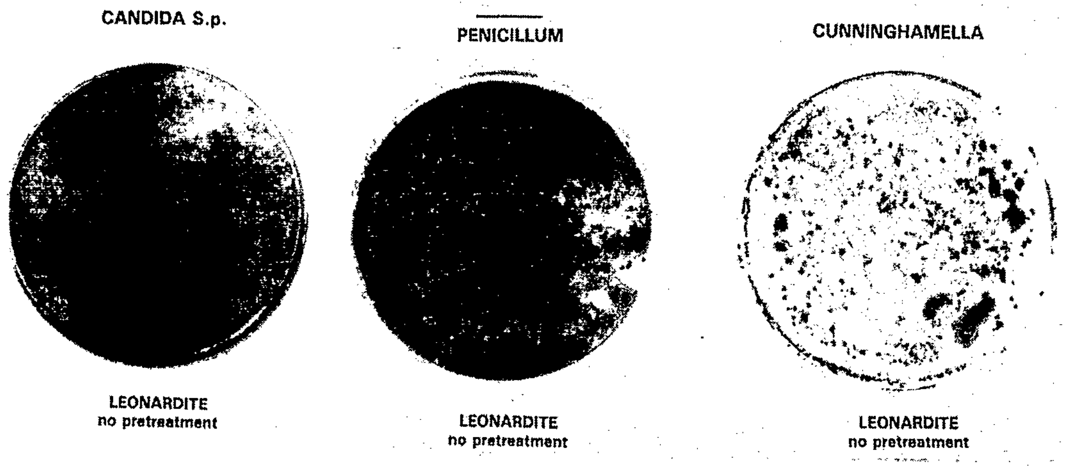

**CANDIDA S.p.**
LEONARDITE
no pretreatment

**PENICILLUM**
LEONARDITE
no pretreatment

**CUNNINGHAMELLA**
LEONARDITE
no pretreatment

Figure 2-1. Leonardite coal incubated with Candida, Penicillium, and Cunninghamella.

**CUNNINGHAMELLA**

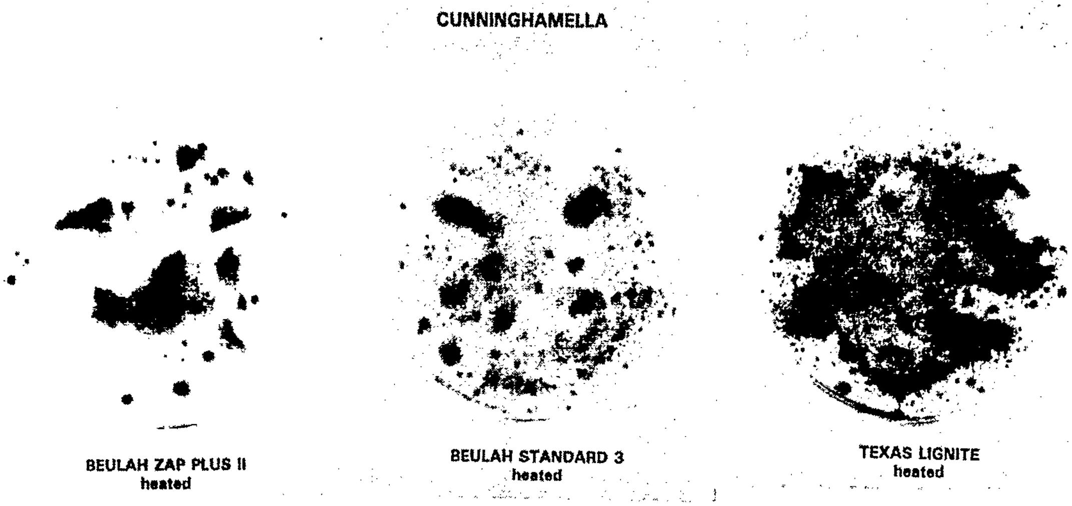

**BEULAH ZAP PLUS II**
heated

**BEULAH STANDARD 3**
heated

**TEXAS LIGNITE**
heated

Figure 2-2. Cunninghamella cultured with various coals that have been pretreated by heating at 150°C.

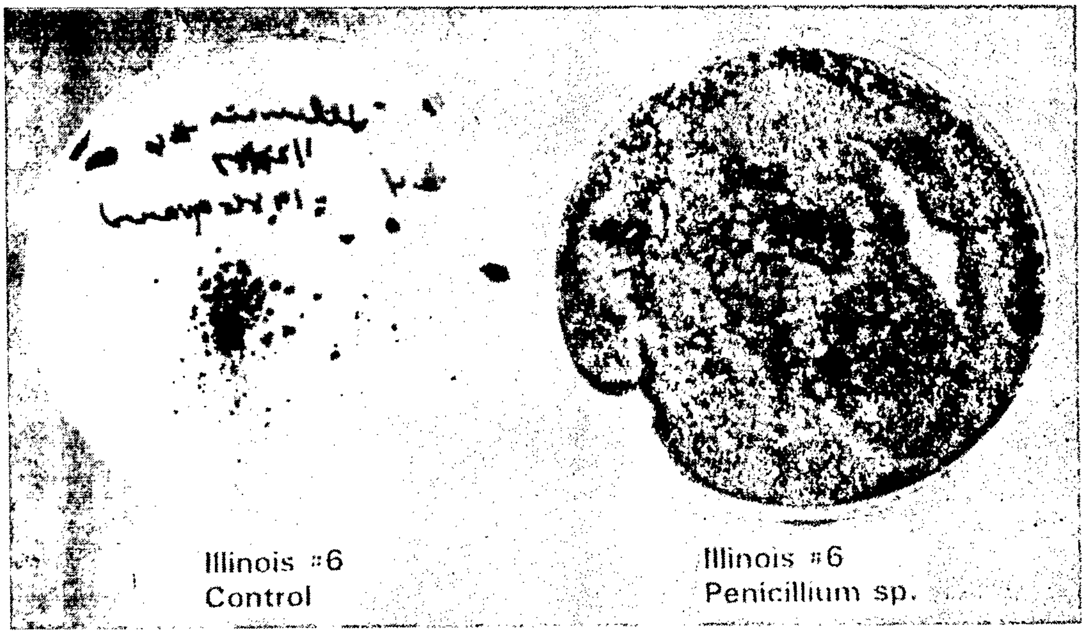

Figure 2-3. Illinois #6 coal incubated at 30°C with _Penicillium_ and with Sabouraud maltose agar.

## ISOLATION AND CHARACTERIZATION OF LACCASE ENZYNE SYSTEMS

Cell-free solubilization of lignite has been accomplished with filtered broth extracts from _P. versicolor_ cultures as well as with more highly purified enzyme fractions. Review of the literature on lignin degradation indicates that the laccase system can break oxygen containing covalent bonds and we have therefore focused on laccase as an enzymatic system likely to effect coal solubilization. Laccase activity is readily detected by a colorimetric assay using syringaldazine. (Syringaldazine oxidase is a more specific designation of the activity indicated in this assay.) To date we have substantial evidence that laccase plays a central role in solubilization of certain coals.

Several tests to confirm that enzymatic activity is responsible for coal solubilization have been conducted using the cell-free extracts. These include enzyme poisoning with azide or cyanide, and acid hydrolysis. Poisoning with cyanide resulted in a 40% inhibition of syringaldazine oxidase activity, and a 10% decrease in solubilization activity, whereas azide inhabited these two activities by 70% and 30%, respectively. Acid hydrolysis completely destroyed both activities.

Using leonardite as a positive control, additional work was carried out with cell-free preparations to determine effects of culture age, coal particle size, pH, and added commercial laccase on solubilization reaction rates. Figure 3-1 shows the appearance of solubilization ability in cell-free filtrates from P. versicolor in Sabouraud maltose broth as a function of time. Figure 3-2 shows the total protein synthesized by the culture. Note that while the synthesis of protein increases in a linear fashion, solubilization activity shows a definite peak around day 6. With regard to particle size, smaller particles result in higher solubilization yields as shown in Figure 3-3. After 3 hours reaction time, the <105 micron material showed approximately twice the yield of the larger sized particles.

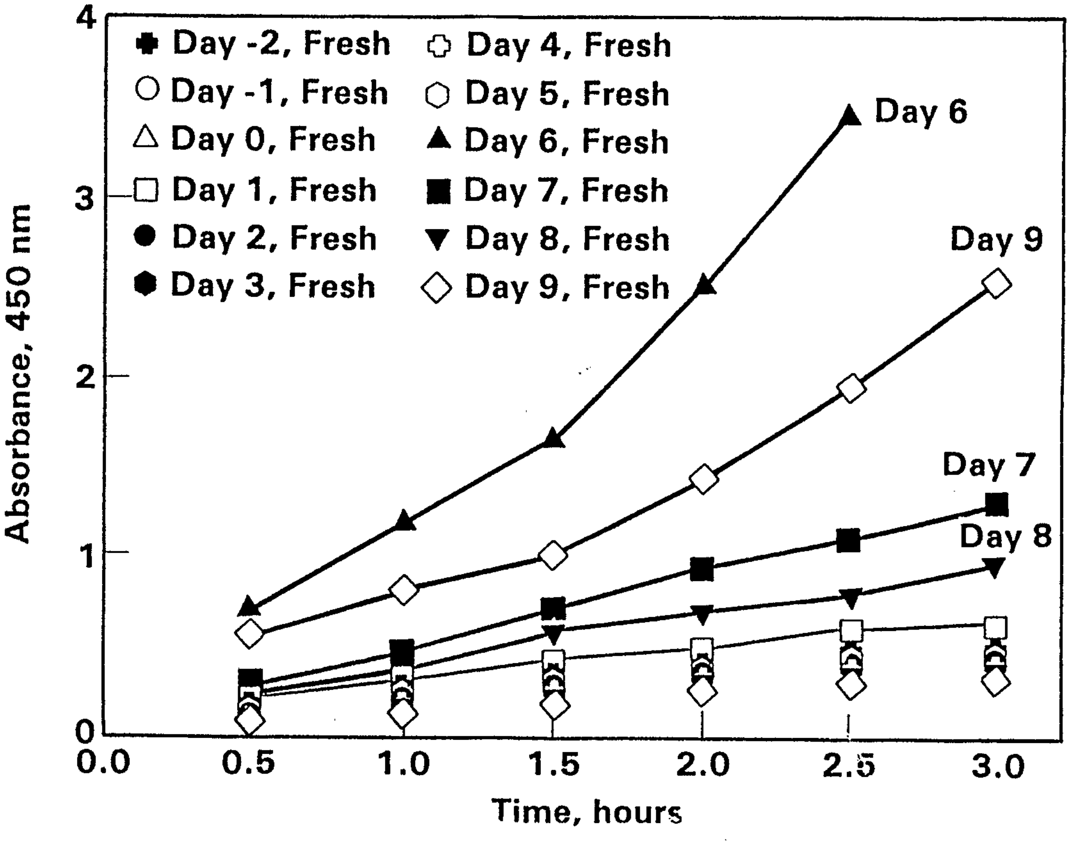

Figure 3-1. Appearance of liquification ability in cell-free filtrates from Sabouraud maltose broth cultures of Polyporus versicolor over a 12 day period.

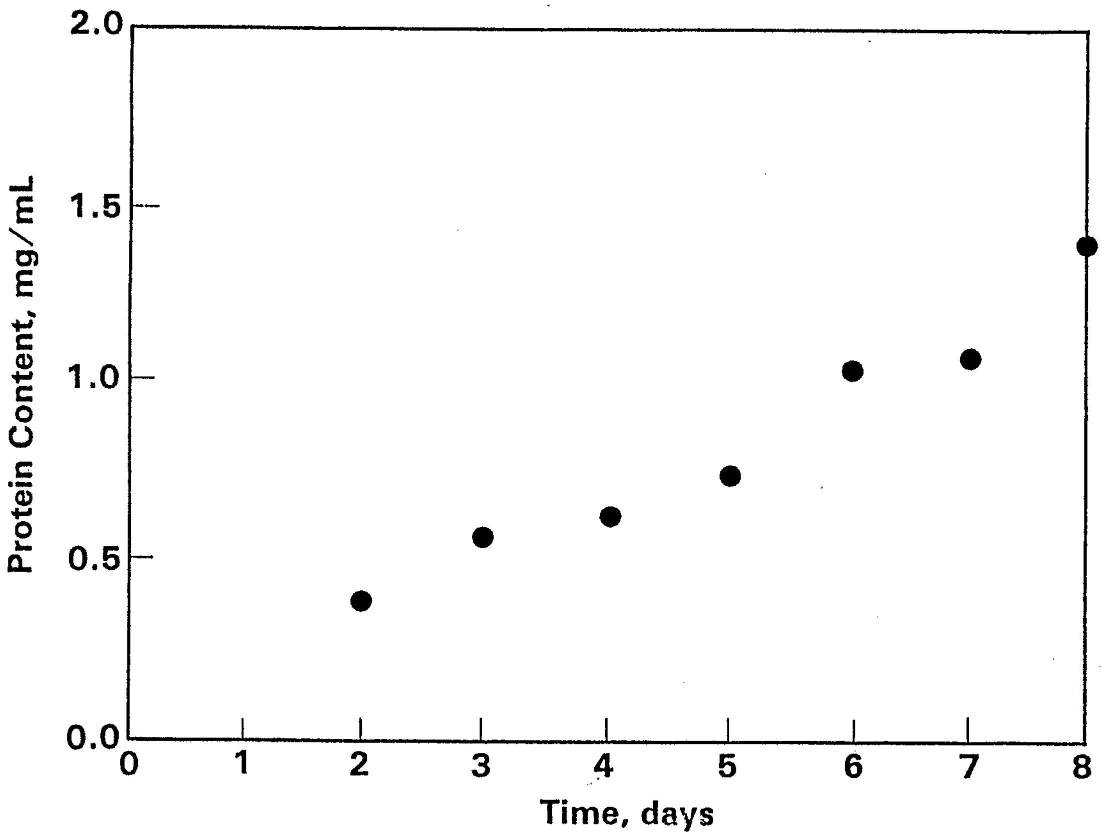

Figure 3-2. Total protein content of cell-free filtrates from Sabouraud maltose broth cultures of Polyporus versicolor.

Although syringaldazine oxidase activity is considered diagnostic for laccase activity, Figure 3-4 shows that added commercial laccase did not increase the solubilization. This result indicates that not all enzyme systems that exhibit syringaldazine oxidase activity are capable of solubilizing coal. Another important parameter in solubilization rates is pH, as illustrated in Figure 3-5. Leonardite is solubilized without added enzyme at higher pHs. We have not yet directly determined the effect of pH on enzyme biosolubilization activity.

An analogous broth extract obtained from a stirred reaction in a fermentor was further filtered to obtain a molecular weight cut between 10,000 and 100,000 daltons. This extract was dialyzed, centrifuged, and fractionated on a DEAE cellulose column. Figure 3-6 shows that, in this extract, leonardite solubilization activity and syringaldazine oxidase activity appear in the same fraction of the eluent as does maximum absorbance at 280 nm (i.e., protein). A typical preparation capable of solubilizing both leonardite and lignite is prepared in our

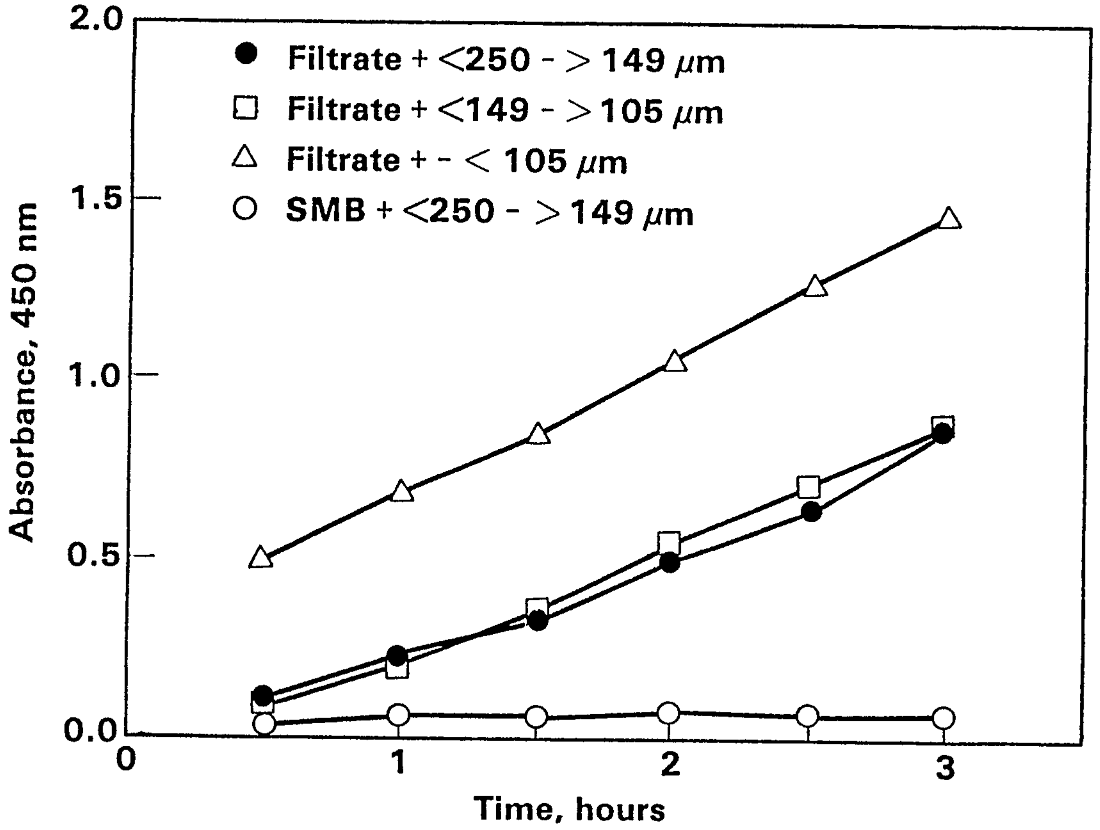

Figure 3-3. Effect of coal particle size on the rate of cell-free liquification by filtrates from Sabouraud maltose broth culture of Polyporus versicolor and by fresh Sabouraud maltose broth.

laboratory as follows: a Sabouraud maltose broth (pH 5.8) is inoculated with P. versicolor, and incubated for 24 days in stationary culture. The cells are then filtered from the broth and the filtrate adjusted to pH 5.4. After dilution of the cell-free preparation with buffer (1:1), coal is added. Solubilization is measured by absorbance at 450 nm. This preparation readily solubilizes Mississippi lignite as shown in Figure 3-7.

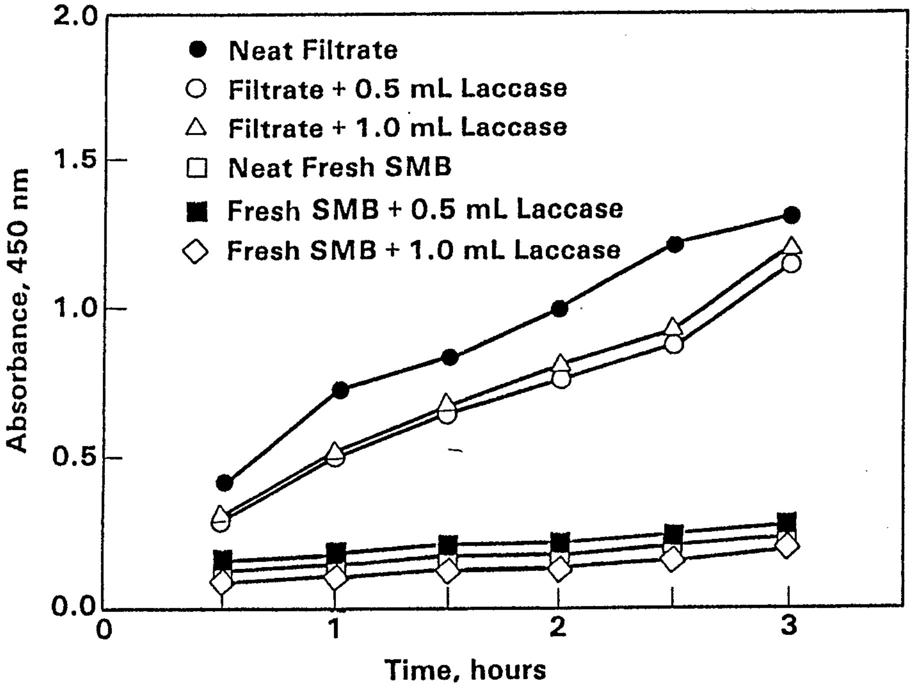

Figure 3-4. Liquification of leonardite coal by cell-free filtrates of Sabouraud maltose broth cultures of _Polyporus versicolor_ and by fresh SMB with and without addition of laccase.

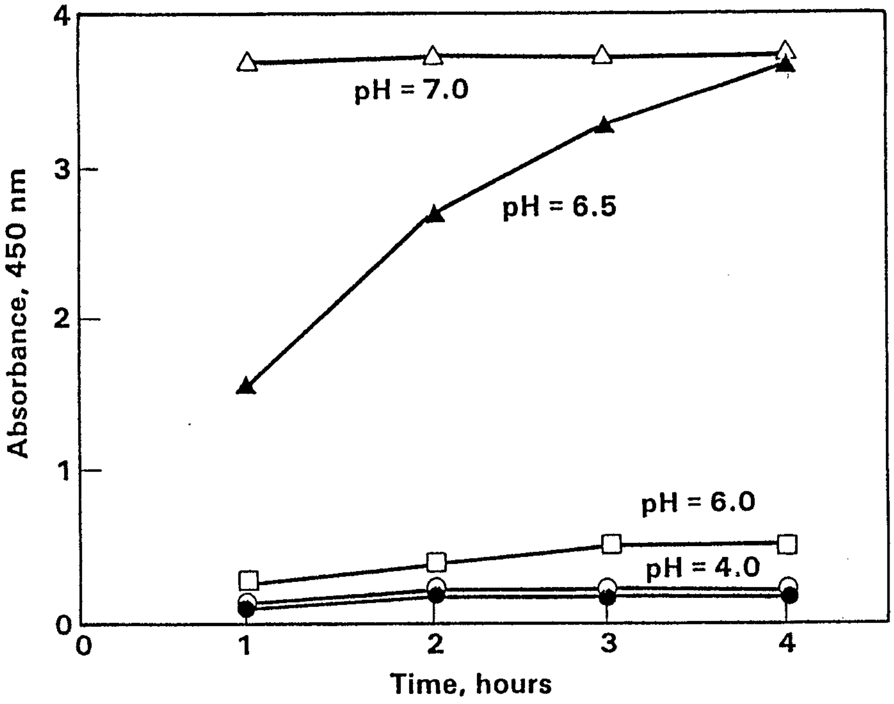

Figure 3-5. Effect of buffers of various pH values on liquification of leonardite coal.

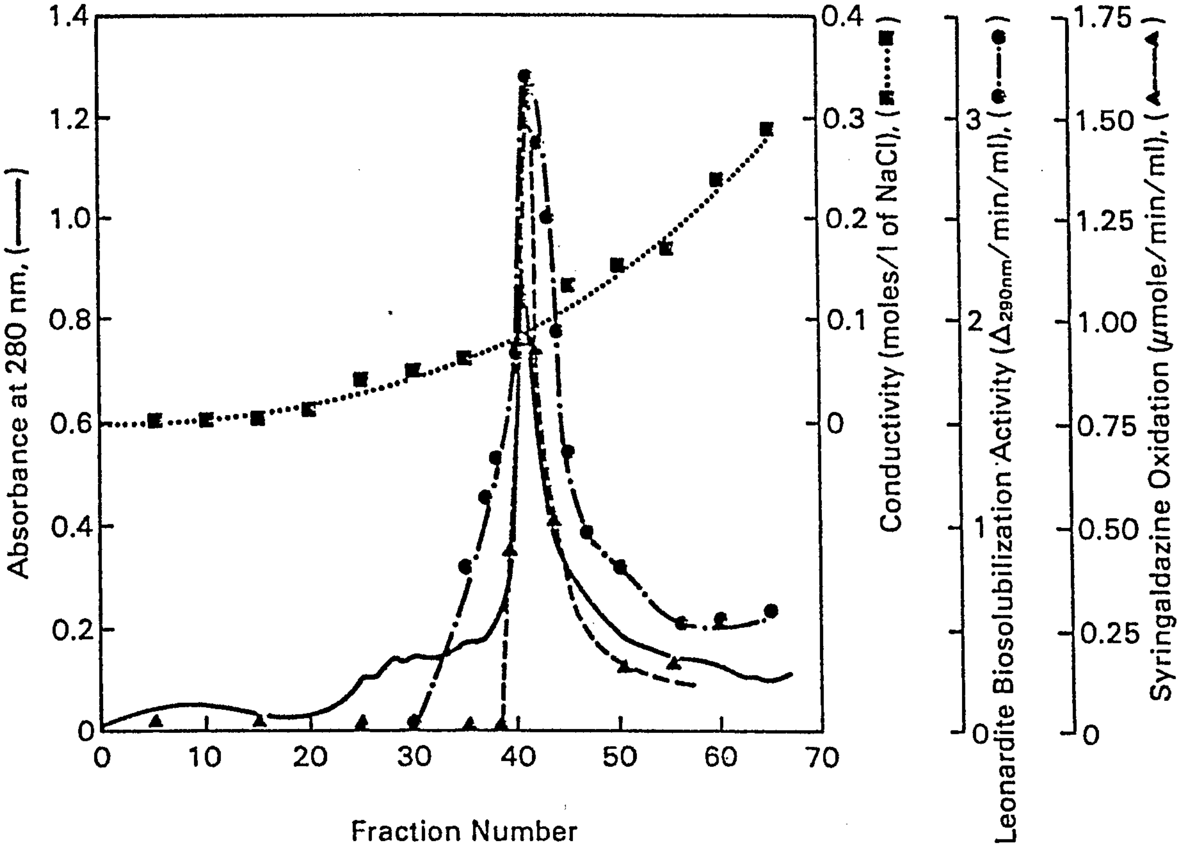

Figure 3-6. Partial fractionation of the concentrated broth in which Polyporus versicolor has grown. The protein content, syringaldazine oxidase activity, and leonardite solubilizing activity all eluted in the same fraction from a DEAE-cellulose column. Syringaldazine oxidase (Δ-Δ) and leonardite biosolubilizing (o-o) activities were estimated as described in text. The elution profile of protein was determined spectrophotometrically as adsorption at 280 nm (__). Protein was eluted with a gradient of zero to 0.3 M sodium chloride and 3 mL were collected. The salt concentration (•-•) was determined by measuring ionic strength.

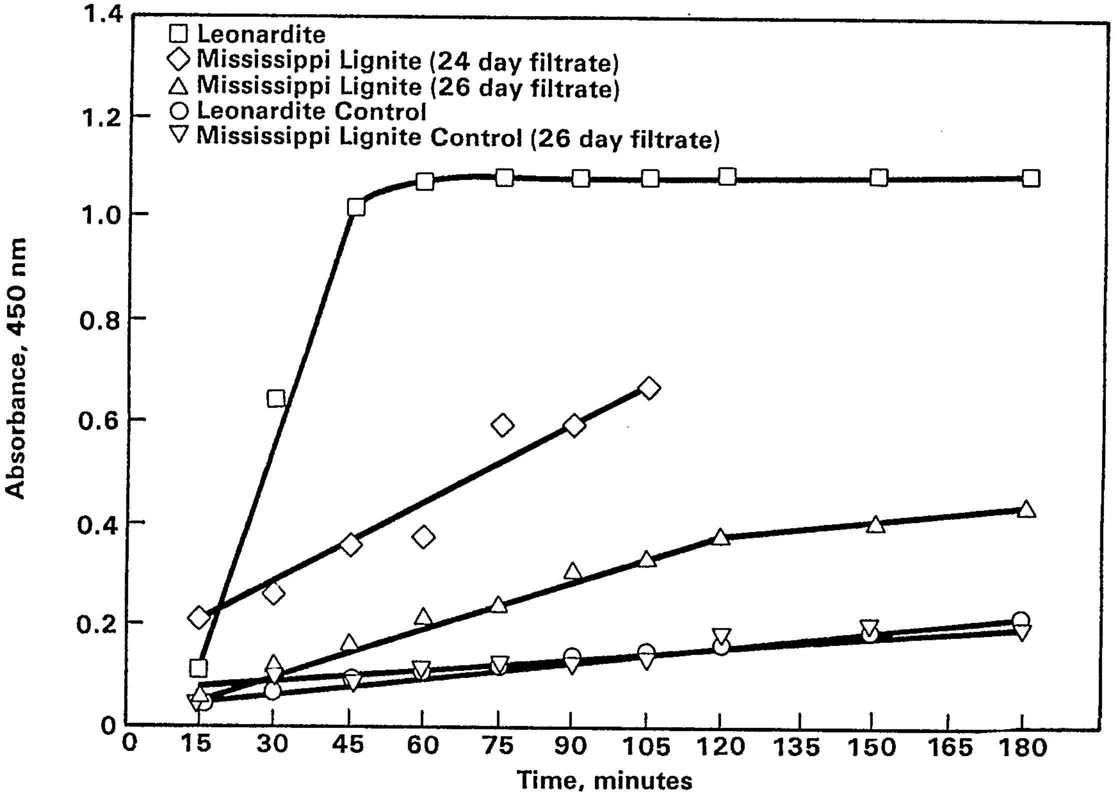

Figure 3-7. Solubilization of leonardite and Mississippi lignite coal by cell-free filtrates of Polyporus versicolor.

BIOREACTOR STUDIES

Three bioreactor types have been used to degrade low-rank coals. These are a packed-bed reactor, a stirred-tank reactor and a cell-free enzymatic system. In all three systems the defined medium of Fahreaus and Reinhammar (2) was used.

In the packed-bed system, leonardite particles were placed in a glass column, which was then filled with growth medium and inoculated with P. versicolor. The column was aerated and temperature maintained at 23°C. After two weeks of operation, the remaining leonardite particles were removed and soxhlet extracted with water. A yield value of 5% was determined based on color of product and the initial weight of leonardite added. Results from the stirred-tank bioreactor are much better than the results from the packed-bed bioreactor. A culture of P. versicolor was grown in a stirred-tank fermentor. A week after inoculation, 50 g of leonardite were added to 15 L of medium in the fermentor. Samples from the fermentor contents were centrifuged to sediment the cells and residual leonardite particles. The absorption at 450 nm was measured and used to determine conversion. The results of the fermentor are shown in Figure 4-1. Product from the fermentor did not require soxhlet extraction to recover as in the packed-bed bioreactor. Based on the formation of the colored material, the yield in the stirred-tank was about 10%.

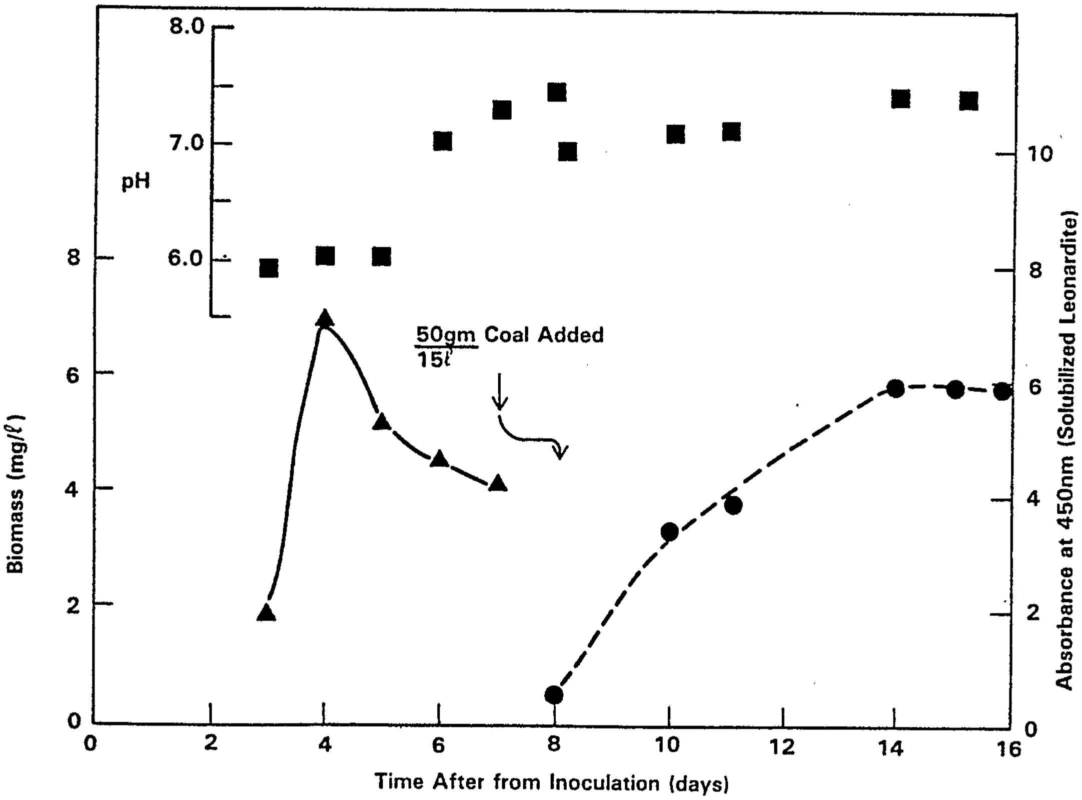

Figure 4-1. Leonardite Biosolubilization in a Stirred-Tank Fermentor

Studies on the cell-free conversion of leonardite have shown that a purified protein-containing preparation with a laccase-like activity can degrade leonardite. Again, based on color formation, yield of product was 44% in the cell-free enzyme system after a twenty hour incubation at 25°C. Present studies are centered on characterizing and on improving levels of formation of the factors important in degrading low-rank coals and improving conditions for degradation.

## CHEMICAL CHARACTERIZATION OF THE BIOSOBULIZED PRODUCT AND A DEVELOPMENT OF A CONVERSION METRIC

Chemical characterization of the initially obtained solubilized product from the action of <u>P. versicolor</u> on leonardite has been completed and published (see ref. 3). Not reported at this meeting in 1986 were the results of $^{13}$C NMR studies on the solubilized product materials. These analyses could account for approximately 60% of the carbon present. Of that 60%, 51% of the carbon was aromatic, 29% was aliphatic, and approximately 20% was present as carboxylate or quinone structures. Data are shown in Figure 5-1.

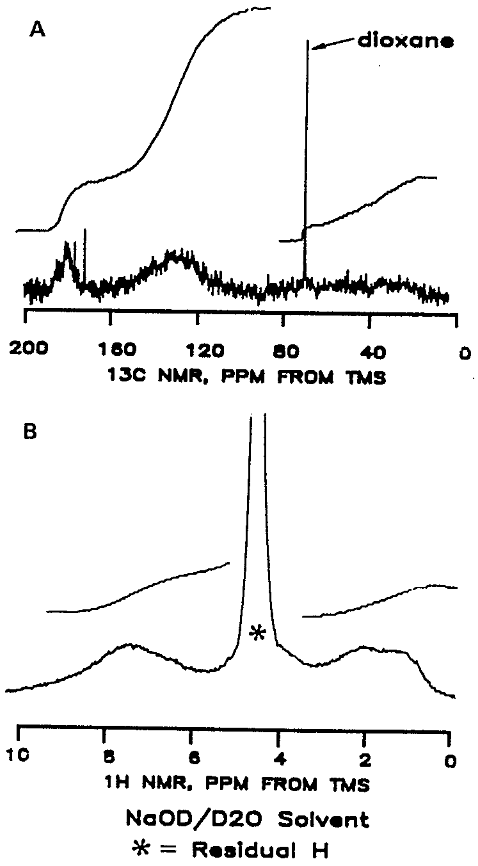

Figure 5-1. $^{13}C$ NMR Studies on the Solubilized Product Material

A continuing problem in comparing the solubilization activity of different cultures and preparations, as well as in comparing results between laboratories, has been the lack of a reliable assay, or conversion metric, for determining the extent of solubilization. Our research group has recently developed such a conversion metric. This was accomplished by freeze drying biosolubilized materials, which had been passed through a 0.22 micron membrane, and reconstituting the material to known concentrations in water. The absorbance spectra of these solutions at 680 nm was plotted and found to be linear with concentration (see Figure 5-2 a, b).

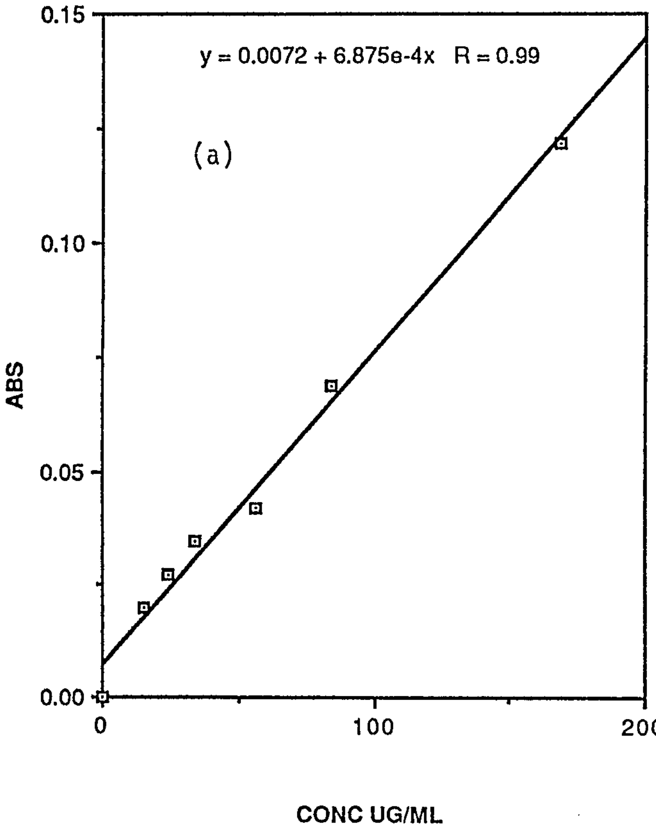

Figure 5-2a. Absorbance of *P. versicolor* Solubilized Leonardite at 680 nm

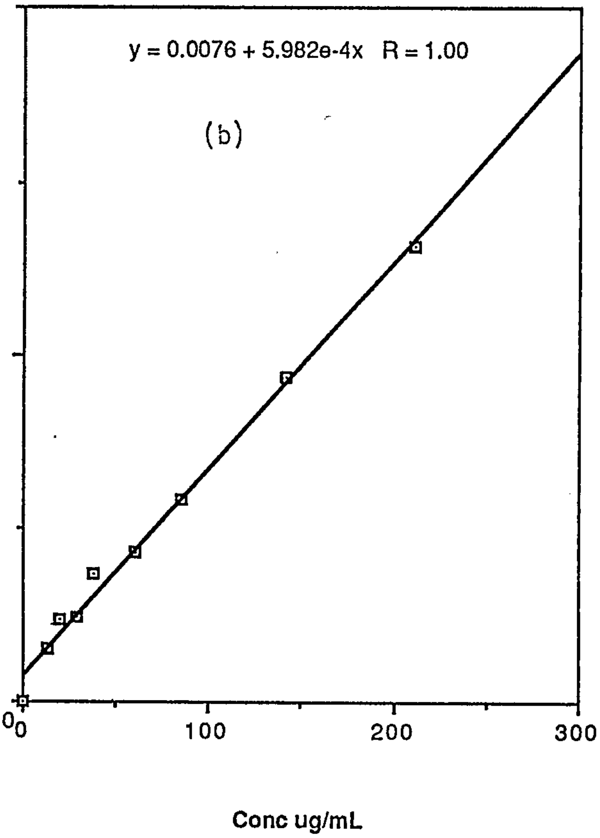

Figure 5-2b. Absorbance of *P. versicolor* Solubilized Nitric Acid Pretreated Texas Lignite at 680 nm.

Interference from agar or microorganism biomass at 680 nm appears to be negligible. This method has been used for determining conversions both on agar plates, where the interference from the media may be significant at wavelengths below 680 nm, and with cell-free systems. (450 nm is also used with cell-free systems when no media is present.) There appear to be essentially no differences between the UV/VIS spectra of materials obtained from coals pretreated with nitric acid and those that are only heat treated or receive no pretreatment. Ultra-violet/visible spectra for materials from three different coals studies thus far were identical.

## MODEL COMPOUND STUDIES

Model compounds have been used to determine the metabolic capabilities of intact organism cultures, crude broth preparations and partially purified enzyme fractions. Model compounds used in these studies to date include benzylbenzoate, methoxybenzophenone, benzylether and phenylbenzoate. Gas chromatography has been used to determine degradation in the reaction mixtures.

Active chromatographic fractions obtained from P. versicolor as described in section 2 were combined and designated the crude enzyme preparation. To determine the metabolic capabilities of this preparation in attacking oxygen containing covalent bonds found in coal, model compounds were introduced at a concentration of 100 ppm in methanol. These reaction mixtures (enzyme and model compound in a buffer solution) were left for 1 day, after which the solution was extracted 3 times with equal columns of chloroform, combined, concentrated to 1 mL, and analyzed by GC/FID to determine the amount of degradation.

For benzylbenzoate, the amount of degradation from this treatment was approximately 50%, while no degradation occurred for methoxybenzophenone. Data from this experiment are shown in Figures 6-1 and 6-2. It should be noted that the analyses of the controls indicated no degradation of the model compound by the buffer solution.

Additional experiments were done to compare the degradation catalyzed by the enzyme preparation from P. versicolor to that of the intact organism. Degradation observed with the intact organism was 95-100% for both compounds. These data are shown in Figures 6-3 and 6-4. Figure 6-3 is a gas chromatogram of the 100 ppm standards of (a) benzylbenzoate and (b) methoxybenzophenone. Figure 6-4 is a gas chromatogram of the degraded (a) benzophenone and (b) methoxybenzophenone by P. versicolor.

The reason for the large discrepancy in degradation amounts between the P. versicolor and the cell-free enzyme may be simply a factor of time in contact with the enzyme (1 week for the total organism vs. 1 day for the cell-free enzyme), or in the case of the intact organism, there may be several enzymes underway to determine the extent of degradation as a function of time with the cell-free enzyme. In addition, other model compounds will be studied with the cell-free enzyme and coal will be added with the model compounds and the cell-free enzyme to determine if there is an induction effect from coal.

In another experiment, P. versicolor was cultured and the broth was subsequently removed but not fractionated or purified as in the previous discussion. This material was also tested for activity using model compounds. Both benzylbenzoate

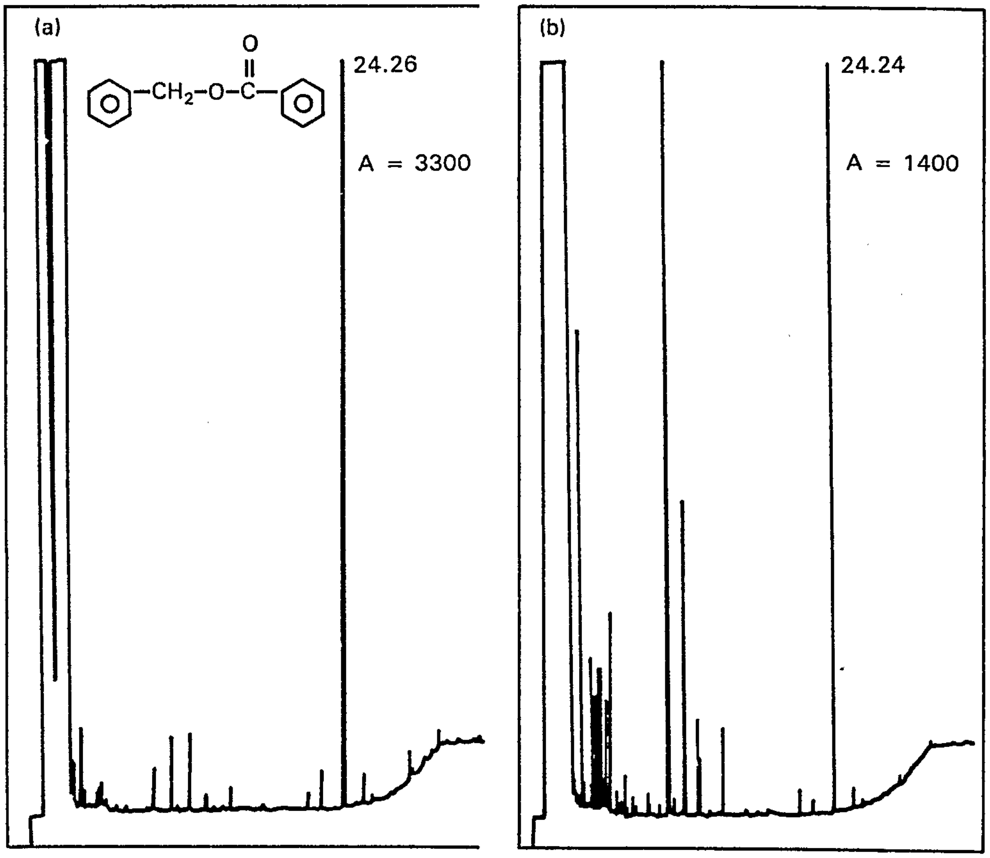

Figure 6-1. Gas chromatogram of (a) 100 ppm standard of benzylbenzoate and (b) after degradation by cell-free enzyme from P. versicolor.

and methoxybenzophenone were used as well as additional compounds, phenylbenzoate and benzylether. Each model compound at 100 ppm was added to the buffer solution and enzyme solution. After 1 day, each sample was extracted with 3 equal volumes of chloroform, combined, and concentrated to 1 ml for analysis by GC/FID. Preliminary results indicate the amount of degradation for each compound is as follows:

| COMPOUND | PERCENT DEGRADATION |
|---|---|
| benzylbenzoate | 60% |
| methoxybenzophenone | 5-10% |
| benzylether | 50% |
| phenylbenzoate | 99% |

These results are illustrated in Figures 6-5 and 6-6. Figure 6-6 is a gas chromatogram of the 100 ppm standard of (a) benzylether and (b) after degradation by cell-free filtrates from cultures of P. versicolor. Figure 6-7 is a gas

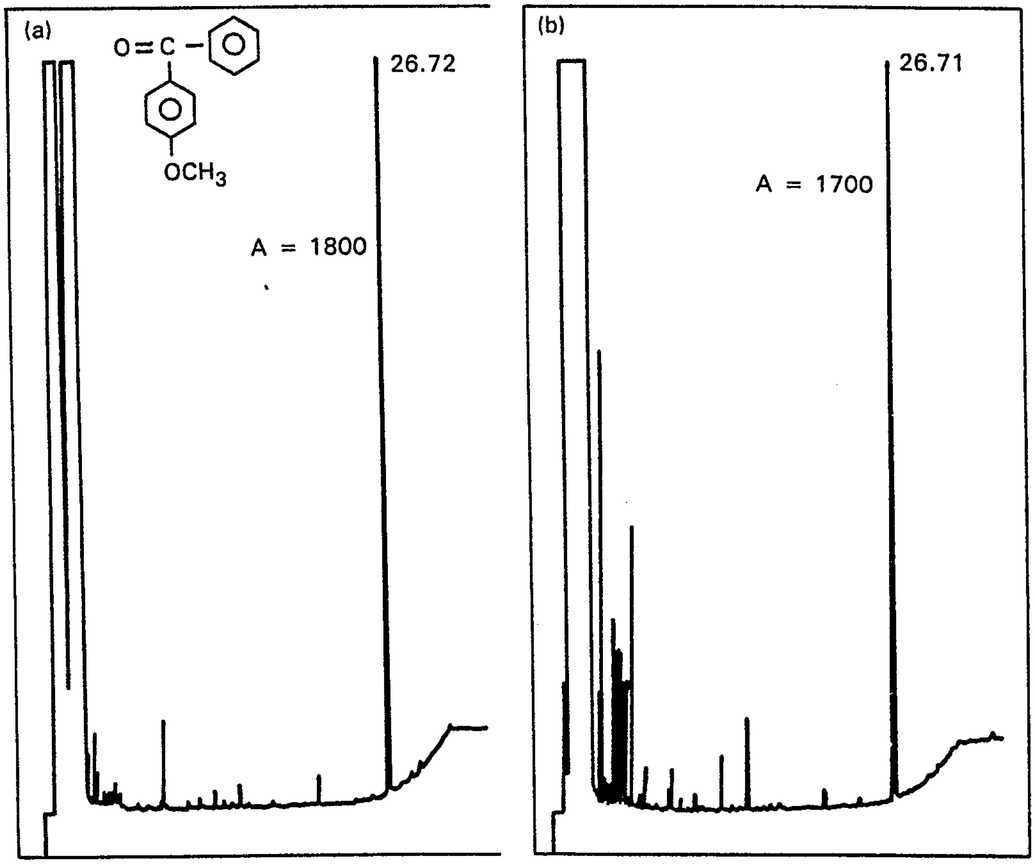

Figure 6-2. Gas Chromatogram of (a) 100 ppm Standard of Methoxybenzophenone and (b) after Degradation by Cell-Free Enzyme from P. versicolor

chromatogram of the 100 ppm standard of phenylbenzoate before (a) and after (b) degradation by cell-free filtrates from cultures of P. versicolor. Again, the discrepancy between these results and the total organism may be a factor of contact time. The amount of degradation does agree fairly well with the cell-free, purified enzyme results of both benzylbenzoate and methoxybenzophenone. Although the solutions have not been analyzed by GC/MS, the mechanism of degradation is thought to be cleavage, followed by hydrolysis as shown below.

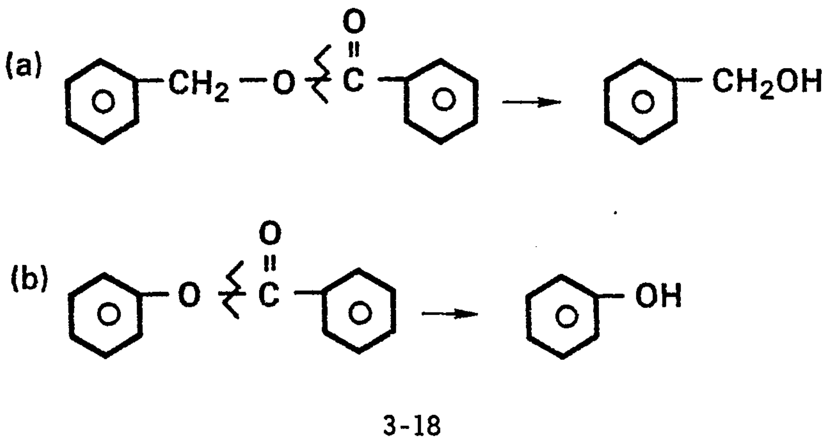

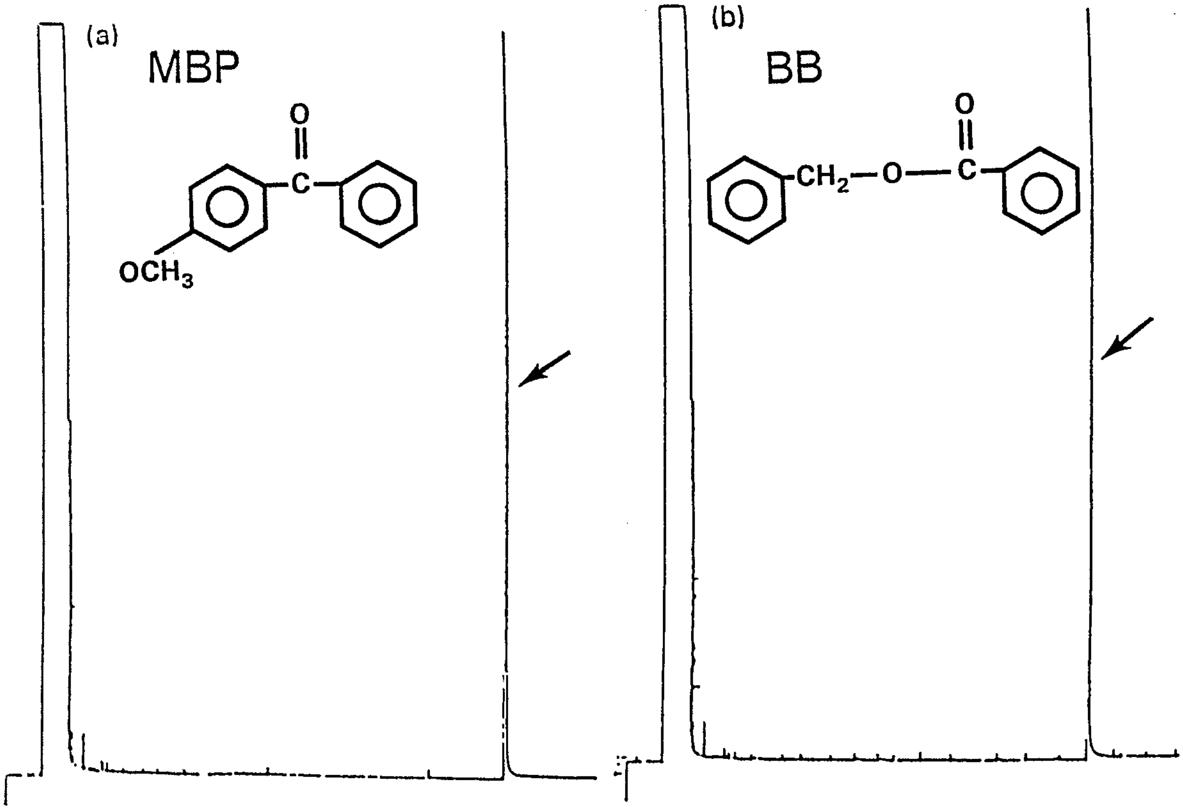

Figure 6-3. Gas Chromatogram of 100 ppm (a) Methoxybenzophenone and (b) Benzylbenzoate

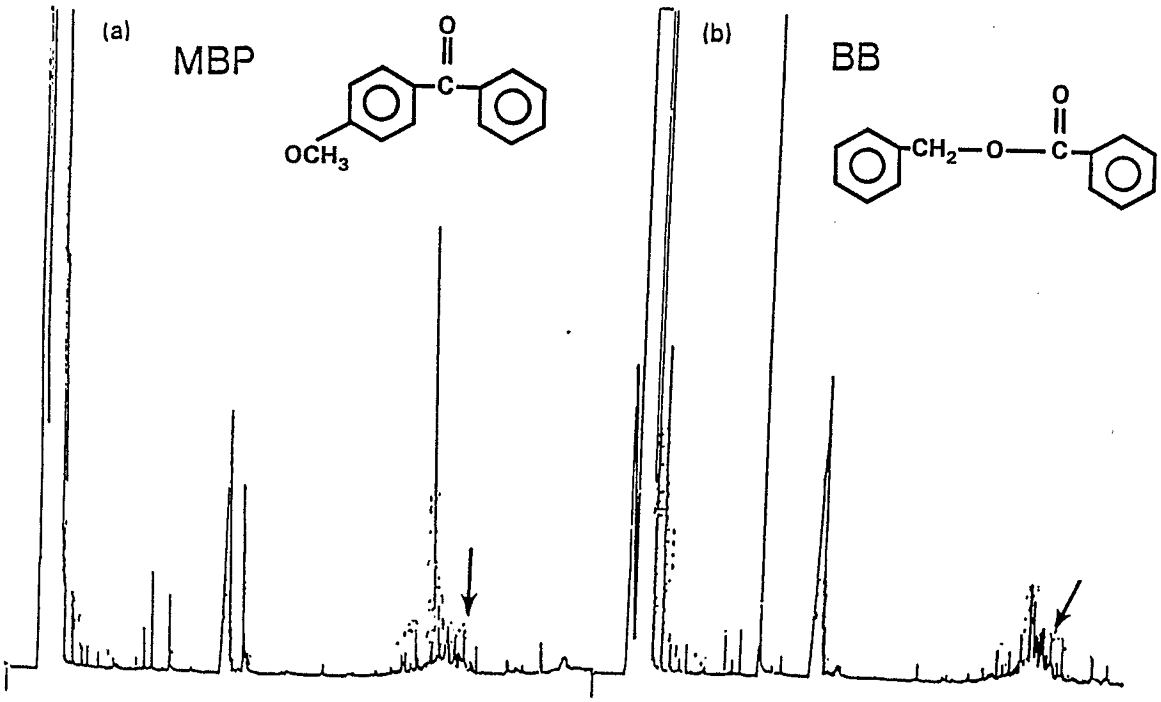

Figure 6-4. Gas Chromatogram of 100 ppm (1) Methoxybenzophenone and (b) Benzylbenzoate after Degradation by *P. versicolor*

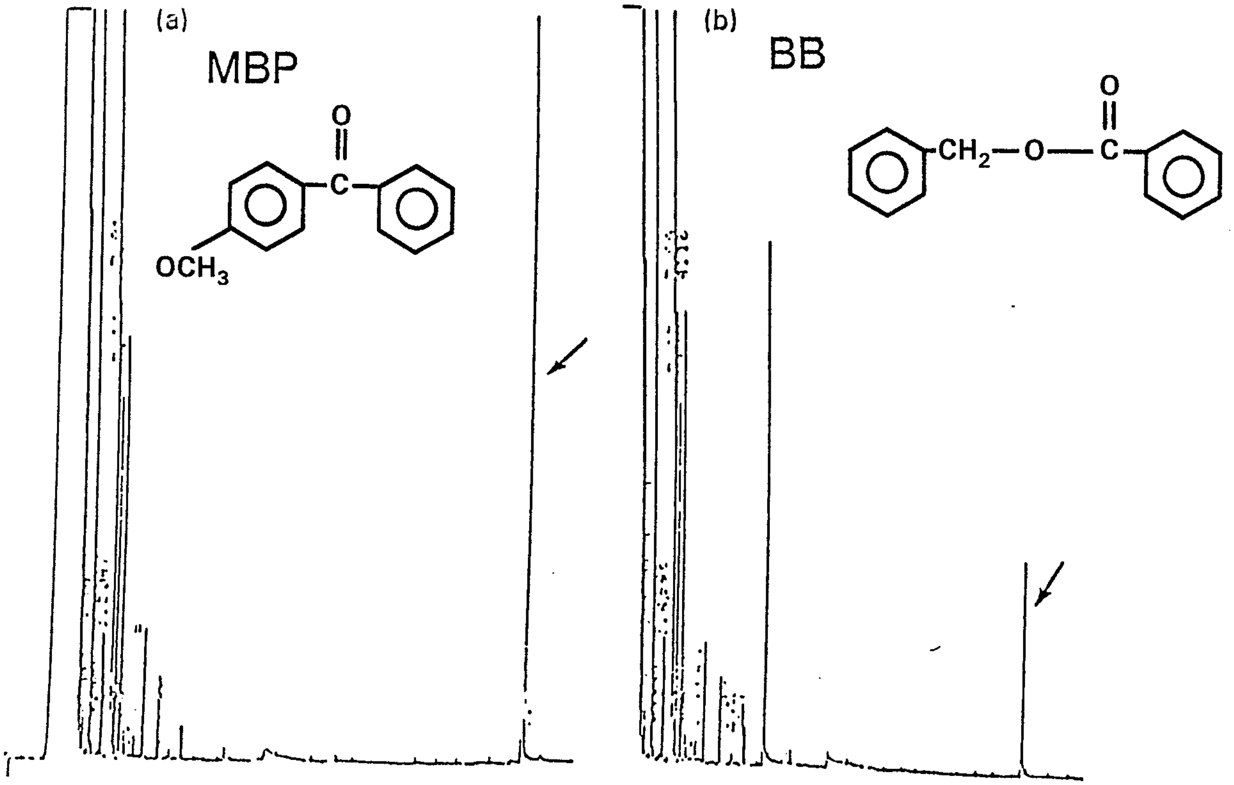

Figure 6-5. Gas Chromatogram of 100 ppm (a) Methoxybenzophenone and (b) Benzylbenzoate after Degradation by <u>P. chrysosporium</u>

In future work, model compounds with sulfur and nitrogen heterocycles will also be tested for degradation. Other model compounds being considered are of the following form:

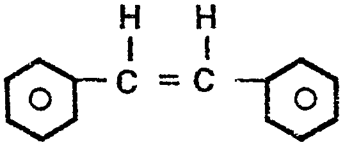

In addition, mixtures of several model compounds will be allowed to react with the enzyme and the amount of degradation will be determined.

## FUTURE WORK

Production of methane from the acid precipitate has been proposed as a possible end use for the biosolubilized product. Initial attempts to effect this reaction have been unsuccessful. We believe that the high molecular weight of the biosolubilized material, as it is currently produced, makes it unsuitable for further

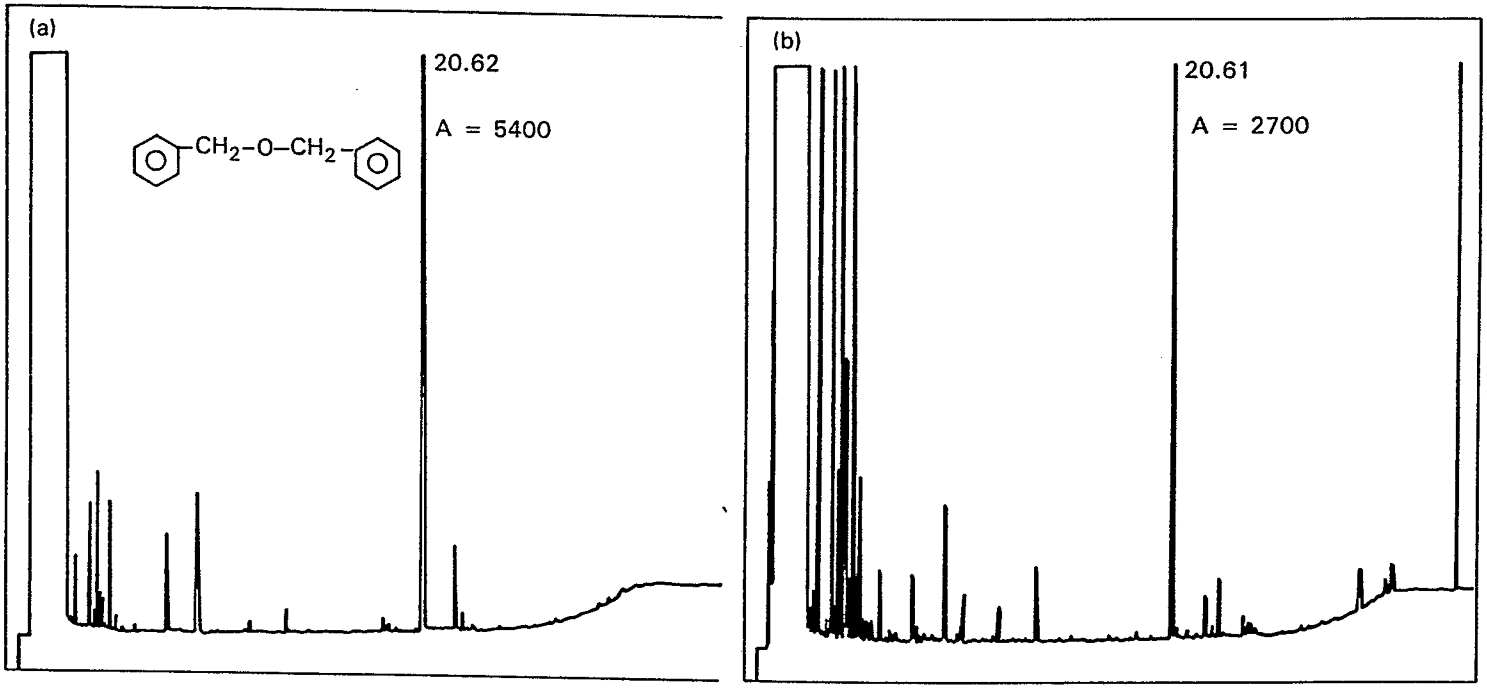

Figure 6-6. Gas Chromatogram of (a) 100 ppm Standard of Benzylether and (b) After Degradation by Cell-Free Filtrates of P. versicolor.

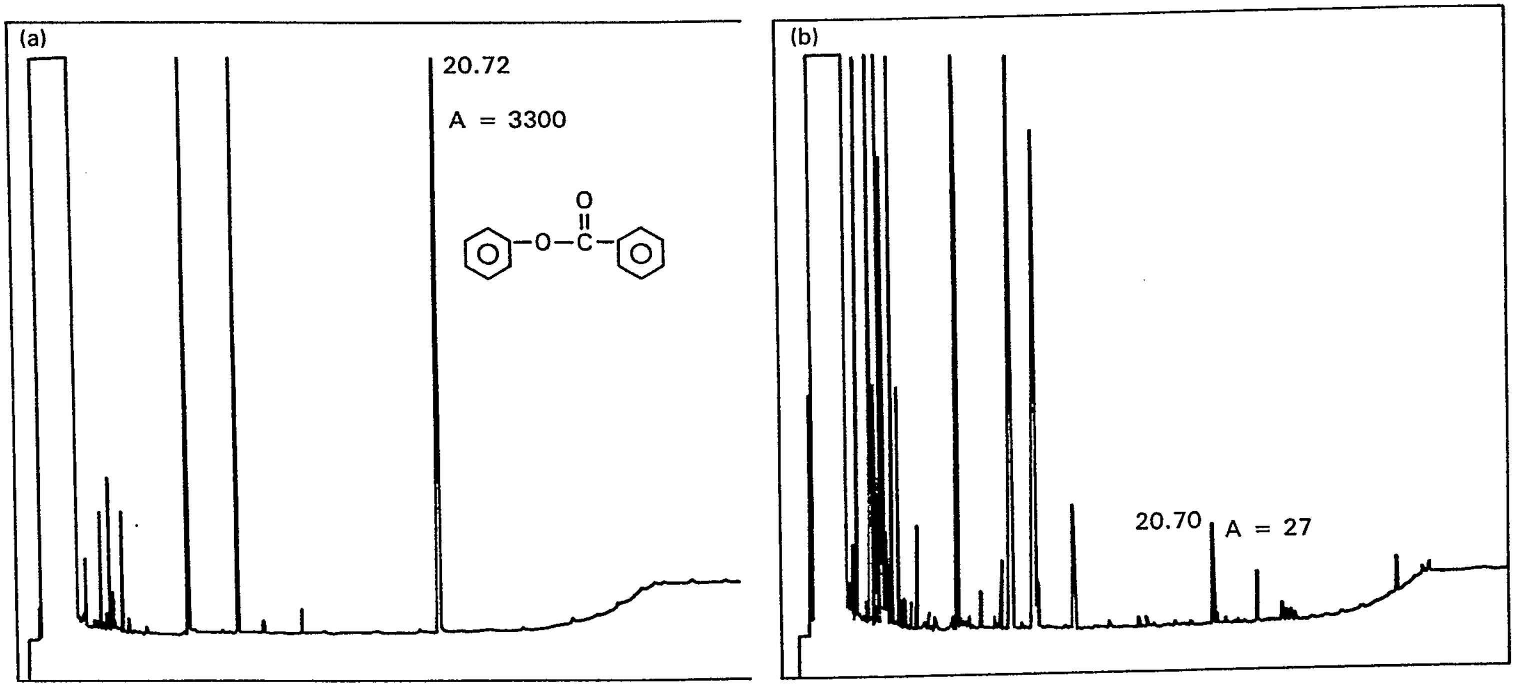

Figure 6-7. Gas Chromatogram of (a) 100 ppm Standard of Phenylenzoate and (b) After Degradation by Cell-Free Filtrates of *P. versicolor*.

microbial degradation to methane. It is currently unclear whether longer reaction times in cell-free systems would reduce product molecular weight to a range that would be amenable to further anaerobic degradation.

Immobilization and eventual recovery of enzymatic catalysts is an attractive approach that has been successfully used in other bioprocesses. We have conducted preliminary experiments to determine if laccase can be encapsulated in reverse micelles, at or near critical conditions, and remain active. Reverse micelle solutions were made using the surfactant AOT, and syringaldazine was used to determine reactivity of the enzyme after encapsulation. Analyses of these reaction mixtures showed the disappearance of syringaldazine in one of the two mixtures used. Formation of the colored oxidase product, however, was not detected. This research is scheduled to continue under alternative funding from the U.S. Department of Energy.

As mentioned in Section 2, there is now clear evidence that coals vary widely in their amenability to biosolubilization. Understanding the characteristics of coal that favor biosolubilization is an important contribution to eventual development of a viable process. We plan to apply advanced surface science techniques including X-ray Photoelectron Spectroscopy (XPS), and Scanning Electron Microscopy (SEM), to determine the surface characteristics of coals. We will compare amenable and non-amenable coals in terms of pore distribution and surface chemistry, including metals, carbon bonding, and oxidation state of constituents on and near the coal surface.

Together with Argonne National Laboratory, we have proposed work to evaluate the use of microbial swelling of bituminous coals as a first step in desulfurization. Enzymes which metabolize sulfur are not active unless bound to the cell wall or membrane of the microorganism. Our goal in this work is to the cell wall or membrane of the microorganism. Our goal in this work is to determine if a Penicillium strain can be used to swell and soften the coal so that sulfur metabolizing bacteria can gain access to the thiophenic sulfur sites.

## REFERENCES

1. Wilson, B. W., R. M. Bean, J. A. Franz, B. L. Thomas, M. S. Cohen, H. Aronson, and E. T. Gray, Jr. 1987. "Microbial Conversion of Low-Rank Coal: Characterization of Biodegraded Product." Energy and Fuels, 1:80-84.
2. Fahraeus, G. and B. Reinhammar. 1967. "Large Scale Production and Purification of Laccase from Cultures of the Fungus polyporus versicolor and Some Properties of Laccase A." Acta Chemica Scan. 21:2367-2378.

# Section 4

# PROGRESS REPORT ON THE SELECTIVE OXIDATION OF PYRITES IN COALS

T. L. Tewksbury, H. E. Carlton and J. H. Oxley

Battelle Columbus Laboratories

# ABSTRACT

A process is being developed to remove pyritic sulfur from coal by selective oxidation at relatively low temperatures in a fluidized-bed system. Essentially all the pyritic sulfur, and perhaps some of the sulfate sulfur as well, can be removed from non-caking or weakly caking steam coals ground to less than about 20 mesh at temperatures of about 725-775 F and at steam to air ratios of about 10 to 1. Heating value loss is in the range of 5 to 20 percent. The product coal is not pyrophoric and can be discharged relatively hot from the reactor apparently without significant further oxidation. Up to at least about 4 percent $SO_2$ in the fluidizing feed gas causes no significant reduction in $SO_2$ removal kinetics. Work is now underway to study continuous feeding and discharge operation as compared to the batch operation previously employed. The process may be especially suitable as an alternative to the fine coal cleaning circuits in conventional coal cleaning plants.

## INTRODUCTION

This paper is based on the second year of a study to determine the possibilities of selectively oxidizing the pyritic sulfur in coal in a low-temperature steam-air fluidized-bed process. The first results from this study were reported at the conference held last year(1), and a summary report for the first year of research issued in October(2).

The idea of oxidation of pyritic sulfur in coal is indeed old. In fact it occurs in nature and is evidenced in at least two ways. With air, the oxidation of pyritic sulfur in coal or gob piles is so exothermic that these piles often ignite spontaneously. In aqueous media, the oxidation by air (often assisted by bacteria) reacts to form highly acidic solutions which cause the well-known acid mine drainage problem that is so difficult to control.

Pyritic sulfur often, if not usually, represents more than half of the sulfur in most steam coals. In view of pending regulations relating to the acid rain issue, which often propose about a 50 percent cutback in $SO_2$ emissions, the oxidation of pyritic sulfur, if it can be done inexpensively, represents an attractive control approach now being reexamined. It is probably also necessary that the alkalinity of the ash in the coals to be treated be relatively small compared to the sulfur content, otherwise this alkalinity would tend to trap and retain the acidic sulfur dioxide formed upon oxidation.

The results of batch shallow-bed experiments carried out last year indicated that an amount of sulfur equivalent to slightly more than the pyritic sulfur in coal could be removed from two Illinois No. 6 coals with losses of heating values of 10 to 15 percent. It was found that a one to two hour treatment time would be required to remove the sulfur based on such batch operation.

With the Rosebud coal about 40 percent of the sulfur was removed without excessive loss of heating values. However, the sulfur removal was delayed from two to four hours after the coal was brought to treatment conditions, and only then was significant sulfur removed in one to two hours of additional treatment time. The reason for the less favorable results with the Rosebud coal were thought to be due to the alkaline nature of its ash.

The study being carried out this year is to determine the feasibility of carrying out such a process in continuous operation, to determine to what levels the $SO_2$ content of the off-gas could be built up without suppressing the reaction in order to be able to specify the $SO_2$ recovery process, and to study the potential of the process with respect to other coals.

## THEORECTICAL DEVELOPMENT

The theoretical basis for the process was developed previously, but is being repeated in this presentation. This is because in this era of fluidized-bed combustion, it is often not understood that significant combustion of the coal can be readily avoided by the proper choice of reaction conditions in an oxidative fluidized-bed treatment process.

The technique used to control a practical selective oxidation process is to withdraw the heat of reaction at a sufficiently rapid rate so that the ignition point of the reaction of coal with air cannot be exceeded. This can be best explained by reference to Figure 1. In this figure the rate of reaction, in this case the combustion rate, has been plotted as a function of the temperature of a single, isolated coal particle. As temperature is increased, the rate increases exponentially but then levels off at higher temperatures where diffusional control of reactants takes over. This "S" shaped curve (A) also represents the heat-generation rate for a reacting particle of coal, at least to a first approximation (the heat liberated by combustion is essentially proportional to the reaction rate). Superimposed on the heat-release rate is the approximately linear heat-transfer rate (B) from a particle to the surrounding gas and solid surfaces. The slope of the heat-transfer curve is the effective heat-transfer coefficient from the coal particle to its surroundings. In general, this heat-transfer rate curve intersects the heat generation rate curve at three points; the maximum gas temperature at which such a multivariant solution occurs is approximately the ignition temperature of the coal. In a selective-oxidation scheme, ignition of the coal must be avoided.

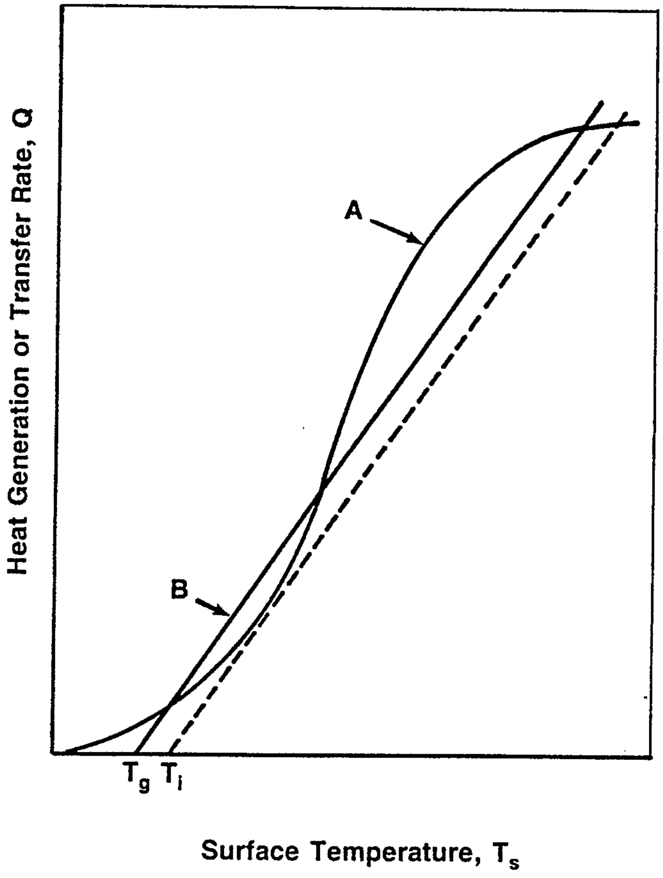

Figure 1. Heat Generation and Transfer Relationships(3)

It is generally impossible to maintain an air fluidized bed of such coal particles at intermediate temperature levels near and above the ignition temperature of coal without a diluent, i.e. the heat cannot be removed rapidly enough to control the particle temperature. In other words, the temperature of the coal would jump to a level which is represented by the intersection of the heat-transfer line and the diffusional part of the reaction-rate curve. However, with the use of a fluidized-bed reactor with mixtures of steam and air, the effective heat-transfer rate can be increased, and the overall heat-release rate reduced, to permit operation at a range of temperature conditions. The range of temperature conditions of interest are those defined by the lower point of intersection in Figure 1, i.e. the temperatures at which selective oxidation of pyritic sulfur to sulfur dioxide occurs without ignition of coal.

## RELATED EFFORTS

As far as is known, the first study indicating that pyritic sulfur might be selectively oxidized from coal in a fluidized-bed process was carried out in 1954-56 at Carnegie Institute of Technology(3). Results from the feeding of Deister rejects, containing about 8.2 percent sulfur, to such a fluidized-bed process are shown in Figure 2. The work was carried out at relatively high temperatures, and although selective burn-off of sulfur was achieved, the selectivity was not very attractive in terms of heating-value loss (organic material burn-off).

A few years later, work was published by United Engineers and Constructors concerning the desulfurization of coal in a fluidized-bed carbonizer in a 1/2-inch diameter reactor(4). With an Illinois No. 6 seam coal, containing about 4.9 percent total sulfur, up to about 70 percent sulfur burn-off could be obtained at temperatures of up to approximately 800°F. The sulfur content of the feed coal was a little more than half pyritic. Desulfurization was found to be sensitive to the particle size of the coal but not to the steam, air, or nitrogen content of the fluidizing gases. This work led to a 10-inch pilot-scale study. However, it was reported that the scale-up work was not as promising as the small-scale test work in terms of sulfur removal.

About 1970, a preoxidation process was developed to avoid coal agglomeration in the HYGAS process at the Institute of Gas Technology and some information

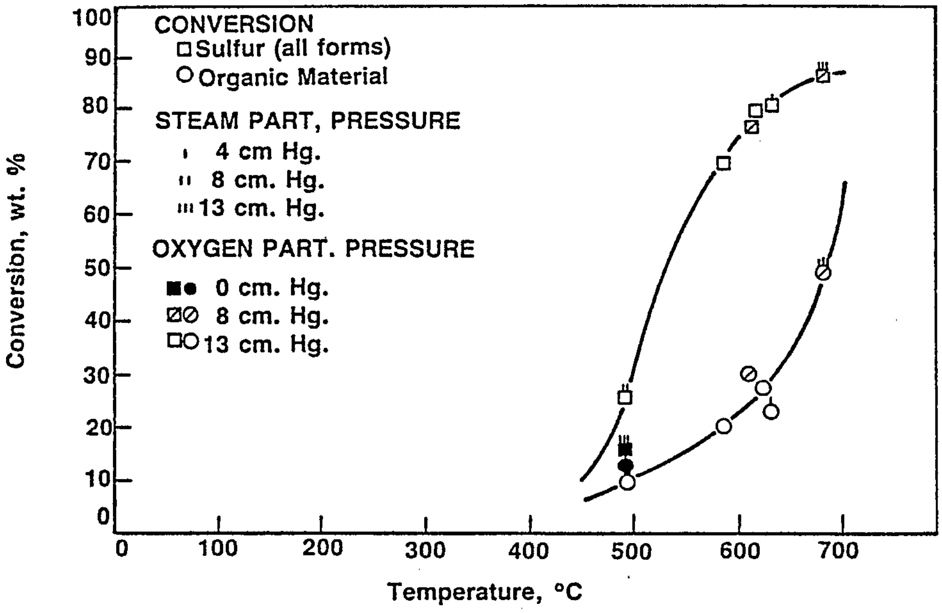

Figure 2. Sulfur and Organic Conversions of Deister Rejects in a Fluidized Bed Flash Oxidizer (3)

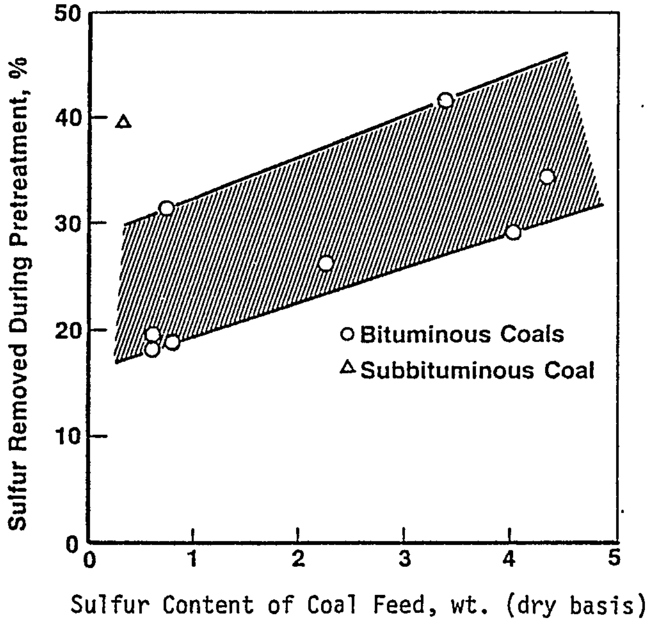

Sulfur Content of Coal Feed, wt. (dry basis)

Figure 3. Sulfur Removal From Coals By IGT Peoxidation Process (5)

on the coal desulfurization aspects of the process was reported(5). Various coals, containing from 0.02 percent pyritic sulfur and 0.85 percent organic sulfur, to 2.84 percent pyritic sulfur and 2.17 percent organic sulfur, were contacted with air at about 800°F. The sulfur-removal levels are plotted in Figure 3. Losses of heating value were probably about ten percent with eastern bituminous coals, but only about half the pyritic sulfur was removed.

Work at the Pennsylvania State University was published in 1972 on treatment of coals by air at temperatures of about 660 to 840°F in thin layers in silica boats in a muffle furnace(6). The total sulfur content of the coals ranged from 3 to 7 percent, with the pyritic sulfur content generally being about 50 percent of the total. More than 90 percent of the pyritic sulfur could be removed at 660°F in 10 minutes in some cases. Most interesting, it was reported that the rate of removal was unaffected by the build-up of $SO_2$ concentration in the air stream (to at least 10 percent).

Since the last EPRI meeting, three more references of interest have been identified. The first is based on research at California Institute of Technology, where oxidation at temperatures of about 320 F was used to increase the ion-exchange capability of coals(7). It was said that the pyrite was converted to iron sulfate, which was subsequently leached out of the coal with weak acid. Work at California State University showed about half the pyritic sulfur in coals could be removed by mixtures of steam and air, the balance could be removed by magnetic treatment of the oxidized coal, in which at least part of the pyrite had been converted to magnetite(8). A third paper by workers at the USGS and at Howard University on careful oxidation of relatively pure pyrites showed optimum temperature conditions for pyritic oxidation to be about 400 C, and reported that the iron sulfate initially formed could be subsequently fully oxidized to iron oxide(9).

## PREVIOUS RESULTS

At the last meeting in Palo Alto, some of the results obtained under the support of EPRI were reported. Three fuels had been fairly well characterized in terms of response to a selective oxidation approach at that time -- a coal from the Peabody Christian County mine in the Illinois No. 6 seam which had already been cleaned by conventional washing, a coal from the Peabody River King mine also in the Illinois No. 6 seam, and a coal from the Rosebud seam in Montana. These coals were ground and seived before use. Typical proximate analyses and sulfur form analyses for these fuels, as well as that for an Illinois No. 2 coal studied this year, are listed in Table 1.

The experimental equipment used at that time is shown schematically in Figure 4. Fluidizing air and steam were metered into the system and then passed through a preheater furnace. These preheated fluidizing gases then passed into the reactor, where they reacted with the coal. As the fluidizing gases left the reactor, a sample was continuously extracted for monitoring the $SO_2$ content of the exhaust gases. The off-gases were exhausted through a stack. No attempt was made to establish an overall material balance. The reactor was only charged once during the run, i.e. at the beginning of the experiment about five pounds of coal were added, but small samples of the bed were withdrawn periodically during the run by means of a dip tube.

Figure 5 shows the heating values lost to obtain a given sulfur removal for the various coals studied. The Christian County coal reacted as expected. Initially, the sulfur is selectively oxidized from the coal and presumably when all of the mineral sulfur is removed, the coal oxidizes without further reduction of the sulfur on a Btu basis. Forty to fifty percent of the sulfur could be removed with little loss in heating value.

The River King coal responded differently to such treatment. Early in the experiment heating value was lost faster than sulfur. This may be due, at least in part, to volatilization of organic components in the coal. Later, the sulfur was removed preferentially. While not shown in the results plotted, if more than 60 percent of the sulfur was removed, a substantial loss in heating value was then observed. About 60 percent of the sulfur in the River King coal sample was pyritic. These initial unfavorable burn-off phenomena were not observed with the Christian County coal, but they were consistently observed with the River King, and also the Rosebud, coals.

With Rosebud coal, analysis indicated an apparent substantial increase in sulfur content on heating to temperature. During the first few hours of a typical experiment with Rosebud coal, sulfur appeared to be lost at about

## Table 1

## ANALYSIS FOR SULFUR CONTENTS IN FEED COALS

| | | Proximate Analysis | | | | | Sulfur Forms | | |
|---|---|---|---|---|---|---|---|---|---|
| Run No. | Coal | Moisture % | Ash % | Volatile % | Fixed Carbon % | Sulfur % | Pyritic % | Sulfate % | Organic % |
| 2-8 | CC | 12.4 | 9.8 | 35.3 | 42.5 | 3.7 | 1.18 | 0.30 | 2.18 |
| 2-8 | CC | 11.9 | 9.6 | 36.0 | 42.6 | 3.6 | 1.05 | 0.34 | 2.18 |
| 2-8 | CC | 12.4 | 10.0 | 35.3 | 42.2 | 3.6 | 1.30 | 0.28 | 1.99 |
| 10 | RK | 7.4 | 22.5 | 33.3 | 36.8 | 4.9 | 2.74 | 0.16 | 1.99 |
| 11 | RB | 19.4 | 11.3 | 29.9 | 39.4 | 1.7 | 1.22 | 0.01 | 0.45 |
| 12 | RB | 19.6 | 12.0 | 29.8 | 38.6 | 2.2 | 1.93 | 0.02 | 0.21 |
| 13 | RK | 7.5 | 21.5 | 32.6 | 38.4 | 5.4 | 3.15 | 0.15 | 2.15 |
| 14 | RB | 18.7 | 10.1 | 38.0 | 33.3 | 1.6 | 1.03 | 0.02 | 0.57 |
| 23 | CC | 12.0 | 9.3 | 35.5 | 43.3 | 3.6 | 0.90 | 0.40 | 2.27 |
| 4-A | CC | 11.3 | 10.5 | 34.8 | 43.5 | 3.7 | 0.95 | 0.77 | 1.97 |
| 6-A | RK | 7.8 | 19.7 | 32.9 | 39.7 | 4.8 | 1.77 | 0.77 | 2.25 |
| 10-A | CC | 12.1 | 9.3 | 34.7 | 43.9 | 3.3 | 0.66 | 0.72 | 1.94 |
| 17-A | IL | 10.4 | 5.5 | 38.1 | 45.9 | 2.6 | 1.72 | 0.06 | 0.84 |
| 18-A | IL | 13.0 | 5.3 | 36.0 | 45.7 | 2.7 | 1.54 | 0.21 | 0.95 |
| 19-A | IL | 13.5 | 5.3 | 35.9 | 45.4 | 2.6 | 1.54 | 0.22 | 0.86 |

CC - Precleaned Christian County (#6)
RK - ROM River King (#6)
RB - Rosebud Seam
IL - Precleaned Illinois (#2)

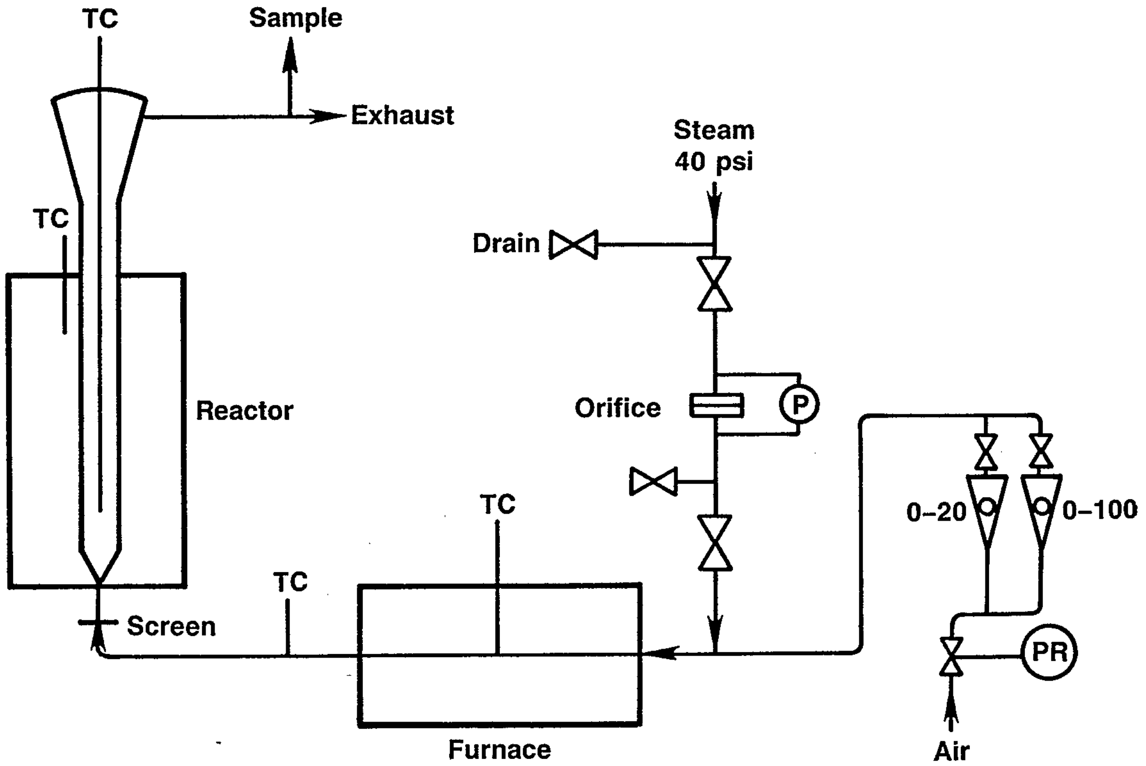

Figure 4. Flow Diagram For Original Experimental Setup

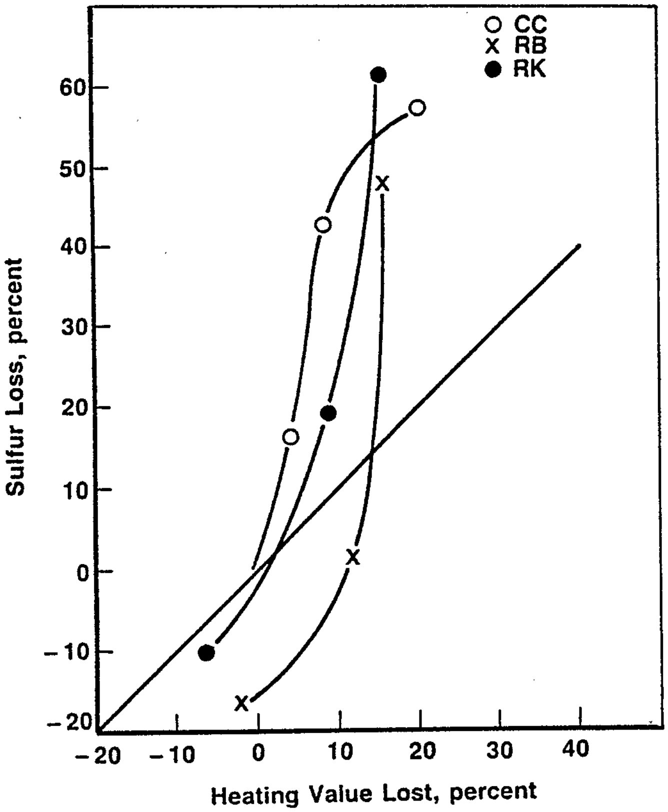

Figure 5. Comparison of Sulfur Removal and Heating Value Lost During Treatment at Selected Conditions (1)

the same rate as the loss in heating value, with a loss of about 15 percent of each. Then, and only then, was the sulfur attacked preferentially. The experiment was somewhat arbitrarily terminated when the $SO_2$ content of the off gas dropped to about 4000 ppm. At that time, however, sulfur was still being oxidized faster than the coal was being burned, and somewhat longer treatments might further reduce the sulfur content on a Btu basis. The amount of sulfur removed was generally less than the fraction analyzed as pyritic sulfur over the range of conditions studied.

## NEW RESULTS

During the past year, the all-glass equipment used during the first year of study was replaced with a new stainless-steel unit, shown schematically in Figure 6. The new reactor included an internal cyclone for returning elutriated fines to the fluidized bed, a hopper and valve system for periodically charging fresh coal to the unit during a run, and a bed withdrawal arrangement at the bottom of the unit. By periodic withdrawal of bed, and addition of feed, continuous operation could be approached as closely as desired. Provision was also made for addition of $SO_2$ to the feed gases.

Some of the results with semi-continuous operation in the new equipment are shown as unshaded squares and triangles in Figure 7 for a Christian County coal feed. The temperature of operation was a nominal 750 F, although significant perturbations occurred with a one-pound feed addition per hour operation, and even with a one-half pound replenishment every half hour. Temperature drops of 50-75 F, and 25-50 F, for periods of time of 10-20 minutes were encountered due to heat input limitations by the reactor system. It will be noticed that although fuel value losses were very low, at the same time sulfur removal levels were of marginal interest. It is believed that this problem results both from mixing of fresh feed with one hour or less treatment times into the product being withdrawn, as well as due to the temperature excursions. However, these interrelationships still need to be further investigated. To verify that the new reactor was capable of duplicating previous results with the glass unit, the equipment was then run for six hours without bed replenishment, and the results shown in Figure 8, as shaded data symbols (circles). The results without bed replenishment are obviously very similar to the results obtained last year.

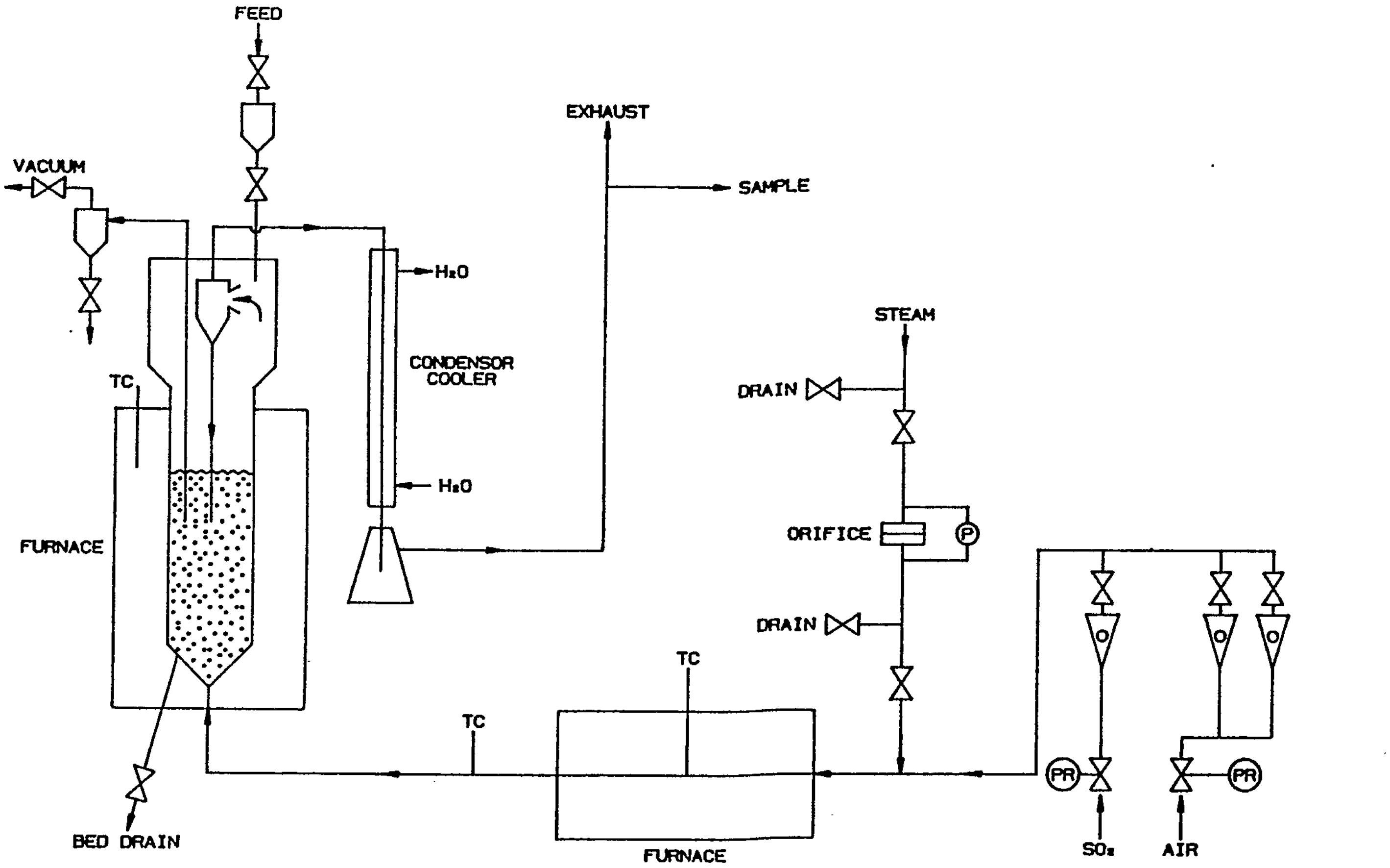

Figure 6. Flow Diagram for the Modified Setup

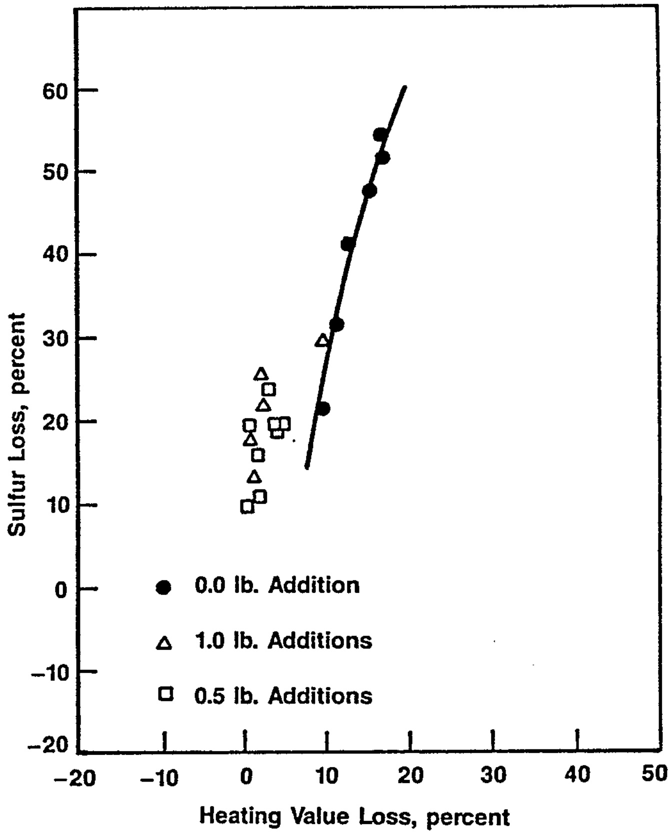

Figure 7. Sulfur Removal and Heating Loss for Christian County Coal at 750°F Nominal Temperature

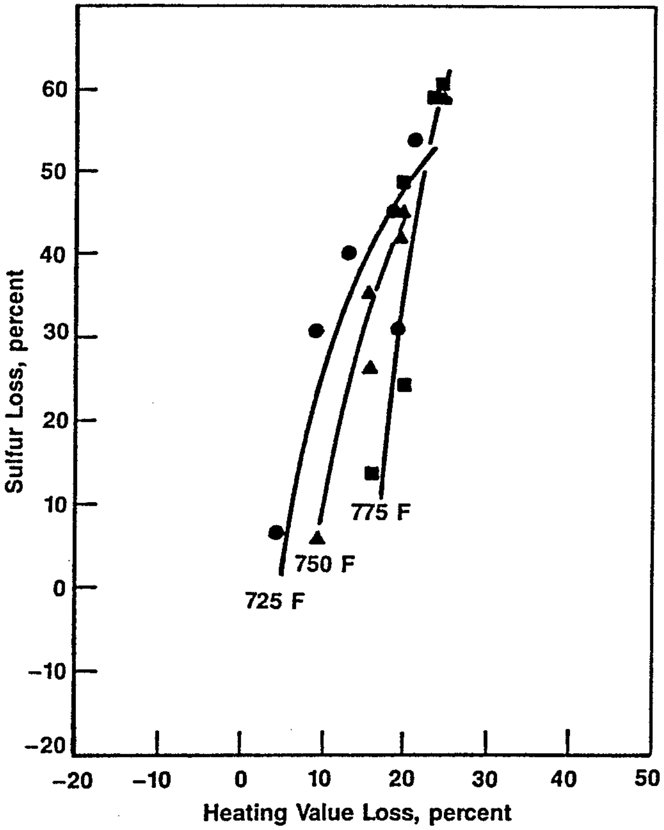

Figure 8. Sulfur Removal and Heating Loss for Illnois No. 2 Coal Without Bed Replenishment

Other studies carried out this year with an Illinois No. 2 coal, whose analysis was shown in Table 1. Three temperature levels were studied to be sure that the near optimum temperature levels measured last year in the glass equipment were being reproduced in the steel equipment. The results are shown in Figure 8. No bed additions were made during these multihour runs. It can be seen that the Illinois No. 2 coal can also be effectively desulfurized, the selectivity and degree of desulfurization being more temperature dependent than previously defined.

Other work this period involved adding $SO_2$ to the feed gas to obtain an independent measure of the effect of that variable. Levels of 4 percent $SO_2$ in the feed gas seemed to have little effect. At 10 percent $SO_2$ in the feed gas, the desulfurization efficiency was reduced by perhaps 20 percent of the value that would otherwise have been obtained. Work on various feed particle sizes of Christian County coal showed no significant effect of particle size on desulfurization or ash content. In addition, because the Christian County coal on hand had been kept almost two years in relatively unprotected storage, and because it had been reported that it already had been physically cleaned before receipt from the supplier, the sulfur as sulfate content had now climbed to almost one percent. It was shown in some experiments with this aged coal that much of the sulfate sulfur could also be selectively oxidized, with the sulfur presumably being liberated as $SO_2$.

Heating value lost, at least as determined by ash balances, was sometimes a little higher in general than that found in full batch operation last year with the all glass unit. On the other hand, in semicontinuous operation, heating value losses based on ash balances were almost negligible. Losses of heating values based on overall material balances, however, still give less than satisfactory agreement with those based on an ash balance.

## CONCLUSIONS

### Based on First Year Results

- Overall the results are most encouraging - up to 60 percent of the sulfur in River King coal, up to 40 percent of the sulfur in precleaned Christian County coal, and 50 percent of the sulfur in Rosebud coal could be removed with Btu losses in the range of ten to fifteen percent.

- It would appear that the fluidized-bed selective oxidation process is attractive for the desulfurization of coal fines in general, and may be especially of interest where sulfur emission regulations could be met by removal of pyritic sulfur only.

Based on Second Year Results

- This year the process was also found to be similarly effective on an Illinois No. 2 coal, and it also appears effective for at least some sulfate removal from coals.

- It would appear that up to at least about 4 percent of $SO_2$ in the fluidizing gases can be tolerated without retarding the desulfurization kinetics.

- It may be desirable for a commercial reactor design to involve several stages if a continuous-fed and continuous-discharge system is to be employed.

## REFERENCES

1. J. H. Oxley, H. E. Carlton and J. Klingspor, "Selective Oxidation of Coal Pyrites in Coals by Steam Air Mixtures in a Fluidized Bed", Proceedings of the Eleventh Annual EPRI Contractors' Conference on Clean Liquid and Solid Fuels, EPRI AP-5043-SR, April 1986.

2. H. E. Carlton, J. Klingspor and J. H. Oxley, "Selective Oxidation of Pyrites in Coal", Battelle Report EPRI AP-4873, October 1986.

3. J. H. Oxley, "The Reactions of Sulfur During the Gasification (Oxidation) of Coal", Ph.D. Thesis, Carnegie Institute of Technology, 1956.

4. J. K. Jacobs and J. D. Mirkus, "Coal Desulfurization in a Fluidized Bed Carbonizer", Ind. Engr. Chem., 50 (1), January 1958, pp 24-26.

5. H. L. Feldkirchner and F. C. Schora, Jr., "Coal Desulfurization Aspects of the Hygas Process", Paper presented at the Second International Conference on Fluidized Bed, Hueston Woods State Park, Ohio, October 4-7, 1970.

6. R. K. Sinha and P. L. Walker, Jr., "Removal of Sulfur from Coal by Air Oxidation at 350-450 C", Fuel, 51, April 1972, pp 125-128.

7. K. K. Chang, R. C. Flagen, G. R. Gavalas, and G. R. Sharma, "Combustion of Calcium-Exchanged Coals", Fuel, 65, January 1986, pp 75-80.

8. S. C. Tsai, "Chemical Desulfurization of West Virginia Coal Using Air and Steam", Ind. Engr. Chem. Proc. Des. Dev., 25, January 1986, pp 126-132.

9. A. N. Thorpe, R. E. Senftle, C. Alexander, F. T. Dulong, R. E. LaCount, and S. Friedman, "Oxidation of Pyrite in an Anoxic Atmosphere", Fuel, 66, February 1987, pp 147-153.

## Section 5

# COAL UPGRADING BY SELECTIVE AGGLOMERATION

W. Pawlak, A. Turlak, Y. Briker and B. Ignasiak
Alberta Research Council

## ABSTRACT

Laboratory-scale research conducted at the Alberta Research Council and supported by U.S. Electric Power Research Institute on beneficiation of coals by oil agglomeration has resulted in the development of AGLOFLOAT and AGFLOTHERM processes. This paper summarizes the results of agglomeration studies of American and Canadian coals of different ranks, and describes the results of work on

- desulfurization and deashing of coals by the AGLOFLOAT process,
- utilization of tar refuse in oil agglomeration, and
- oil recovery from agglomerates by the AGFLOTHERM process.

## INTRODUCTION

In recent years the emphasis in coal preparation has been placed on reducing the sulfur content of coal and improving the recovery of combustible material. Removal of sulfur is probably the most difficult problem in coal preparation. Sulfur in coal exists in three forms: organic, pyritic and as sulfates. Organic sulfur is an integral part of the coal matrix and can be removed by chemical cleaning processes. Pyritic sulfur may be removed to varying extents by physical cleaning. The amount of sulfate sulfur, except for oxidized or weathered coals, is less than 0.1% and is not an important factor in coal clean-up.

Chemical methods for coal clean-up are capable of removing both pyritic and organic sulfur, but the degree of desulfurization depends on the particular method used. Chemical desulfurization usually causes a significant decrease in coal volatile matter and heating value. The operating cost of chemical methods tend to be prohibitively high and some of these processes can potentially produce toxic wastes. Therefore, increased attention is being given to the development of advanced physical coal cleaning techniques such as froth flotation, selective floculation, oil agglomeration, magnetic separation, etc. Physical cleaning methods are capable of removing only pyritic sulfur that is liberated from the coal during comminution. The degree of mineral matter (pyrite) removal is dependent upon mineral matter size and distribution, coal particle size, and other physical characteristics.

Oil agglomeration, one of the physical cleaning methods, is based on the principle that coal particles are naturally hydrophobic and can therefore be agglomerated and separated from hydrophilic mineral matter by addition of a suitable bridging liquid that wets the carbonaceous consitutents. The work carried out at the Alberta Research Council over the last six years has shown that by using light oils or appropriately formulated mixtures of heavy oils with light oils, it is possible to successfully agglomerate coals of different ranks in terms of deashing and dewatering and with high recovery of combustibles. However, a questionable aspect of the agglomeration process is its tendency to retain pyrite in the clean coal. The surface of clean pyrite tends to be hydrophobic, and oil agglomeration experiments have shown that pyrite particles were readily wetted by the bridging liquid and were agglomerated. To overcome this deficiency a modified oil agglomeration process ("Aglofloat") has been developed and investigated at the Research Council laboratories. The process has been found to be very effective for ash and pyritic sulfur removal and clean-up of waste materials containing heavy hydrocarbons; at the same time the process is characterized by high recovery of combustibles. The modified "Aglofloat" process followed by size enlargement and thermal treatment of agglomerates seems to be very promising for simultaneous beneficiation of low rank subbituminous coals and heavy non-conventional oils. It results in significant reduction in ash and moisture contents and in an increase in calorific value of agglomerated coal, as has been reported earlier (1).

This communication summarizes the results of studies carried out at the Research Council in 1986 in the following areas:

- desulfurization and deashing of coals by the AGLOFLOAT process,
- utilization of highly contaminated and viscous tars in oil agglomeration, and
- oil recovery from agglomerates

## EXPERIMENTAL

Agglomeration experiments were carried out with selected American and Canadian coals of various rank. The coals were crushed and pulverized to a top size of 0.6 mm. Diesel oil, kerosene and blends of bitumen and coal tar with some light additives were applied as bridging liquids. AGLOFLOAT experiments were performed in a standard Denver flotation machine equipped with a 2.5 l flotation cell. Single stage AGLOFLOAT experiments were carried out as shown in Fig. 1. The experimental details of the two-stage procedure, which also includes interstage wet grinding, is depicted in Fig. 2. Agglomeration experiments with subbituminous coal were performed in small, stirred tanks according to standardized procedures developed and used for subbituminous coals (1,2). The oil recovery tests were performed in an apparatus designed and built in the Research Council laboratories. A detailed description of the unit and its operation has been given earlier (3).

Standard analytical procedures were used in analysis of feed coals, agglomerates, and de-oiled product.

## RESULTS AND DISCUSSION

### Desulfurization of High Sulfur Coals

Recent work on physical coal cleaning at the Alberta Research Council has focussed mainly on inorganic sulfur removal. A modified agglomeration-flotation process, AGLOFLOAT, has been developed and its effectiveness has been tested using several different rank coals characterized by varying contents and proportions of pyritic and organic sulfur. The origin of the test coals, their ash contents, sulfur distributions and calorific values are presented in Table 1.

Results of studies with Montana subbituminous coal agglomerated with bitumen and heavy oil based bridging liquids are summarized in Table 2. Initially, the experiments were carried out according to standardized procedures developed and used for subbituminous coals (1,2). Microscopic examination revealed excellent separation between the created coal flocs and pyrite particles at very early stages of the agglomeration process. However, at that point the size of microagglomerates was still small and this precluded the usage of screening techniques for separation. To increase the size of agglomerates, the agitation time was extended to 20 minutes and this resulted in the incorporation of liberated pyrite particles into the agglomerates. Only a slight decrease in total sulfur from 4.4% to 3.8% was observed. A better inorganic sulfur removal was observed when pyrite depressants were used in the agglomeration process (i.e., sulfur content was reduced from 4.4% in the feed coal to 3.1% in agglomerates).

The observation that separation of coal flocs at very early stages of the process could improve the efficiency of pyrite removal led to the development of the agglomeration-flotation (AGLOFLOAT) process; the schematics of which are presented in Figure 1. Application of the early version of this process to Montana coal resulted in 50% reduction in ash content and a decrease in total sulfur content from 4.4% in the feed coal to 1.6% in the agglomerated product. About 95% of inorganic sulfur was removed by the AGLOFLOAT process. Combustible material recovery generally exceeded 92%. Results of the tests with Montana subbituminous coal indicated that the AGLOFLOAT process might be applicable for deashing and desulfurization of subbituminus coals.

Five samples of bituminous run-of-mine or pre-cleaned coals were tested using various modifications of the "Aglofloat" process.

The results of cleaning of cyclone overflow from the Homer City Coal Cleaning Plant are summarized in Table 3. Initially, the experiments were performed using the single stage AGLOFLOAT procedure. The process resulted in about a 70% ash reduction and about 23% of total sulfur removal which corresponded to 40% pyritic sulfur rejection. The combustible material recovery was generally greater than 96%. However, at 40% pyrite rejection the $SO_2$ emission for clean product was still above EPA standards. The AGLOFLOAT experiments performed in the modified system were successful at producing a compliance coal. About 80% of pyritic sulfur was removed which resulted in lowering the $SO_2$ emission to 1.00 lbs per million Btu; this is significantly below EPA standards.

The AGLOFLOAT process has also been employed for cleaning Kentucky No. 9 raw coal. Initially the objective of the work was to maximize pyritic sulfur removal and achieve high (90-95%) combustible material recovery. Subsequently, the additional task of obtaining a product with very low ash content (below 5%) was added. Preliminary experiments were carried out using the single stage AGLOFLOAT process type and 600$\mu$m by 0 coal sample. The results presented in Table 4 showed a reduction in ash and total sulfur contents from 14.6% to 6.8% and from 5.08% to 3.62%, respectively. About 40% of pyritic sulfur was retained in the product and there were indications that a considerable portion of this pyrite was not liberated during grinding. It was expected that better liberation of mineral matter resulting from deeper grinding would increase ash and sulfur rejection. Therefore, a series of experiments were carried out with a sample which was dry ground to -74$\mu$m. Surprisingly, the degree of deashing and desulfurization was lower with this sample than with the coarser sample (600 $\mu$m by 0). A similar negative effect has been reported in a study on the effect of dry grinding on the flotation of coals (4). To improve the quality of the product, two stage AGLOFLOAT experiments were performed. The two-stage procedure consists of the standard "Aglofloat" process (using 600$\mu$m x 0 coal sample) followed by wet grinding of the precleaned microagglomerates and reagglomeration. In the two-stage AGLOFLOAT process Kentucky No. 9 coal was cleaned from 14.6% ash and 5.08% total sulfur to 4.4% ash and 2.81% sulfur with high combustible material recovery of about 94%. Despite the fact that 84% of pyritic sulfur present in the feed coal was removed, $SO_2$ emissions remained high because of the high organic sulfur content in this particular coal.

The two-stage AGLOFLOAT process was also tested for desulfurization of Devco Metallurgical, Devco Thermal and Pittsburgh Seam coals. The Pittsburgh Seam sample was a run-of-mine coal; the other two coals were precleaned. The degree of deashing and desulfurization was dependent upon the initial ash and sulfur contents in feed coals (see Tables 5 and 6). For Pittsburgh Seam coal, a 44% reduction in total sulfur (74% reduction in pyritic sulfur), 85% reduction in ash and about 92% combustibles recovery were obtained by the two-stage AGLOFLOAT process. For precleaned Devco Metallurgical coal, the AGLOFLOAT process resulted in further ash reduction and about 60% pyritic sulfur removal (Table 6).

The potential of the two-stage AGLOFLOAT process for deashing and desulfurization of different rank coals seems to be very promising. It also seems that the efficiency of the process can be further improved particularly in terms of pyritic sulfur removal.

## Utilization of Tar Refuse in Oil Agglomeration

Recently completed laboratory tests at the Alberta Research Council resulted in the development of a process for recovery and utilization of tar refuse contaminated with large quantities (30% to 60%) of solids. The tars were composed of very heavy hydrocarbons and the moisture content in the refuse was 15% to 20%. The Research Council AGLOFLOAT process was modified to handle contaminated viscous binder. A block diagram of the developed process is given in Figure 3. The refuse material, which contains 20% to 30% tar, up to 60%

solids and a substantial amount of water, is introduced into a hot slurry of fine coal and water. The temperature is maintained at the level required to lower the viscosity of the binder so that the agglomeration process can be initiated. After sufficient agitation the agglomerates are separated from the slurry by froth flotation. A typical material balance for the process is given in Table 7. The very high recoveries of tar and chars from the refuse were accompanied by high selectivity which resulted in the generation of a solid fuel which had improved properties compared to the coal used in process. The tailings from the process contained a negligible amount of tar and posed no disposal problems. Important process variables were the coal/tar ratio, slurry temperature, pH and agitation time. Preliminary data on the effects of some of these variables on product properties are presented in Figures 4-6. The fact that the modified "Aglofloat" process can be used to recover and utilize the hydrocarbon contents of refuse material, clean the material and, at the same time, beneficiate the coal underlines the versatility and potential of the process.

## Oil Recovery from Agglomerates

To agglomerate subbituminous coals, a significant amount of bitumen or heavy oil based bridging liquid has to be used. This fact precludes the application of oil agglomeration on a commercial scale because of the cost of oil. Therefore, major effort has been devoted to lowering the oil consumption through recovery of oil from agglomerates. The process for recovering the distillable part of the bridging liquid from agglomerates has been studied at the Research Council over past three years. The thermal treatment of agglomerates at optimum conditions resulted in

- high recoveries of oils (i.e., amounts of recovered oil were higher than would be expected from bridging liquid composition),
- drastic reduction in moisture capacity of de-oiled agglomerates, and
- insignificant decrease in calorific values of de-oiled agglomerates compare to oil-loaded agglomerates

At 350°C, the whole diluent and up to 50% of bitumen (heavy oil) were recovered in the form of distillable, asphaltene free oil. The results on thermal treatment of the agglomerates have been reported earlier (3). Recent work on the recovery of oil from agglomerates was aimed at evaluating the properties of recovered oils. Two samples of agglomerates which were generated with blends of bitumen and diesel oil in different ratios, were used in this study. Properties of feed coal, agglomerates and de-oiled agglomerates are presented in Table 8. Heat treatment of agglomerates at a temperature of 350°C resulted in about 65% oil recovery for the blend of bitumen and diesel oil in ratio 3:2 and about 54% recovery when a mixture of bitumen and diesel in ratio 4:1 was used as a bridging liquid. For both bridging liquids, the moisture capacity of de-oiled agglomerates was drastically reduced, while calorific value slightly decreased compared to the oil-loaded agglomerates. Table 9 compares the properties of the oils distilled off from bridging liquids at 525°C using the standardized distillation procedure with the properties of oils recovered from the agglomerates during thermal treatment at 350°C. The amount of oil recovered from agglomerates at 350°C was essentially the same as that obtained during ASTM distillation of bitumen at 525°C. The amount of light hydrocarbons distilled off from agglomerates at 350°C was almost twice as high as that from direct distillation of bitumen at the same temperature. The reasons for the improved distillable recoveries during heat treatment of agglomerates as compared to direct distillation of the raw hydrocarbon feedstock are not clear; it may be a physical and/or chemical phenomenon. It is possible that due to the high dispersion of the bitumen on the surface of coal particles which form the agglomerates and because of the carrier gas used, very efficient distillation takes place which results in evaporation of considerable amounts of +350°C fraction. The distillation curves of the recovered oils presented in Fig. 7 seem to support such speculation. API gravity of the oils recovered from agglomerates is in the range 26.1 to 23.1, which is typical for NO. 2 fuel oil.

## CONCLUSION

The results of studies on oil agglomeration carried out at the Alberta Research Council lead to the following conclusions:

1. Significant ash and inorganic sulfur removal can be achieved through a modified oil agglomeration process called AGLOFLOAT. The process results in

    - Very low bridging liquid addition (5% or less).
    - Reduction in mineral matter by (50%-85%).
    - High recovery of combustible material (90%-96%).
    - Removal of inorganic sulfur (60%-95%).

2. The AGLOFLOAT process operated in hot mode can be used to recover and utilize the hydrocarbon contents of refuse material, clean the material and beneficiate the feed coal.

3. Results of tests on oil recovery from agglomerates produced from subbituminous coals show that

- Quantities of recovered distillable oils are higher than would be expected on the basis of the volatility of oil mixture used for agglomeration.
- API gravities of recovered oils are comparable to No. 2 fuel oil.
- Moisture capacity of the de-oiled agglomerates was reduced by about 67%.

## REFERENCES

1. W. Pawlak, A. Turak, J. Janiak, Y. Briker and B. Ignasiak, Oil Agglomeration of Low-Rank Coals and Development of Method for Recovery of Oil from Agglomerates, Proc. 11 Annual Clean Liquid and Solid Fuels Contractors' Conference, May 1986, Palo Alto, California, U.S.A.

2. B. Ignasiak, Process for Selective Agglomeration of Subbituminous Coal Fines, Canadian Patent 1 216 551, Jan. 13, 1987.

3. W. Pawlak, R. Goddard, J. Janiak, A. Turak and B. Ignasiak, Oil Agglomeration of Low Rank Coals, Proc. 10 Annual Clean Liquid and Solid Fuels Contractors' Conference, April 1985, Palo Alto, California, U.S.A.

4. K.J. Miller, Fine Grinding and Flotation to Desulfurize Coal, Proc. The First International Conference on Processing and Utilization of High Sulfur Coals, October 1985, Columbus, Ohio, U.S.A.

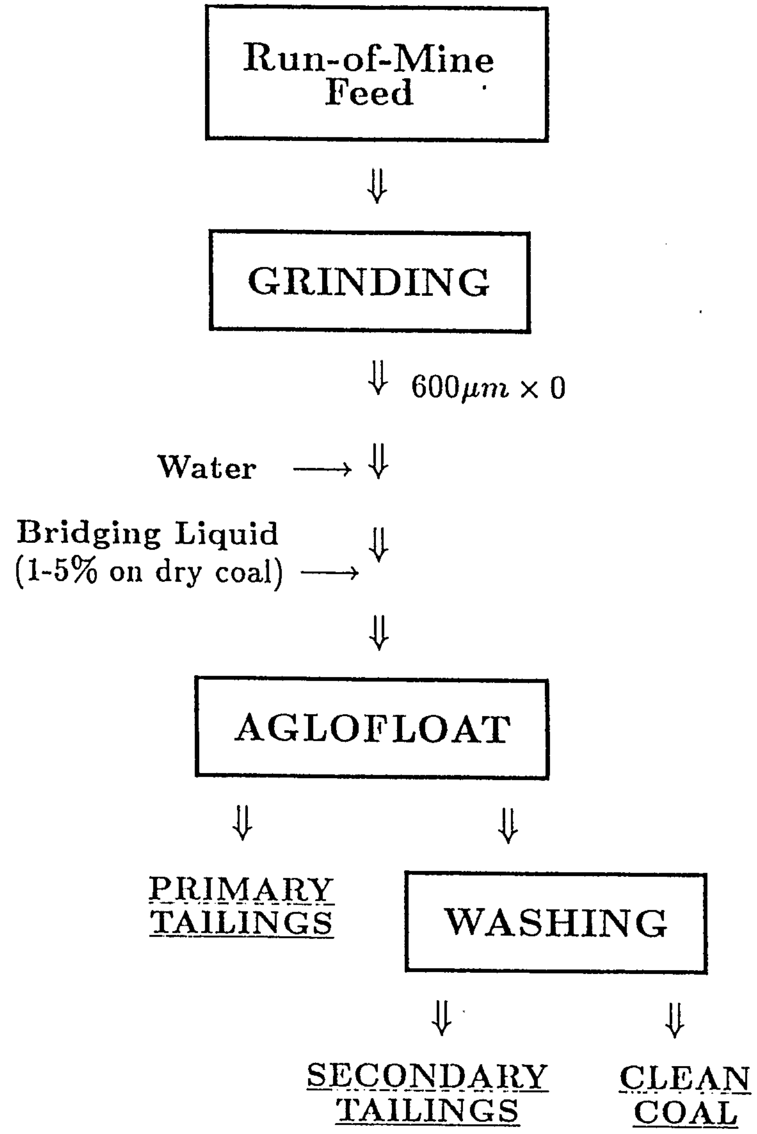

Figure 1. Schematic Illustration of the Single Stage Aglofloat Process

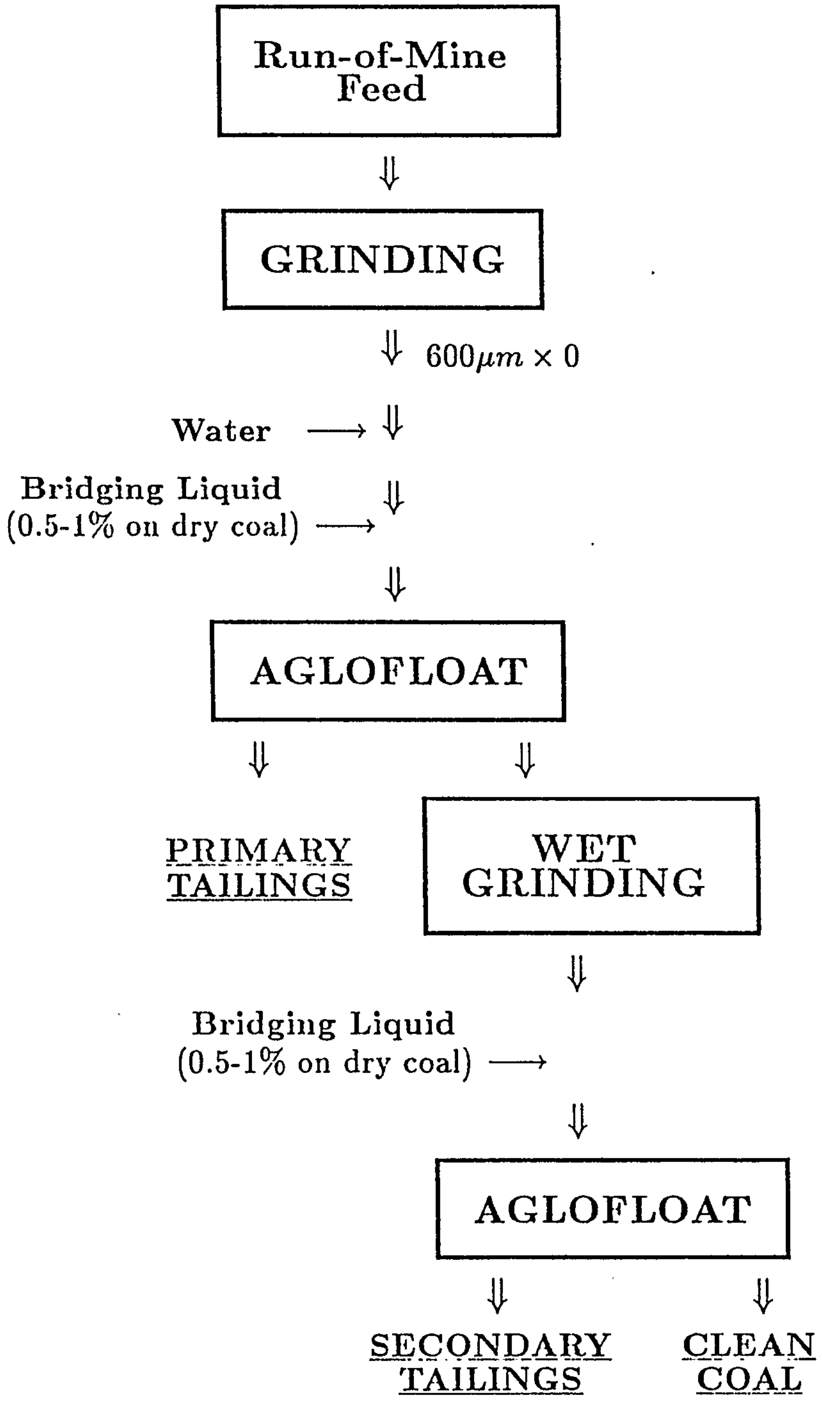

Figure 2. Schematic Illustration of the Two-Stage Aglofloat Process with Interstage Wet Grinding

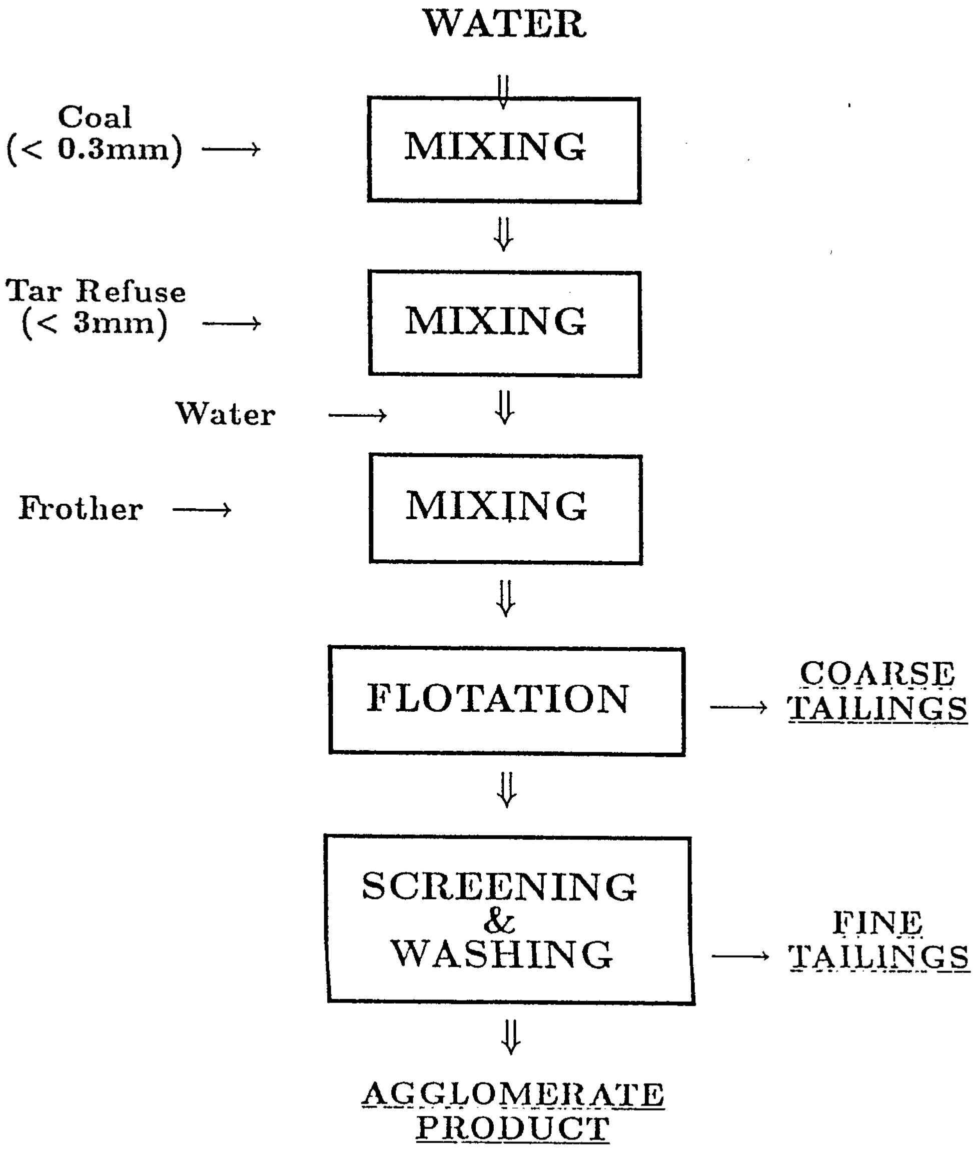

Figure 3. The Hot Aglofloat Process

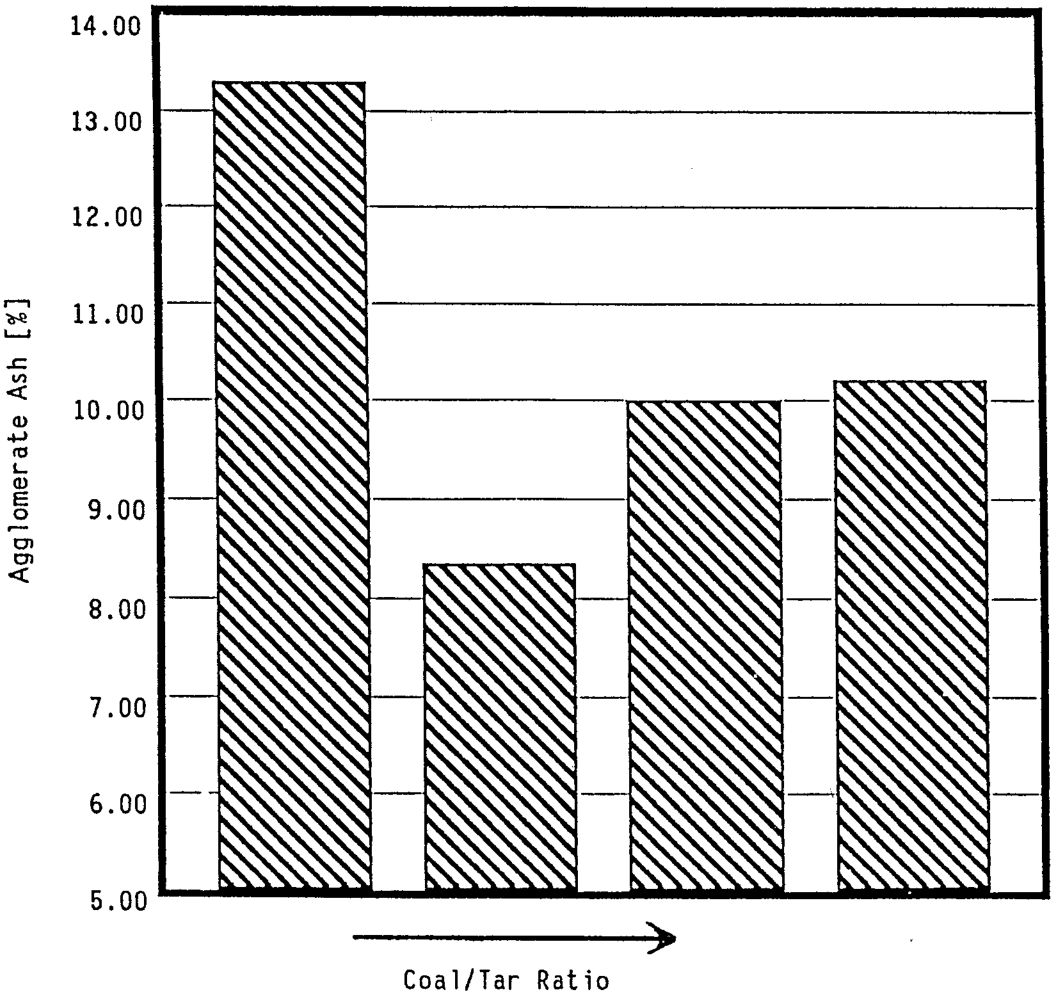

Figure 4. Effect of Coal/Tar Ratio on Agglomerate Ash

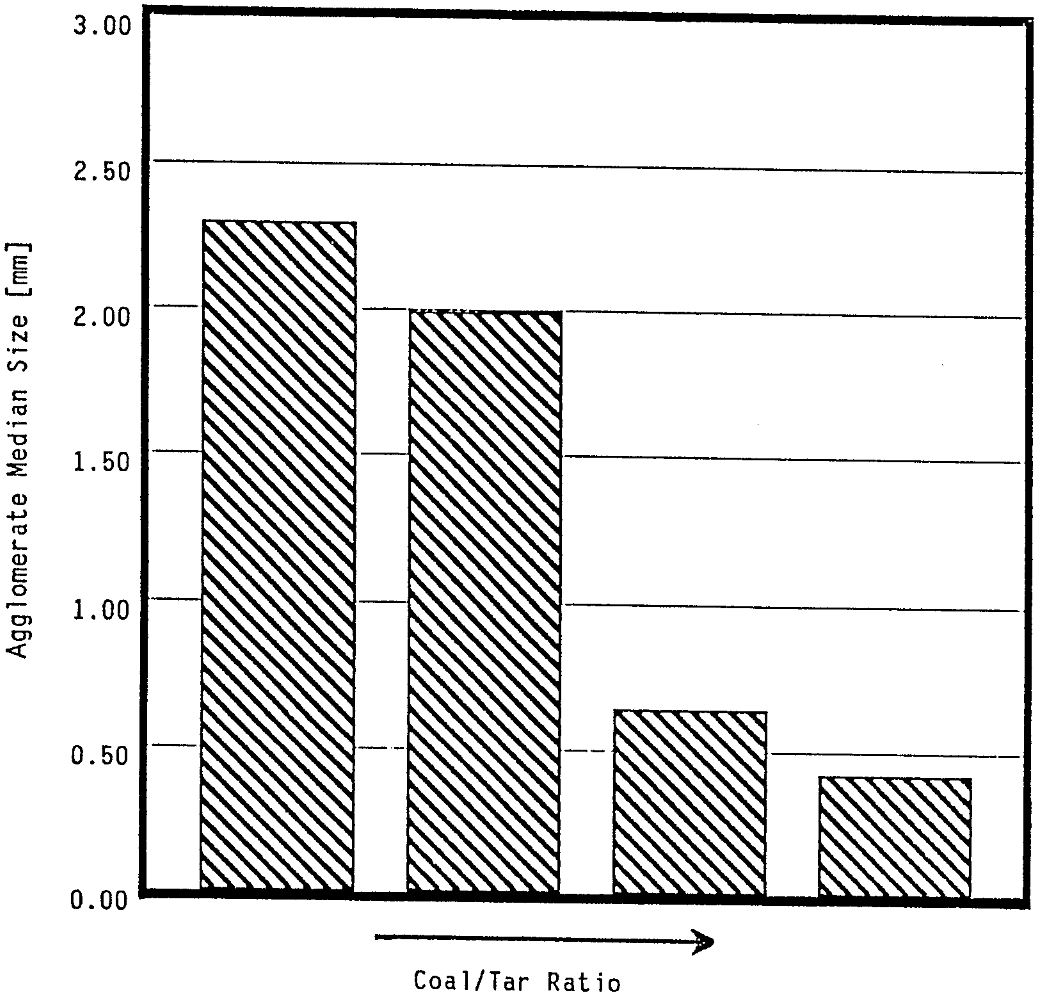

Figure 5. Effect of Coal/Tar Ratio on Agglomerate Size

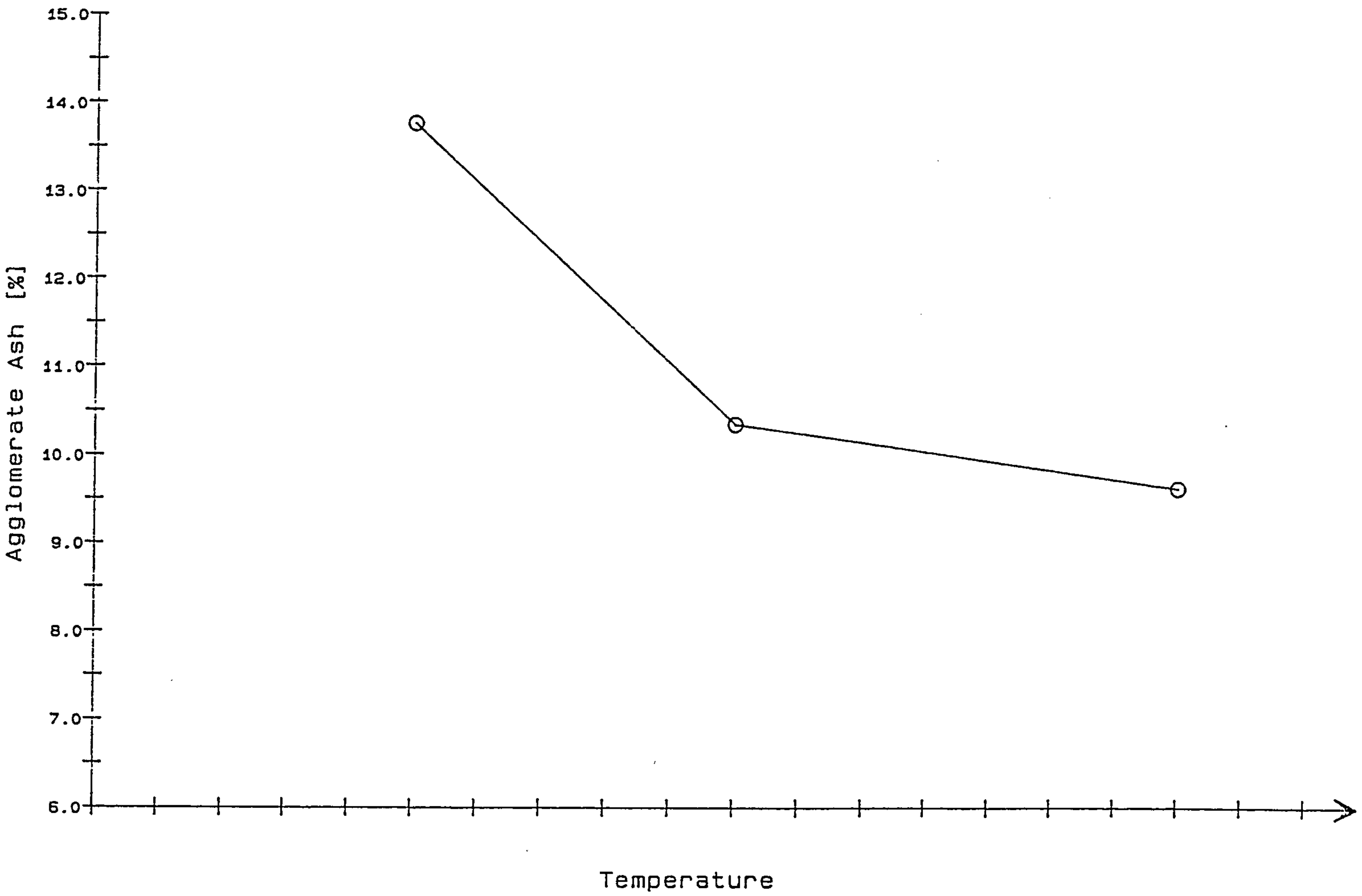

Figure 6. Effect of Temperature on Agglomerate Ash

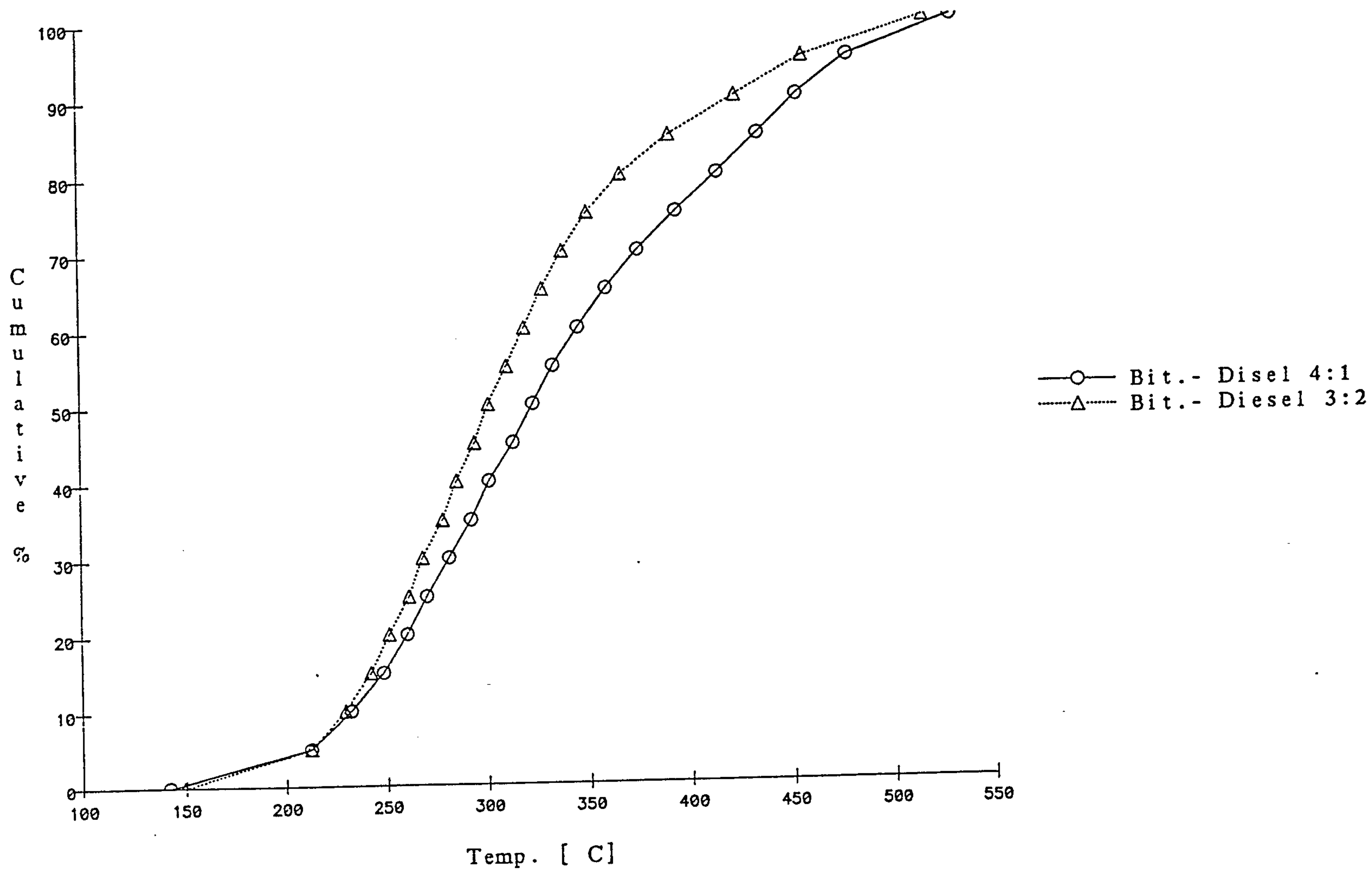

Figure 7. Distillation Curves of Oil Recovered from Agglomerates

## Table 1

## PROPERTIES OF TEST COALS

| Sample | Ash [%] | Sulfur [%] |  | Calorific Value [Btu/lb] | lbs $SO_2/10^6$ Btu |
|---|---|---|---|---|---|
|  |  | Total | Pyritic |  |  |
| Montana reject | 17.8 | 4.40 | 2.83 | 10,780 | 8.16 |
| Kentucky No. 9 | 14.6 | 5.08 | 3.09 | 12,430 | 8.21 |
| Pittsburgh Seam | 22.0 | 1.70 | 0.95 | 11,530 | 2.95 |
| Penn. C.O. | 19.2 | 1.13 | 0.58 | 12,240 | 1.81 |
| Devco Thermal | 5.7 | 2.90 | 1.88 | 14,500 | 4.00 |
| Devco Met. | 4.9 | 1.43 | 0.63 | 14,640 | 1.91 |
| EPA Standard |  |  |  |  | 1.20 |

All values on dry basis

## Table 2

## COMPARISON OF STANDARD AGGLOMERATION AND AGLOFLOAT PROCESS FOR MONTANA REJECT

| Process Procedure | Oil Addition* [% on dry coal] | Depressants | Combustible Recovery [%] | Ash [%] | Sulfur [%] |
|---|---|---|---|---|---|
| Feed Coal | | | | 17.8 | 4.4 |
| Standard | 21 | - | 91.4 | 10.9 | 3.8 |
| Agglomeration | 21 | + | 90.2 | 10.8 | 3.1 |
| Aglofloat | 10 | + | 91.3 | 8.2 | 1.6 |
| Process | 5 | + | 93.9 | 9.1 | 1.8 |

*Bitumen and Diesel Oil in ratio 4:1
All values on dry basis

Table 3

CLEANING OF PENNSYLVANIA CYCLONE OVERFLOW BY AGLOFLOAT PROCESS

| Experimental Procedure | Oil Addition* [% wt on dry coal] | Yield of Clean Coal [%] | Combustibles Recovery [%] | Ash [%] | Total Sulfur [%] | % Sulfur Removal | | lbs $SO_2/10^6$ Btu |
|---|---|---|---|---|---|---|---|---|
| | | | | | | Total | Pyritic | |
| Feed coal | | | | 19.2 | 1.13 | | | 1.81 |
| Single Stage Aglofloat | 5.0 | 82.3 | 96.2 | 5.6 | 1.06 | 23 | 41 | 1.42 |
| | 2.5 | 82.8 | 96.1 | 6.2 | 1.08 | 21 | 38 | 1.47 |
| Single Stage Aglofloat in Modified System | 10.0 | 77.0 | 89.5 | 6.1 | 0.75 | 49 | 84 | 0.97 |
| | 5.0 | 79.0 | 92.1 | 5.8 | 0.78 | 45 | 78 | 1.04 |

*Diesel Oil
All values on dry basis.

Table 4

CLEANING OF KENTUCKY NO. 9 COAL BY SINGLE
AND TWO STAGE AGLOFLOAT PROCESS*

| Test No. | Depres-sants | Yield of Clean Coal [%] | Combustibles Recovery [%] | Ash [%] | Total Sulfur [%] | % Sulfur Removal |  | lbs $SO_2/10^6$ Btu |
|---|---|---|---|---|---|---|---|---|
|  |  |  |  |  |  | Total | Pyritic |  |
| Feed Coal |  |  |  | 14.6 | 5.08 |  |  | 8.21 |
| K-1 Single Stage | + | 86.6 | 94.5 | 6.8 | 3.62 | 39 | 60 | 5.33 |
| K-2 Two Stage | + | 83.8 | 93.7 | 4.6 | 2.90 | 52 | 83 | 4.17 |
| K-3 Two Stage | - | 83.8 | 93.8 | 4.4 | 2.81 | 54 | 84 | 4.04 |

*Bridging liquid: Diesel Oil 2% on dry coal
All values on dry basis

## Table 5

## CLEANING OF PITTSBURGH SEAM COAL BY TWO STAGE AGLOFLOAT PROCESS*

| Test No. | Depressants | Yield of Clean Coal [%] | Combustibles Recovery [%] | Ash [%] | Total Sulfur [%] | % Sulfur Removal | | lbs $SO_2/10^6$ Btu |
|---|---|---|---|---|---|---|---|---|
| | | | | | | Total | Pyritic | |
| Feed Coal | | | | 22.0 | 1.70 | | | 2.95 |
| C-22 | + | 74.2 | 91.9 | 3.4 | 1.30 | 43 | 68 | 1.79 |
| C-24 | - | 74.0 | 91.8 | 3.2 | 1.30 | 43 | 70 | 1.79 |
| C-25 | + | 74.7 | 92.1 | 3.8 | 1.26 | 44 | 74 | 1.76 |

*Bridging liquid: Kerosene 1% on dry coal
All values on dry basis.

## Table 6

## CLEANING OF DEVCO METALLURGICAL AND THERMAL COALS BY TWO STAGE AGLOFLOAT PROCESS*

| Test No. | Depressants | Yield of Clean Coal [%] | Combustibles Recovery [%] | Ash [%] | Total Sulfur [%] | % Sulfur Removal | | lbs $SO_2/10^6$ Btu |
|---|---|---|---|---|---|---|---|---|
| | | | | | | Total | Pyritic | |
| Devco Metallurgical Feed | | | | 4.9 | 1.43 | | | 1.91 |
| D-6 | - | 93.6 | 96.5 | 1.8 | 1.10 | 28 | 59 | 1.45 |
| D-5 | + | 92.4 | 95.4 | 1.6 | 1.10 | 29 | 55 | 1.45 |
| Devco Thermal Feed | | | | 5.7 | 2.90 | | | 4.00 |
| DT-4 | - | 92.6 | 95.0 | 3.2 | 2.10 | 33 | 49 | 2.82 |
| DT-5 | + | 91.6 | 94.3 | 2.9 | 1.90 | 40 | 60 | 2.54 |

*Bridging liquid: Kerosene 1% on dry coal
All values on dry basis.

Table 7

MATERIAL BALANCE OF TAR RECOVERY PROCESS

| Streams | Weights | | Assays (%) | | | Distribution (%) | | |
|---|---|---|---|---|---|---|---|---|
| | (g) | (%) | Coal/Coke | Tar | Ash | Coal/Coke | Tar | Ash |
| Coal | 34.58 | 36.46 | 90.01 | - | 9.99 | 69.80 | - | 10.03 |
| Tar | 60.27 | 63.54 | 22.35 | 26.25 | 51.40 | 30.20 | 100.00 | 89.97 |
| Total Feed | 94.85 | 100.00 | 47.02 | 16.68 | 36.30 | 100.00 | 100.00 | 100.00 |
| Total Prod. | 90.43 | 95.34 | 45.23 | 16.11 | 34.00 | 96.19 | 96.57 | 93.67 |
| Agglomerates | 68.65 | 63.94 | 67.10 | 24.53 | 8.37 | 91.25 | 94.03 | 14.74 |
| Tailings | 29.78 | 31.40 | 7.40 | 1.35 | 91.25 | 4.94 | 2.54 | 78.93 |

All values on dry basis.

Table 8

EFFECT OF BRIDGING LIQUID COMPOSITION ON PROPERTIES OF AGGLOMERATES AND DE-OILED AGGLOMERATES[*]

| Sample | Bridging Liquid | Oil Recovery[a] [% wt] | Moisture[b] [%] | Ash[c] [%] | Volatile Matter[c] [%] | Moisture Capacity [%] | Calorific Value [Btu/lb] | |
|---|---|---|---|---|---|---|---|---|
| | | | | | | | Dry | Air-dry |
| Feed coal | - | - | 17.4 | 5.4 | 41.6 | 20.6 | 12,470 | 10,300 |
| Agglomerates | Bitumen + Diesel Oil in ratio 3:2 | - | 7.5 | 3.3 | 48.9 | 13.3 | 13,540 | 12,520 |
| De-oiled Agglomerates | | 64.6 | 1.6 | 3.0 | 41.2 | 6.7 | 13,380 | 13,170 |
| Agglomerates | Bitumen + Diesel Oil in ratio 4:1 | - | 7.3 | 3.2 | 49.4 | 14.2 | 13,640 | 12,640 |
| De-oiled Agglomerates | | 53.6 | 1.6 | 2.9 | 41.7 | 6.5 | 13,450 | 13,230 |

[*] Heat treatment at 350°C using nitrogen as a carrier gas

[a] Direct determination of condensed oil

[b] Air dry

[c] Dry basis

## Table 9

## COMPARISON OF OILS DISTILLED OFF DIRECTLY FROM BRIDGING LIQUIDS AND OILS RECOVERED FROM AGGLOMERATES DURING HEAT TREATMENT AT 350°C

| Bridging Liquid Composition | Bitumen + Diesel Oil 3:2 | | Bitumen + Diesel Oil 4:1 | |
|---|---|---|---|---|
| Properties | Standard Distil. (-525°C) | Oil from Agglom. | Standard Distil. (-525°C) | Oil from Agglom. |
| Yield, % wt | 65.3 | 64.6* | 54.5 | 53.6* |
| Density, g/ml at 15.6°C | 0.8920 | 0.8973 | 0.9126 | 0.9156 |
| API Gravity | 27.1 | 26.1 | 23.5 | 23.1 |
| Carbon, % wt | 87.1 | 85.9 | 85.6 | 85.7 |
| Hydrogen, % wt | 12.2 | 11.8 | 11.9 | 11.7 |
| Sulfur, % wt | 1.2 | 1.0 | 1.9 | 1.6 |
| Nitrogen, ppm | 291 | 244 | 505 | 329 |
| Calorific Value | n/a | 18,990 | n/a | 18,960 |

*Direct determination of condensed oil.